ISBN: <ask the JACoW BoD> ISSN: <ask the JACoW BoD> doi: 10.18429/JACoW-HB2025-MOLBA01

# HEAVY LON BEAM LOSS CONTROL AT THE FACILITY FOR RARE ISOTOPE BEAMS*

T. Maruta†, K. Fukushima, A. Gonzalez, K. Hwang, P.N. Ostroumov, A.C. Plastun, T. Zhang, Q. Zhao
Facility for Rare Isotope Beams, Michigan State University, East Lansing, USA

*Abstract*

The power of heavy ion beams at FRIB fragmentation target has gradually increased from 1 kW to 30 kW over the past three years, and maintaining relative beam losses below $10^{-4}$ is a high priority. This paper presents the discussion of primary sources of the beam halo in heavy ion linacs, accelerating multiple charge-state beams and beam physics applications to control beam losses for the full spectrum of accelerated ion species from oxygen to uranium. It will also discuss the effect of liquid lithium film fluctuations on beam losses and the challenge of maintaining extremely low beam losses, <10 mW/m, in cryomodules.

## INTRODUCTION

The driver linac is designed to provide a 400 kW continuous wave beam to the production target [1]. The detailed description of FRIB and driver linac was provided in our paper at the previous HB workshop [2]. To avoid lengthy repetitions, this paper will use the same abbreviations as in Ref. 2 for the linac components. The layout of the linac is shown in Fig. 1. The beam accelerated by the LS1 interacts with the charge stripper, a highly beneficial technique for heavy ion accelerators [3]. The electrons are stripped off the ions while passing through a thin material, which boosts the charge-to-mass ratio ($q/A$) of beams for efficient acceleration. FRIB has developed a 20 – 30 μm thick liquid lithium film as the stripper (LLCS) [4] due to its high capability for thermal load and radiation resistance. Due to the stochastic nature of the stripping process, the output beam is distributed to several charge states. In most cases, the charge state distribution is similar to a Gaussian function, and the fraction of beam intensity in a single charge state is low. Table 1 shows recently operated beams, including the stripping efficiencies measured in FRIB. The yield of the central charge state of the $^{238}$U beam is only 21% of the initial intensity.

To provide higher stripping efficiency, the FRIB linac has been designed to accelerate multiple charge states simultaneously. To minimize effective emittance growth of multi-charge ion beam, the bending systems in FS1, FS2 and BDS have been designed to satisfy achromat conditions and merge all charge states' central trajectories after the bends [5]. The aperture in the dispersive plane is sufficient to accept five charge states of the uranium beam with charge state spread $\Delta q/q_{cen}$, equal to 5.3%. The multi-charge acceleration substantially reduces the deposited power of unwanted charge states on the Charge Selection Slits (CSS) installed after the first bending dipole in the FS1, thereby reducing the required radiation shielding. In the current CSS, absorbed beam power at a single spot is limited to 500 W. For example, after the stripping, the $^{48}Ca^{19+}$ fraction is 26% and the 500 W limit corresponds to approximately 13 kW of $^{48}Ca^{20+}$ only delivered to the target.

Mitigation of beam loss is an essential requirement in high-intensity accelerators. Hands-on maintainability is compromised if the loss exceeds the empirical limit of 1 W/m. FRIB operates 324 Super-Conducting (SC) cavities to accelerate heavy ions, and there is a hypothesis that the beam loss in the SC cavities degrades the surface condition and can limit the available accelerating gradient due to field emission.

Table 1: Beam Parameters During the Recent Beam Operations (the stripping efficiencies were measured at 17 MeV/u for $^{124}$Xe and $^{238}$U, and 20 MeV/u for the rest of ions)

| Ion | Charge states after stripper | Energy at the target [MeV/u] | Stripping efficiency 1q / Multi-q |
|---|---|---|---|
| $^{48}$Ca | 19+, 20+ | 225 | 72% / 98% |
| $^{58}$Ni | 26+, 27+ | 250 | 66% / 94% |
| $^{64}$Zn | 28+, 29+ | 240 | 71% / 88% |
| $^{82}$Se | 32+, 33+ | 200 | 74% / 88% |
| $^{124}$Xe | 48+ to 50+ | 240 | 30% / 76% |
| $^{238}$U | 73+to 77+ | 177 | 21% / 83% |

## NEW BEAM DEVELOPMENT

The development of a new primary beam starts with a pre-calculation of the accelerator setting by simulation tools. The RF cavities' setting from MEBT to the target is calculated by a model-based Instant Phase Setting (IPS) application [6]. The amplitude and synchronous phase of each cavity are optimized to meet the energy requirement and provide sufficient stability area for all selected charge states in the longitudinal phase space. The calculated RF cavities' settings are loaded to the 3D beam envelope code FLAME to calculate the required focusing fields. The solenoids in the acceleration segments LS1 and LS2 are set to provide the transverse phase advance per period below 90°. Then, five sections of quadrupoles (upstream of the

* Work supported by the U.S. Department of Energy Office of Science under Cooperative Agreement DE-SC0023633, the State of Michigan, and Michigan State University.
† maruta@frib.msu.edu

ISBN: <ask the JACoW BoD> ISSN: <ask the JACoW BoD> doi: 10.18429/JACoW-HB2025-MOLBA03

# THE MUON COLLIDER DESIGN CHALLENGES*

E. Métral†, CERN, Geneva, Switzerland
on behalf of the International Muon Collider Collaboration (IMCC)

*Abstract*

The International Muon Collider Collaboration (IMCC) was established following the 2020 Update of the European Strategy for Particle Physics, with the aim of assessing the feasibility of a muon collider operating at a centre-of-mass energy of 10 TeV. The concept of colliding beams of oppositely charged muons dates back to the late 1960s, with foundational work by F. F. Tikhonin, G. I. Budker, and A. N. Skrinski. Interest in muon colliders has recently been revitalized due to technological advances that address longstanding obstacles, many of which were first tackled by the Muon Accelerator Program (MAP) in the United States (2010–2017) and have since been advanced by the IMCC. The large mass of the muon (207 times that of the electron) suppresses synchrotron radiation, making circular colliders feasible. However, the short muon lifetime (2.2 μs at rest) constrains the number of usable turns, making the design and operation of such a collider uniquely challenging. Despite the many hurdles linked to the muon decay, no fundamental showstopper has been identified to date. A muon collider thus remains a highly promising candidate for the next-generation high-energy physics facility.

## INTRODUCTION

The conceptual layout of the IMCC muon collider and its target parameters are shown in Fig. 1 and Table 1 respectively, while the technically-limited timeline, for the initial stage, is presented in Fig. 2. Two conceptual layouts, for both CERN and FNAL sites, can be found in Fig. 3.

The huge beneficial effect of using muons instead of electrons comes from the fact that the energy lost from synchrotron radiation, given by $U_{\rm lost} \propto E^4/(\rho E_0^4)$ (with $E$ the muon total energy, $E_0$ the muon rest energy and $\rho$ the dipole bending radius) is reduced by more than $10^9$ thanks to the larger rest energy of the muon. Therefore, in the TeV energy scale, synchrotron radiation can be considered to be negligible with muons (as well as Beamstrahlung and disruption at the interaction point), which opens again the possibility to use relatively small circular machines to accelerate and collide leptons. However, the first and main challenge of a muon collider is the short muon lifetime at rest $\tau_{\mu 0} = 2.2$ μs, which corresponds to only ~ 660 m at the speed of light $c$. Fortunately, thanks to special relativity, the muon lifetime increases with its energy [1]: $\tau_\mu = \gamma \tau_{\mu 0}$ with $\gamma = E/E_0$ the relativistic mass factor. Therefore, the muon lifetime is ~ 20 ms per TeV, i.e., ~ 30 ms at 1.5 TeV total muon energy (corresponding to 3 TeV in the center of mass) or ~ 100 ms at 5 TeV total muon energy. Note then that a total muon energy of ~ 50 TeV would be needed to reach a muon lifetime of ~ 1 s. The short muon lifetime is therefore the main challenge of a muon collider and all the muon beam manipulations will need to be done (much) faster than 1 s!

## MUON SURVIVAL AND REQUIRED AVERAGE ACCELERATING GRADIENT

At constant energy, the muon decay is given by

$$\frac{N(t)}{N(0)} = e^{-\frac{t}{\tau_\mu}} = e^{-\frac{t}{\gamma \tau_{\mu 0}}} \quad , \tag{1}$$

where $N$ is the number of muons and $t$ is the time. The muon decay as a function of time is depicted in Fig. 4 for several energies. IMCC has been analyzing the scenario with an energy of $E = 5$ TeV per beam (resulting in a center-of-mass energy of 10 TeV) and a repetition frequency of $f_r = 5$ Hz. Under these conditions, approximately 15 % of the muons survive until the arrival of the second injection, with about 2 % remaining by the time of the third injection. Therefore, for each collision energy, the repetition frequency or/and injection/colliding schemes should be optimised. For the moment, IMCC assumes that the remaining muons are removed before each injection into the same bucket, such that only two bunches collide at the interaction point.

During acceleration (with acceleration time $\tau_{\rm acc}$), assuming a linear acceleration from initial (i) to final (f) energies, the muon decay is given by

$$\frac{N(\tau_{\rm acc})}{N(0)} = \left(\frac{\gamma_{\rm f}}{\gamma_{\rm i}}\right)^{-\frac{1}{\tau_{\mu 0}}\frac{\tau_{\rm acc}}{\gamma_{\rm f}-\gamma_{\rm i}}} \quad . \tag{2}$$

For large $\gamma$, the total energy can be approximated by the kinetic energy and the average accelerating gradient, over the accelerating length $d_{\rm acc}$, can be obtained

$$G_{\rm acc,avg} = \frac{E_{\rm f} - E_{\rm i}}{d_{\rm acc}} = \frac{m_{\mu 0} c}{\tau_{\mu 0}} \ln\left(\frac{E_{\rm f}}{E_{\rm i}}\right) / \left[-\ln\left(\frac{N_{\rm f}}{N_{\rm i}}\right)\right] \quad , \tag{3}$$

where $m_{\mu 0} \approx 105.7$ MeV/c$^2$ is the muon rest mass. A muon survival of ~ 90 % during the acceleration processes seems to be a good compromise and for a muon survival of 90 % during acceleration, the required average accelerating gradient is a few MV/m.

## LUMINOSITY

The luminosity values reported in Table 1 have been calculated under the following nine assumptions: one bunch of $\mu^+$ colliding against one bunch of $\mu^-$ (as for the same total number of particles, it is more efficient to have all the particles in one bunch); densities uncorrelated in the three

* This work was supported by the European Union grant agreement 101094300 and it was endorsed by the IMCC

† Elias.Metral@cern.ch

ISBN: <ask the JACoW BoD> ISSN: <ask the JACoW BoD> doi: 10.18429/JACoW-HB2025-TUIAB02

# RANDOM RESONANCE COMPENSATION FOR FURTHER BEAM POWER RAMP-UP IN THE J-PARC RCS

K. Kojima*, H. Harada, M. Chimura, P. K. Saha
Japan Atomic Energy Agency, 2-4 Shirakata, Tokai-mura, Naka-gun, Ibaraki 319-1195, Japan

*Abstract*

A detailed study on random resonances was conducted to facilitate further beam power ramp-up in the 3 GeV rapid cycling synchrotron of the Japan Proton Accelerator Research Complex. Systematic experiments employing a low-intensity beam revealed considerable excitation of linear random resonances, namely horizontal half-integer and linear sum resonances, located just above the current operating point. The half-integer resonance was well compensated by using trim quadrupole magnets. This resonance compensation scheme has been confirmed to mitigate beam loss even for high-intensity beams and effectively improve the operating point tunability. Similarly, the linear sum resonance was found to be compensated by making local bumps in the location of sextupole fields. We identified the source of lattice imperfection driving the random resonances as the leakage field from the extraction DC magnets by implementing a theoretical procedure based on resonance driving terms.

## INTRODUCTION

A 3 GeV rapid cycling synchrotron (RCS) of the Japan Proton Accelerator Research Complex (J-PARC) is a high-intensity proton driver for the pulsed muon and neutron target at the Material and Life Science Experimental Facility and also serves as an injector for the main ring synchrotron [1]. As shown in Fig. 1, the RCS has a threefold symmetric lattice, with each superperiod comprising one dispersion-free straight section and one arc section. The injected proton beam is accelerated from 400 MeV up to 3 GeV at a repetition rate of 25 Hz and simultaneously delivered to the two destinations mentioned above. Owing to the sophisticated beam commissioning technique, the RCS currently delivers a beam at the design output beam power of 1 MW for routine user operation with very low fractional beam loss [2–5].

The RCS beam power ramp-up aiming beyond the design is proceeding steadily, and minimizing the resonance-induced beam loss is crucial to ensure stable and sustainable operation. In the low-energy region of 400 MeV, the space charge effect plays a particularly important role and pushes the tune spread toward the lower tune side. The tune spread for the intensity of 1.5 MW-eq. overlaps the structure resonances $\nu_{x(y)} = 6$ as shown in Fig. 2. To mitigate the beam loss due to the structure resonances, the operating point has to be shifted higher tune side from the current operating point $(\nu_x, \nu_y) = (6.46, 6.36)$. However, previous studies employing a 1 MW beam indicated a substantial increase in beam loss, even a minor shift in the horizontal tune from 6.46 to 6.49 as shown in Fig. 3, and the change in the position of the operating point is strictly restricted by such beam loss.

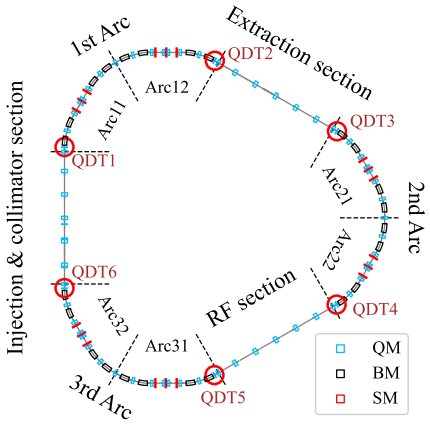


Figure 1: Schematic view of the RCS. Red circles indicate the locations of the trim quadrupole magnets (QDTs). BM, bending magnet; QM, quadrupole magnet; SM, sextupole magnet.

In this study, the random resonances, which are positioned on the higher tune side and are likely to restrict the tunability of the operating point, were studied. The random resonances enhanced by the lattice imperfections were exclusively investigated by employing a low-intensity beam. Our tune survey result indicates the severe excitation of the horizontal half-integer resonance ($2\nu_x = 13$) and linear sum resonance ($\nu_x + \nu_y = 13$). To expand the tunability of the operating point, we attempted to compensate for these resonances. This paper presents these experimental results.

## IDENTIFICATION OF THE CAUSES OF THE BEAM LOSS

To identify the random resonances that lead to the beam loss, a tune survey was conducted with the operating points indicated by red circles in Fig. 2; namely the operating point was shifted from $(\nu_x, \nu_y) = (6.5, 6.4)$ to $(6.57, 6.47)$ linearly in the betatron tune space. Proper beam conditions are required to observe the resonance-induced beam loss clearly. Figure 4 shows the injected beam distributions in the horizontal and vertical phase spaces. The horizontal and vertical painting emittances of $\varepsilon_{p,x}$ and $\varepsilon_{p,y}$ can be arbitrarily adjusted by controlling the offset [3]. In this case, the painting emittances were set at $200\pi$ mm·mrad in both directions to enhance the resonance-induced beam loss. The beam was injected in the longitudinal direction with minimal momentum spread to mitigate the chromaticity-induced tune shift

* kunihiro.kojima@j-parc.jp

ISBN: <ask the JACoW BoD> ISSN: <ask the JACoW BoD> doi: 10.18429/JACoW-HB2025-TUIAB03

# RECENT OPTICS MEASUREMENTS AND CORRECTIONS FOR HIGH-INTENSITY OPERATION OF THE J-PARC MAIN RING

T. Aasami*, H. Hotchi, S.Igarashi, T. Koseki[1], Y. Sato, T. Yasui, KEK, Tsukuba, Japan
[1]also at Deaprtment of Physics, The University of Tokyo, Tokyo, Japan

*Abstract*

In the intensity-frontier proton synchrotron J-PARC Main Ring (MR), a power upgrade plan is underway to achieve 1.3 MW beam power for neutrino experiments. The upgrade has generally progressed as planned, with the beam power for the user operation reaching 830 kW as of May 2025. A major obstacle to upgrading the beam power of the MR is the radioactivation of accelerator components caused by beam loss. One significant contributor to beam loss is the betatron resonances, which are sensitive to the symmetry of optics. Precise optics corrections during beam tuning have therefore been playing a critical role in suppressing these resonances and reducing beam losses. This paper presents the strategies and recent results of optics measurements and corrections for the MR.

## INTRODUCTION

The J-PARC Main Ring (MR) is an intensity-frontier synchrotron with three-fold symmetry. Its fundamental parameters are summarized in Table 1. The MR accelerates protons from 3 to 30 GeV, and a power upgrade program is underway to deliver 1.3 MW for neutrino experiments [1]. The upgrade aims to shorten the repetition period and increase the number of protons per pulse (ppp) to 1.16 s and $3.3 \times 10^{14}$ ppp, respectively. A large-scale hardware upgrade was completed by July 2022, enabling 1.36 s operation [2, 3]. By May 2025, the MR achieved 830 kW in user operation and demonstrated 950 kW during beam studies.

A critical obstacle in enhancing beam power is the degradation of accelerator component maintainability caused by beam-loss-induced radioactivation. In the MR, the dominant source of loss is the betatron resonances, which depend on symmetry of optics. Precise adjustment of quadrupole fields to compensate three-fold symmetry has been essential, successfully reducing the amount of beam losses by several tens of percent in past operations [4]. Since beam losses must remain below a threshold for stable operation regardless of intensity, precise correction of quadrupole field errors is becoming increasingly important.

Nevertheless, residual quadrupole errors as large as $\Delta K/K \sim 1\,\%$ are still estimated [5]. Two main factors are considered responsible. First, some quadrupole power-supply families were divided in ways that no longer preserved three-fold symmetry, requiring substantial compensation during beam tuning after the upgrade [4, 6]. Second, eddy currents induced in the vacuum ducts by the steeper ramping pattern produce quadrupole field responses. Because the vacuum ducts are not arranged symmetrically, these effects break optics' symmetry during acceleration and are likely to worsen as the repetition rate increases.

Table 1: Basic Parameters of MR

| Parameter | Value |
|---|---|
| Circumference | 1567.5 m |
| Superperiodicity | 3 |
| Injected particles | proton $p$ |
| Injection energy | 3 GeV |
| Extraction energy | 30 GeV |
| Harmonic number | 9 |
| Number of bunches | 8 |
| Number of quadrupole magnets | 216 |

Steering magnets are small bending magnets used to correct closed orbit distortion.

To evaluate residual errors of $\Delta K/K \sim 1\,\%$ with sufficient significance, a method with accuracy at the 0.1 % level is required. Furthermore, identifying the underlying sources necessitates error evaluation at each quadrupole magnet around the ring. The purpose of this paper is to present the development and demonstration of such a method, as discussed in detail in Ref. [5].

## EVALUATION OF QUADRUPOLE FIELDS

This section introduces a method for detecting time-varying quadrupole field errors at individual magnets around the MR, referred to as QCPLM (Quadrupole field analysis by Closed orbits using the Perturbation-based Linearized Model ). QCPLM is a variant of the Orbit Response Matrix (ORM) method [7–9], where steering magnets are excited one by one and the resulting closed-orbit distortions are fitted to an optics model. Unlike many other ORM methods, which require fitting a nonlinear response function, QCPLM employs a perturbation-based linearized model to reduce the impact of measurement errors. The principles of QCPLM are described here, and its precision and validity are evaluated in later sections.

### *QCPLM*

QCPLM determines quadrupole field errors by comparing closed orbits produced with opposite steering kicks. A closed orbit $\chi(s, \vec{\theta}_\chi)$ is measured, then re-measured with reversed kicks $\chi(s, -\vec{\theta}_\chi)$. Their difference, $\Delta\chi_i \equiv [\chi(s_i, \vec{\theta}) - \chi(s_i, -\vec{\theta})]/2$ satisfies $\overrightarrow{\Delta\chi} = A(\vec{\theta}_\chi)\overrightarrow{\Delta K}$, from which the error vector $\overrightarrow{\Delta K}$ is obtained.

Here, $A(\vec{\theta}_\chi)$ is the response matrix defined by the unperturbed orbit and steering settings. $\overrightarrow{\Delta K}$ includes both quadrupole field errors (in $[\mathrm{m}^{-1}]$) and calibration errors

* tasami@post.kek.jp

ISBN: <ask the JACoW BoD> ISSN: <ask the JACoW BoD> doi: 10.18429/JACoW-HB2025-TUIAB04

# RECENT DEVELOPMENTS OF THE TRIUMF 520 MeV CYCLOTRON IN SUPPORT OF HIGH INTENSITY OPERATION

L. G. Zhang*, R. A. Baartman, I. Bylinskii, P. Jung[1], H. W. Koay, M. Marchetto, T. Planche[1], Y. N. Rao, S. Saminathan, O. Shelbaya[1]
TRIUMF, Vancouver, Canada
[1]also at University of Victoria, Victoria, Canada

*Abstract*

The TRIUMF 520 MeV cyclotron continues to serve as a reliable driver for high intensity proton beams, supporting a broad range of applications. To sustain and enhance high intensity operation, recent developments have focused on reducing beam losses and improving overall reliability. This paper will highlight progress in several key areas: cyclotron tune optimization and the avoidance of linear coupling resonances to suppress beam spills; the implementation of a refined degaussing procedure for the main magnet to improve reproducibility; and upgrades to the new horizontal section of the injection beamline.

## INTRODUCTION

The TRIUMF 520 MeV cyclotron [1] is a powerful and long serving high intensity proton accelerators. Since its first operation in 1974, the cyclotron has undergone continuous upgrades to increase beam current, improve reliability, and support an expanding range of experimental programs [2, 3]. Over the past decades, sustained developments in ion source performance, beam dynamics understanding, and refurbishment of the key component [4–6] have enabled routine operation above 300 µA of average extracted proton current with the beam availability of around 90 % as shown by the beam delivery statistics in Fig. 1.

The layout of the TRIUMF cyclotron is shown in Fig. 2. The beam is simultaneously extracted to three beamlines using stripping foils, providing approximately 3 × 5000 beam hours annually. With the upcoming installation of the Advanced Rare Isotope Laboratory (ARIEL) facility [7], the total beam-hour requirement will increase to 4×5000. Consequently, the demand for higher beam intensity and improved operational reliability has become more pressing.

In this paper, we report recent developments of the TRIUMF 520 MeV cyclotron undertaken to support high-intensity operation. These include (1) theoretical and experimental studies of the linear coupling resonance to better understand and mitigate beam loss; [8,9] (2) implementation of a demagnetization procedure to improve the reproducibility of the main magnetic field; [10, 11] and (3) design, construction, and commissioning of a new electrostatic injection line [12, 13] to enhance reliability, and beam quality.

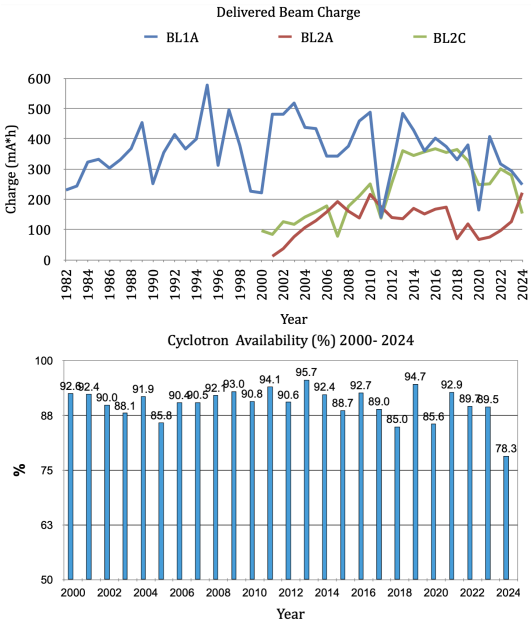


Figure 1: Annual beam delivery and cyclotron availibility.

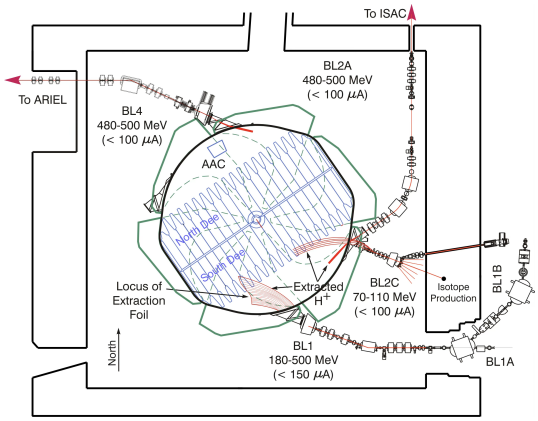


Figure 2: Layout of the TRIUMF 520 MeV cyclotron and the primary beamlines.

## COUPLING RESONANCE

In TRIUMF cyclotron, the tune diagram, as shown as the dashed line in Fig. 3, passes through the linear coupling resonance line $\nu_r - \nu_z = 1$ multiple times with acceleration. Because cyclotron has a much larger radial aperture than the vertical one, the betatron oscillation amplitude of halo particles in the radial direction is larger. When these oscillations are transferred into the vertical plane through linear

* lzhang@triumf.ca

ISBN: <ask the JACoW BoD> ISSN: <ask the JACoW BoD> doi: 10.18429/JACoW-HB2025-TUIAC02

# BEAM DYNAMICS COMPARISON OF DIFFERENT STRUCTURES TOWARDS A COMPACT ACCELERATOR BASED NEUTRON SOURCE

R.E. Laxdal[1], Mina Abbaslou[1], O. Kester[1], P. Kolb[1], M. Marchetto[1], D. Marquardt[2]
[1]TRIUMF, Vancouver, BC, Canada
[2]University of Windsor, Windsor, ON, Canada

*Abstract*

A prototype Canadian compact accelerator-driven neutron source (PC-CANS) is under study. The source utilizes a high-intensity compact proton RF linear accelerator, delivering a peak current of 20 mA with a 5% duty factor of protons at 10 MeV to the target. The accelerator baseline concept includes a short radio-frequency quadrupole (RFQ) to 3 MeV, followed by a drift tube Linac (DTL) structure accelerating to 10 MeV. Various room temperature DTL variants, including Alvarez, and H-mode variants using APF, KONUS, and NSP (negative synchronous phase) beam dynamics are considered at a frequency of 352.2 MHz. This paper compares the beam dynamics and characteristics of the various structures.

## INTRODUCTION

A Canadian consortium of neutron users, BNCT researchers and technical experts is proposing a compact accelerator-based neutron source (CANS) [1]. The PC-CANS (prototype Canadian CANS) is a relatively low-cost facility that would serve the local university community of neutron users, allow the development of BNCT in Canada and supply 18F for PET at a local hospital. It is envisaged that the PC-CANS could serve as a model to set up other similar CANS facilities across Canada and serve as a technical development centre towards a more powerful facility, that would be a national-scale facility.

A schematic of PC-CANS is shown in Fig. 1. Briefly, it consists of a proton linear accelerator with a peak intensity of 20 mA at 5% duty factor (1 mA average current) to 10 MeV for a peak/average beam power of 200/10 kW. For neutron time-of-flight (TOF) considerations, repetition rates are in the range from 20 Hz to 200 Hz. For upgrade potential, simulations to higher intensities are also considered as part of the design study. The beam intensity limit is due to present target technology that is foreseen to be developed in a staged way as target experience develops.

A conceptual design study has been completed [2,3] that supports a technical design report as a basis for a funding proposal. This paper summarizes the work that has been done to characterize the performance of various DTL variants including their potential for further intensity upgrades. Given the end use of PC-CANS as a tool for neutron scientists and medical practitioners in a university setting simplicity of operation and maintenance are a consideration in technical choices.

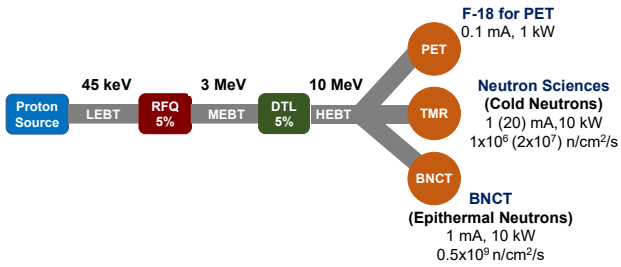


Figure 1: Schematic layout of PC-CANS [2].

## LINAC CONSIDERATIONS

The pulsed low duty cycle high intensity scheme for the PC-CANS and final end-use favours a normal conducting linac. Important optimization parameters are capital and operating cost, low losses for hands-on maintenance, footprint and ease of operation. The PC-CANS parameters allow some flexibility in the technical choice as the space charge forces are not extreme and the RF duty factor at ~7% (for 5% beam duty factor) reduces RF power density in the structures. Several high current proton linacs (up to 70 mA) have been built or proposed in this regime (ie LINAC4, ESS, SNS) with rf frequencies ranging from 300-400 MHz, though lower frequency linacs [4] have been proposed for higher beam intensities (>100 mA) requiring larger acceptances. The present PC-CANS studies consider 352 MHz as the baseline since rf sources are common and standard linac cost optimization would favour the highest frequency that supports the beam dynamics. For a small linac like PC-CANS choosing a common frequency between RFQ and DTL is prudent to limit required spares and technical support knowledge.

Commercial ECR sources are available in this intensity range. A source potential of 45 kV is suitable for moderate space charge applications like PC-CANS. The choice is a compromise between considerations of beam space charge effects that may increase the transverse emittance at low energy and limiting initial energy to promote efficient bunching in the RFQ, where the longitudinal emittance and length favours decreasing injection energy. A short LEBT consisting of two solenoids is assumed in the design.

The handover energy from RFQ to DTL of 3 MeV is a compromise where a higher energy helps control space charge forces at higher intensities at the expense of higher acceleration efficiency in the DTL. At 3 MeV the RFQ length is modest and the initial cell length of the DTL ($\beta\lambda$=68mm) allows reasonably efficient acceleration for the chosen DTL bore size of 20 mm.

ISBN: <ask the JACoW BoD> ISSN: <ask the JACoW BoD> doi: 10.18429/JACoW-HB2025-TUIBB03

# COMMISSIONING OF NICA INJECTION COMPLEX

O. I. Brovko, A. V. Butenko, D. K. Chumakov, E. E. Donets, A. R. Galimov, B. V. Golovenskiy, E. V. Gorbachev, V. N. Karpinskiy, S. A. Kostromin, V. A. Lebedev†, I. N. Meshkov, D. N. Nikiforov, I. Yu. Nikolaichuk, Yu. V. Prokof'ichev, V. L. Smirnov, A. S. Sergeev, V. S. Shpakov, E. M. Syresin, Y. S. Tamashevich, G. V. Trubnikov, A. V. Tuzikov, A. A. Volodin
Joint Institute of Nuclear Research, Dubna, Russia

*Abstract*

Construction of the NICA collider is approaching to its end with the beam circulation in the collider rings expected by the beginning of 2026. Successful collider commissioning requires obtaining high intensity heavy ion beams in its injector string. The talk discusses upgrades of the injection complex aimed at radical increase of the injection complex intensity. In general, there are two major efforts. The first one is the beam accumulation in Booster with help of electron cooling; and the second one is a drastic reduction of beam loss in the course of beam acceleration. This work actually includes large number of different efforts ranging from solving simple engineering problems to the detailed measurements and correction of beam optics for all rings and transfer lines, optimization of beam acceleration, as well as optimization of beam accumulation with electron cooling.

## INTRODUCTION

The NICA accelerator complex (JINR, Dubna, Russia) [1] consists of collider rings, two synchrotrons (Booster and Nuclotron), a linear accelerator, and several transport lines connecting them. The complex is designed to accelerate and collide light and heavy ions with a magnetic rigidity of up to 44.5 T·m. Currently and during the first years of the complex's operation we will use a beam of $^{124}Xe^{26+}$ ions from the KRION-6T heavy ion source. Initially, the ion beam is accelerated using RFQ and a linear accelerator to an energy of 3.2 MeV/n and then injected into the Booster. After acceleration in the Booster to an energy of ≈500 MeV/n, the beam is transferred to the Nuclotron. At the beginning of Booster-Nuclotron beamline the beam is stripped on the thin foil to bare nuclei. After acceleration in the Nuclotron to the collision energy the beam is transferred to the collider rings where, before coming to collisions, the beams are accumulated in the barrier-bucket RF with help of electron and stochastic cooling. After accumulation the beams are rebunched with two RF systems operating at harmonics 22 and 66, and then brought to the collisions.

Commissioning of the collider rings is expected to start at the end of this year. The injection complex, which includes Booster and Nuclotron, is in the operational state. Currently, the main goal of its commissioning is an achievement of the design beam intensity and commissioning of fast extraction from the Nuclotron. It requires ion accumulation at the Booster injection energy and minimization of beam loss throughout the accelerator chain. The Booster is planned to accumulate (2-5)·$10^8$ ions, injected in 10 pulses at a rate of ~3 Hz. The beam accumulation happens in the longitudinal plane with help of electron cooling. The total acceleration cycle duration is ~7 s.

This article discusses commissioning of the injection complex carried out in 2024 - 2025 which includes: (1) optimization of operation for the ion source (KRION-6T) and the heavy ion linac (HILAC), (2) measurement and correction of beam optics for the HILAC-Booster transfer line, (3) finalization of orbit correction software and hardware for the Booster and Nuclotron, (4) beam optics measurements through the entire complex, and (5) optimization of beam cooling and accumulation at the Booster injection energy. This work also included rewriting software controlling the rate of acceleration which matched available RF voltage to the dipole field growth rate. The growth rate was designed to prevent a reduction of RF bucket size in the course of acceleration, so that to avoid beam loss observed at the beginning of acceleration in the previous Runs.

## KRION AND HILAC

The beam extraction in the KRION ion source was modified in 2023 to shorten duration of the extracted beam. Before modification the extraction system consisted of 15 cylindrical electrodes - 50 mm long and 4 mm internal diameter. To extract the beam a linearly grown voltage was applied to the cylinders. The corresponding voltage distribution was obtained with resistive divider fed by ~1.5 kV pulse. Since the extraction voltage did not penetrate into the cylinders the ion pulse had long tail which duration was determined by temperature of heavy ions. Depending on the ion type the total duration of the pulse was in the range of 12-18 μs, while the revolution time at the Booster injection energy is 8.2 μs. Since longitudinal electron cooling is much faster than the transverse one, we chose the beam accumulation in the longitudinal plane. That requires the total duration of the beam to be ≤4 μs. To address this problem, we changed the shape of ion holding cylinders. New electrodes have long fingers which penetrate into nearby cylinders. New extraction system has the same period but due to the fingers the extraction field is almost uniform along the ion column [2]. Figure 1 shows the beam current measurements for xenon and nitrogen beams after the source upgrade. The 10 pulses at the top picture go every 100 ms. As one can see the major fraction of particles fits into 4 μs and there is relatively small pulse to pulse intensity variation. In operation with xenon a typical total charge coming out

† valebedev@jinr.ru

ISBN: <ask the JACoW BoD> ISSN: <ask the JACoW BoD> doi: 10.18429/JACoW-HB2025-TUIBC03

# HADRON SOURCES AND LINACS ACTVITIES IN THE ACCELERATOR BEAM PHYSICS GROUP AT CERN

J. B. Lallement[†,1], A. Ajanovic[1,2], B. Bhaskar[1], G. Bellodi[1], S. Bertolo[1], F. Di Lorenzo[1], D. Küchler[1], A. M. Lombardi[1], A. Mamaras[1,3], C. Mastrostefano[1], M. O'Neil[1], E. Pasino[1], E. Sargsyan, M. Slupecki[1]
[1]CERN, Geneva, Switzerland
[2]University of Sarajevo, Sarajevo, Bosnia and Herzegovina
[3]Aristotle University of Thessaloniki, Thessaloniki, Greece



*Abstract*

This paper reviews various activities regarding primary particle production for the entire CERN accelerator complex, the Linac3 lead ion and Linac4 $H^-$ operation and studies possible future upgrades and consolidation of the injectors. Besides lead ions, Linac3 provides a variety of different ions for the LHC and fixed target experiments. The Linac4 $H^-$ source was recently improved with a new extraction system that allowed reliable routine operation with unprecedented beam current and quality. A spare RFQ will be commissioned in 2025 at a dedicated test stand where the critical low-energy beam dynamics will be studied with a dedicated diagnostics line. The expertise and competences gained over the past decades with the renovation of the CERN injectors have been applied to sources and linacs for societal and medical applications: a series of compact MeV range accelerators based on the frequency of 750 MHz have been built at CERN and in industry. They are used both at CERN and elsewhere for ion beam analysis and as a pre-injector for a linac-based hadron-therapy facility for protons or carbon ions.

## INTRODUCTION

The Hadron Sources and Linacs (HSL) section is part of the Accelerator and Beam Physics (ABP) group within the Beams Department at CERN. The team is responsible for the primary beam production across the entire accelerator complex. Composed of experts in source and linac physics, it oversees the installation, maintenance, and operation of the Linac3 and Linac4 ion sources, manages the operation of Linac3, plays a key role in supporting the Linac4 operation team, and leads all studies, projects, and upgrades related to hadron sources and linacs. There is a growing interest within the CERN physics community in accelerating different ion species through the accelerator complex, both for fixed-target and collider experiments. Presently, these experimental requests can only be fulfilled by Linac3 after developing requested beams. The operation of Linac4 has now reached a smooth and stable regime: the machine performs in line with beam dynamics models and meets the requirements of downstream accelerators. However, the low-energy front end has been identified as the main bottleneck to further increasing the peak current. As a result, studies of the ion source and low-energy section are being carried out in parallel with ongoing operations. The development and validation of beam dynamics tools and measurement techniques—especially during the Linac4 design and commissioning phases—together with the team's experience in machine optimization and upgrades, have had a visible and positive impact on the overall performance and reliability of the CERN complex. These assets also enable valuable knowledge transfer to societal and medical applications. Following the recent success of projects based on 750 MHz RFQ technology for hadron therapy and non-destructive material and surface analysis, several similar machines are now being designed, built, and commissioned, while maintaining the key features of simplicity, compactness, and cost-effectiveness.

## LINAC3: NOT ONLY LEAD

The construction of Linac3 began in the early 1990s and it was commissioned in 1994. It is a normal-conducting machine consisting of an ECR ion source capable of delivering a variety of ions at 2.5 keV/u, a Low Energy Beam Transport (LEBT) system with two spectrometer magnets, a 250 keV/u Radio Frequency Quadrupole (RFQ), and three Interdigital H-mode (IH) structures, accelerating beams up to 4.2 MeV/u. It is designed to accelerate ions with a mass-to-charge ratio of up to 8.3. As part of the LHC ion injector upgrade [1], a new ion source (GTS-LHC) and the Low Energy Ion Ring (LEIR) were developed to meet the required intensity and emittance. The GTS-LHC is an ECR-type ion source based on the Grenoble Test Source. It operates with a 50 ms, 14.5 GHz microwave pulse at 10 Hz, with up to 2.2 kW of power. The two micro-ovens can be operated independently, and a sample lock system allows oven maintenance without venting the source, resulting in only ~10 hours of downtime for oven refilling. A schematic of the source is shown in Fig. 1.

### *Ion Species Tests and Runs*

During physics runs, which typically span weeks to months, the source and linac deliver ion beams continuously (24/7). The source and machine setup time required for each ion species usually does not allow the production of more than two different species per year and development of new ion beams can only take place when no beam is requested by downstream machines or users. Over the past 10 years, a variety of ions of interest have been produced and delivered to different destinations. A summary is given in Table 1. This year, exceptionally, the oxygen run was immediately followed by a short neon run. Because

† jean-baptiste.lallement@cern.ch

ISBN: <ask the JACoW BoD> ISSN: <ask the JACoW BoD> doi: 10.18429/JACoW-HB2025-TUICC01

# FIRST BEAM THROUGH THE SUPERCONDUCTING LINAC OF ESS

S. Johannesson*, R. Miyamoto, N. Milas, I. Gorgisyan, M. Eshraqi,
D. Noll, E. Salehi, A. Gorzawski, European Spallation Source, Lund, Sweden



*Abstract*

The European Spallation Source in Lund, Sweden, is a facility under the final stages of its commissioning process, with the first user program planned in 2027. The 600 m long proton linac underwent beam commissioning in Spring 2025 with first beams through the superconducting part of the accelerator and to the tuning beam dump. This last commissioning run aimed to test all the critical linac components and establish their operations, as well as to establish a stable beam with the final energy larger than 800 MeV at a low beam intensity and short pulse length. These were achieved, and a low-power beam of 6 mA and 5 µs pulse length was successfully accelerated to 810 MeV. Basic tuning schemes, such as phase scans, for setting cavity amplitudes and phases, and beam steering, were also successfully tested. This paper will give an overview of the results from this commissioning phase and the challenges ahead for the initial operations.

## THE ESS LINAC

The European Spallation Source (ESS) is the fourth facility to be constructed following the OECD's 1998 call for new neutron sources, after the completion of the SNS in the United States, J-PARC in Japan, and CSNS in China. All three facilities have MW capabilities, but the design beam power of ESS will be the highest of the three [1]. The high-level parameters of the proton linac are summarized in Table 1. The linac is designed to produce neutrons through spallation with an average flux comparable to that of the continuous ILL source, while maintaining a low pulse repetition rate that enables the production of high-flux, low-energy neutrons.

A schematic overview of the high-power LINAC currently being built at ESS can be seen in Fig. 1. A 6 ms and 80 mA proton beam at 75 keV is produced in the Ion Source (ISrc) and is then focused by two solenoid magnets as well as reduced in length with a slow chopper in the Low Energy Beam Transport (LEBT) section. This is done in order to match the beam to the four-vane Radio-Frequency Quadrupole (RFQ), which is the first accelerating structure of the ESS LINAC, and also transversely focuses and introduces a longitudinal bunch structure of the beam. The 3.62 MeV bunched beam pulse is then focused, both transversely by quadrupoles and longitudinally by three buncher cavities in the Medium Energy Beam Transport (MEBT) section. The MEBT also includes an additional chopper to further clean the head and tail of the beam pulse, as well as collimators and beam diagnostics. The last part of the normal conducting LINAC (NCL) is the Drift Tube LINAC (DTL) section, comprised of five DTL tanks accelerating the beam up to 90 MeV. Transverse focusing of the beam is done by permanent quadrupole magnets placed in every other drift tube. Transverse correctors and beam diagnostics are housed in some of the empty drift tubes. [2]

Table 1: ESS High-Level Parameters for Production and Probe Beam Modes During BOD (Beam on Dump) Commissioning 2025

| Parameter | Unit | Beam Mode | |
|---|---|---|---|
| | | Production | Probe |
| Beam Power (probe) | MW | 2 | $2{\cdot}10^{-5}$ |
| Beam energy | GeV | 0.8 | 0.8 |
| Peak beam current | mA | 62.5 | 6 |
| Beam pulse length | µs | 2860 | 5 |
| Beam pulse rep. rate | Hz | 14 | 1 |
| Duty cycle | % | 4 | $5{\cdot}10^{-4}$ |
| RF frequency | MHz | 352.21/704.42 | |

Downstream of the DTL the accelerating structures are superconducting, and this part of the accelerator is referred to as the Superconducting LINAC (SCL). Three families of superconducting RF-cavities are used at ESS. The cavities are arranged in cryomodules with LINAC Warm units (LWUs) in between, each housing a quadrupole doublet and beam diagnostics. 26 Spoke-cavities (SPK) arranged two in each cryomodule, operating at 352.21 MHz, take the beam to 216 MeV. Both the 36 medium-$\beta$ cavities (MBL) and 84 high-$\beta$ cavities (HBL) are arranged four cavities in each cryomodule and operate at a frequency of 704.42 MHz, twice the SPK frequency. [3]

The medium-$\beta$ cavities accelerate the beam to 571 MeV, and the high-$\beta$ cavities take the beam to the final 2 GeV. Note that during the 2025 commissioning, only 5 cryomodules of HBL, meaning 20 cavities, were installed and operational, making the final design energy 877 MeV. In Fig. 1, each blue rectangle represents a functioning cryomodule and a grey rectangle represents cryomodules to be installed.

The final section, High Energy Beam Transport (HEBT), is a contingency space for future upgrades, currently housing quadrupole doublets and beam diagnostics. In this schematic figure, only the tuning beam dump is drawn, as this was the destination for the commissioning in 2025. During neutron production, two dipole magnets will steer the beam from HEBT to a tungsten target located at ground level, in contrast to the underground accelerator.

## GOALS OF COMMISSIONING 2025

The main objective of the 2025 commissioning campaign was to establish beam transport to the tuning beam dump. To achieve this, several key activities were carried out: beam

* sofia.johannesson@ess.eu

ISBN: <ask the JACoW BoD> ISSN: <ask the JACoW BoD> doi: 10.18429/JACoW-HB2025-TUICC04

# CURRENT STATUS AND UPGRADE PLANS OF THE KOMAC PROTON ACCELERATOR

S. Lee, S. H. Moon, H.-S. Kim, H.-J. Kwon
Korea Multipurpose Accelerator Complex, Korea Atomic Energy Research Institute, Gyeongju, Republic of Korea



*Abstract*

The Korea Multipurpose Accelerator Complex (KOMAC) has been operating a 100 MeV Proton Linear Accelerator (linac) since 2013, supporting various research and industrial applications by providing proton beams to users through four regularly used beam lines. In addition to these, a neutron beam line has completed pilot operations and is set to begin user services. In parallel, maintenance and replacement of aging equipment, including Radio Frequency Quadrupole and Drift Tubes, are underway. To enhance beam diagnostic techniques, we conducted beam physics studies using a Beam Test Stand for beam phase space distribution measurements and space charge compensation. An energy upgrade of the proton linear accelerator is also planned. The proposed upgrade of the 100 MeV proton lianc consists of the 200 MeV linac section, two beam lines and target rooms, building expansion, and utility upgrade. This paper discusses our recent progress and the upgrade plans for the KOMAC linac.

## INTRODUCTION

The Korea Multi-purpose Accelerator Complex (KOMAC) has been providing user beam services using a 100-MeV proton linac and several beamline facilities since the second half of 2013 [1-4]. The proton beam service covers various application and research fields, including material science, biomedical science, semiconductor technology, nuclear physics, and basic science. The 100 MeV linac consists of an injector based on a 50 keV microwave ion source [5,6] and a two-solenoid low-energy beam transport (LEBT) system, a 3 MeV four-vane-type radio-frequency quadrupole (RFQ), and a conventional drift tube linac (DTL), where the proton beam is accelerated from 3 MeV to 100 MeV. KOMAC layout is shown in Fig. 1. The main specifications of the 100 MeV linear proton accelerator are detailed in Table 1. As the operational period of the proton accelerator has exceeded a decade, we consider it an appropriate time to establish a long-term plan to address the aging of the accelerator. To replace the currently operating RFQ, which shows degradation in performance, we are designing a new RFQ with several modifications. For the DTL, we plan to replace the quadrupole magnets inside each drift tube from the electromagnet type to the permanent magnet type, as the electromagnets have shown issues in terms of long-term stability. To advance both device and utilization technologies, we have completed the construction of a new facility called the Beam Test Stand (BTS), which has a structure similar to the beam injection system (ion source, LEBT, and RFQ) of the 100 MeV linear accelerator. We plan to actively conduct beam physics and accelerator research using this facility. Furthermore, we are planning to upgrade the proton linac to 1 GeV for spallation neutron source applications as a long-term goal. In the short term, we are taking a phased approach, with the first phase focusing on an energy upgrade to 200 MeV.

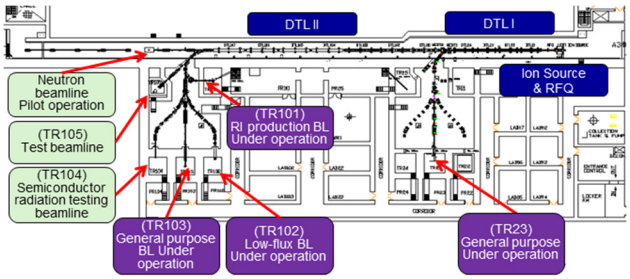


Figure 1: Layout of KOMAC proton accelerator.

Table 1: Main Specifications of 100 MeV Proton Linac at KOMAC

| Parameters | | Specification |
|---|---|---|
| Output energy [MeV] | 20 | 100 |
| Max. peak current [mA] | 20 | 20 |
| Max. beam duty factor % | 24 | 8 |
| Avg. beam current [mA] | 4.8 | 1.6 |
| Beam pulse length [ms] | 2.0 | 1.33 |
| Max. repetition rate [Hz] | 120 | 60 |
| Avg. beam power [kW] | 96 | 160 |
| RF frequeny [MHz] | 350 | 350 |
| No. of beamlines | 1 | 5 |

## AGING MANAGEMENT OF ACCELERATOR OPERATION

The total operational hours have amounted to 36,161 by the end of 2024, more than a decade after its pilot service in mid-2013. Continued enhancements in the accelerator's operational framework and proactive maintenance have increased its operational rate from 82.0% in 2013 to 95.8% in 2024. Recently, improvements to the ion source system—traditionally compromised by high-voltage discharges and insulation breakdowns—along with securing spare parts, have significantly curtailed unplanned downtimes that previously restricted user services.

As the official operational period of the proton accelerator surpasses a decade, with some components like the RFQ extending beyond 20 years of post-development use,

ISBN: <ask the JACoW BoD> ISSN: <ask the JACoW BoD> doi: 10.18429/JACoW-HB2025-TUIDC01

# CERN PROTON SYNCHROTRON BOOSTER HIGH-INTENSITY OPERATION

M. Marchi*[1], S. Albright, C. Antuono, F. Asvesta, C. Bracco, G. P. Di Giovanni, M. A. Fraser, T. Prebibaj, P. Skowronski, C. Zannini
CERN, Geneva, Switzerland
[1]also at Dipartimento di Fisica, Università di Roma La Sapienza, Rome, Italy

*Abstract*

The CERN Proton Synchrotron Booster (PSB) produces a wide variety of high-intensity and high-brightness beams for the fixed target experiments and the Large Hadron Collider (LHC). As part of the LHC Injectors Upgrade (LIU) project, many upgrades were made to the accelerator, including a new injector, Linac4, charge-exchange injection, increased injection and extraction energies and a new RF systems. With the approval of the Search for Hidden Particles (SHiP) facility, a new era of PSB operation approaches which will require higher intensities to ensure the requirements of existing facilities will still be met. This contribution discusses optimisations that have been implemented for present and upcoming operational beams, as well as longer term studies to probe the ultimate performance limit of the accelerator.



## INTRODUCTION

The Proton Synchrotron Booster (PSB) at CERN is the first synchrotron in the Large Hadron Collider (LHC) injector chain. During Long Shutdown 2 (LS2, from 2019 to 2021), as part of the LHC Injectors Upgrade (LIU) project, the PSB underwent a comprehensive upgrade [1]. LIU objective was to double the intensity and to increase the brightness of nominal LHC beams by a factor of ≈ 2, to meet the specifications for the High-Luminosity LHC (HL-LHC). These targets were successfully reached in the PSB.

A core element of the upgrade was the replacement of Linac2 by Linac4 (L4), raising the injection energy from 50 MeV protons to 160 MeV $H^-$ ions [2]. The higher injection energy mitigates space charge effects at low energy. The switch to $H^-$ also required a new charge-exchange injection system in the PSB, a key step for efficient accumulation of high-intensity beams.

Beyond injection, the PSB was extensively improved to the increased performance: the entire injection region was rebuilt, new power converters and Finemet RF systems were installed, and the transfer lines to the Proton Synchrotron were adapted to the upgraded beam parameters. Particular emphasis was placed on reliability and operational flexibility, ensuring that the upgraded PSB can deliver a large variety of beam types across the CERN complex.

With the completion of LS2, the PSB successfully restarted in 2021 with beams from Linac4, marking a major milestone for LIU, enabling the higher-brightness beams required for the HL-LHC, and reaffirming the PSB's role as a versatile and indispensable workhorse of CERN's accelerator chain.

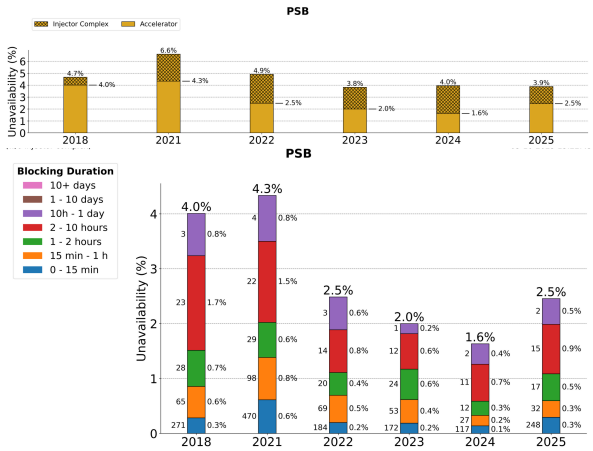


Figure 1: PSB yearly availability since 2018. Data from 2025 is updated until the end of September.

## PSB MACHINE STATUS

PSB reliability and efficiency are crucial for the entire CERN accelerator chain, as any interruption at this early stage propagates downstream to all users, including the LHC. To monitor and assess performance systematically, the availability of the PSB is tracked using the Accelerator Fault Tracking (AFT) system [3]. Specifically, AFT provides a centralised platform to record, categorise, and analyse faults affecting accelerator equipment and operation. Each incident that causes a partial or total interruption of beam delivery is logged with its cause, duration, and the systems involved. This structured reporting allows operators and equipment groups to identify recurring issues, assess the effectiveness of corrective actions, and prioritise future improvements. The availability is expressed as the fraction of scheduled operational time during which the facility is able to deliver beam to its users.

During the run after LS2 (Run3), PSB availability has been closely monitored to verify that the new systems meet expectations. The AFT data, illustrated in Fig. 1, shows that, despite the complexity of the new injection scheme and the extensive hardware interventions, the upgraded PSB achieved an excellent level of operational reliability, comparable to or exceeding pre-LS2 values. A collection of the

* mariangela.marchi@cern.ch

ISBN: <ask the JACoW BoD> ISSN: <ask the JACoW BoD> doi: 10.18429/JACoW-HB2025-TUIDC05

# BEAM LOADING IN THE SUPERCONDUCTING CAVITIES AT THE EUROPEAN SPALLATION SOURCE LINAC

Emanuele Laface*, Paolo Pierini, European Spallation Source ERIC, Lund
Francesco Grespan, INFN/LNL, Legnaro, Italy

*Abstract*

During the commissioning of the ESS LINAC in early summer 2025, we recorded beam-loading transients from a 5 µs, 5 mA beam in 47 superconducting cavities: 26 Spoke and 21 Elliptical Medium Beta. We compare the beam-induced cavity voltage and current phasors with a standard beam-loaded cavity model that includes coupling, loaded $Q$, and detuning, thereby validating model parameters across the installed sections. Leveraging this agreement, we invert the measured response to compute the beam's synchronous phase on a cavity-by-cavity basis without external timing references. The inferred phase is then used to set the optimal accelerating phase and to quantify residual phase errors and detuning during routine operation. We report sensitivity to measurement noise, pulse-to-pulse reproducibility, and the robustness of the method over the commissioning dataset, and we outline a practical procedure to commission and periodically retune SRF sections at ESS using beam-loading observables alone.

## INTRODUCTION

The superconducting linac of ESS is composed of three families of superconducting cavities [1].

The first family consists of double-spoke cavities with an optimum $\beta$ value of 0.5. There are two such cavities per cryomodule across 13 cryomodules, for a total of 26 double-spoke cavities. They use classical tetrode amplifiers at 352.21 MHz, with two tubes providing 400 kW to each cavity.

These are followed by two families of elliptical cavities with geometrical $\beta$ values of 0.67 and 0.86, referred to as medium-$\beta$ and high-$\beta$ cavities, respectively. The medium-$\beta$ cavities have six cells, while the high-$\beta$ ones have five cells. Because of this, they have almost identical lengths, and the cryomodules—housing four cavities—can be of very similar design for the two types. The medium-$\beta$ section of the linac has 9 cryomodules (36 cavities), while the high-$\beta$ section has 84 cavities in 21 cryomodules; during this commissioning phase, however, only 2 cryomodules (for a total of 8 high-$\beta$ cavities) were installed.

The elliptical cavities operate at 704.42 MHz, which is twice the frequency of the preceding structures. Klystrons with a pulsed power of 1.5 MW feed the medium-$\beta$ cavities. Each cavity is powered by one klystron, while one modulator feeds four klystrons. The 660 kVA modulators use a stacked multi-layer topology to maximize performance and reliability while minimizing the floorspace required in the klystron gallery.

* emanuele.laface@ess.eu

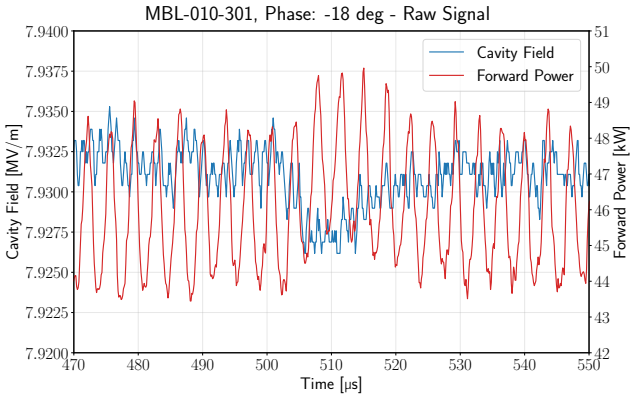


Figure 1: Footprint of the beam passage in the cavity in the raw signal.

Each cavity is equipped with 4 pk-probes to measure the power amplitude and the phase. For these studies we specifically used the forward power and the cavity field, i.e., the transmitted power calibrated to return the field expressed in MV/m. A description of a typical RF system for superconducting cavities is given in [2], while the specific setup used at ESS is described in [3].

In order to accelerate the beam to the design energy, the cavity phases must be set to the values obtained from TraceWin simulations [4] and then optimized during operations.

The current technique consists of scanning the cavity phase over 360° and evaluating the beam time of flight between two BPMs downstream of the cavity, as described in [5]. This process is time-consuming and can be error-prone due to the need to calibrate the BPMs for nanosecond-level measurements.

During the ESS LINAC commissioning in early summer 2025, we observed that the energy exchange between the superconducting cavity and the beam is visible in the pk signal of the cavity field probe (see Fig. 1), opening the possibility of exploiting the beam-loading signal to determine the phase that maximizes acceleration.

## THEORY

We analyze the cavity-voltage phasor under beam loading using the description of P. B. Wilson [6]. We denote by $\theta$ the generator-current phase, by $\psi$ the detuning phase, and by $\phi$ the phase of the cavity voltage with respect to the beam current. To clarify the approach, we separate "steady-state" phasors from transient phasors. Transient phasors have an exponentially varying magnitude as $e^{-\frac{t_{pulse}}{\tau}}$ and a rotating phase as $e^{j\tan(\psi)\frac{t_{pulse}}{\tau}}$; viewed on the complex plane as a

ISBN: <ask the JACoW BoD> ISSN: <ask the JACoW BoD> doi: 10.18429/JACoW-HB2025-TUCDB01

# THE ANTHEM PROJECT: DESIGN AND CONTRUCTION OF A RFQ DRIVEN NEUTRON SOURCE FOR BNCT

F. Grespan, L. Antoniazzi, C. Baltador, L. Bellan, A. Bianchi, D. Bortolato, M. Comunian, V. Conte, J. Esposito, L. Ferrari, E. Fagotti, M. Giacchini, M. Montis, Y.K. Ong, A. Palmieri, A. Selva, A. Pisent, INFN/LNL, Legnaro, Italy
P. Mereu, C. Mingioni, M. Nenni, E. Nicoletti, INFN sezione di Torino, Torino, Italy
A. Passarelli, L. Gialanella, INFN sezione di Napoli, Napoli, Italy
V. Vercesi, S. Bortolussi, S. Fatemi, I. Postuma INFN sezione di Pavia, Pavia, Italy

*Abstract*

The project Anthem, funded within the Next Generation EU initiatives, includes the realization of an accelerator based BNCT (Boron Neutron Capture Therapy) facility at Caserta, Italy. The INFN (LNL, Pavia, Napoli, Torino) has in charge the design and construction of the epithermal neutron source, that will assure a flux of $10^9$ n/(s cm$^2$) with characteristics suited for deep tumours treatment. The proton accelerator for ANTHEM BNCT project is based on a single accelerator stage which is a CW Radio Frequency Quadrupole (RFQ), able to produce proton beam of 30 mA at 5 MeV. The protons will collide to a Beryllium target to produce neutrons. The target is designed following a three-layered concept. The transport line (MEBT) between RFQ and target has been optimized to guarantee uniform footprint of the beam on the target and make possible the dissipation of 1kW/cm$^2$ power density. In the paper an overview of the scientific challenges and the project status will be given.

## INTRODUCTION

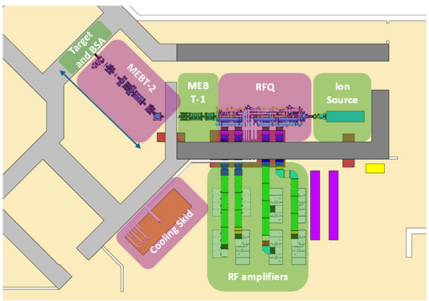


Figure 1: Layout of the ANTHEM BNCT facility.

A new building will host the ANTHEM-BNCT facility in Caserta. The map of the installation is shown in Fig. 1. The design here presented has some differences in the MEBT with respect to [1]. Nonetheless, the key points are confirmed and listed in Table 1. The core of the accelerator is the CW-RFQ cavity, which will bring 30 mA of H+ from 80 keV up to 5 MeV. The RFQ is powered by 8 solid state amplifiers (SSPA) via 8 power couplers, each one delivering 125 kW. The development of RFQ, SSPAs and ion source (ISRC) started in the last years at INFN LNL and INFN LNS in the TRASCO and MUNES [2-4] projects and are now being completed. A two-branches dispersive MEBT line transports and manipulates 150-kW proton beam to the target. The beam will collide perpendicularly to the target, conceived following a three-layered (Be-Pd-Cu) concept. The total length is 25 m. A preliminary BSA design and the operational data from similar facilities [5, 6] show that the required epithermal neutron flux can be achieved with beam currents 2-to-5 times lower than the design value. If confirmed, pulsed operation of the ANTHEM linac will then be possible.

Table 1: ANTHEM Accelerator Parameters

| Parameter | Value | Notes |
|---|---|---|
| Ion source | MDIS | H+, 80 kV |
| Accelerator type | RFQ | 352.2 MHz, 7.13 m |
| Output energy | 5 MeV | |
| Beam current | 30 mA | accelerated |
| Duty cycle | 100 % | Lower DC possible |
| p-n Converter | Beryllium | 150 kW, 1kW/cm$^2$ |
| Neutron yield | ~$10^{14}$ s$^{-1}$ | ave. energy 1.2MeV (4π) |
| Neutron flux | ~$10^9$ s$^{-1}$cm$^{-2}$ | Epithermal @ BNCT port |
| RF power | 1.0 MW | $(P_{Cu} + P_{Beam}) \cdot 1.3$ |
| Installed Power | ~3.5 MVA | |
| Total length | 25 m | ISRC extraction to target |

## THE ACCELERATOR

The choice of a single stage acceleration simplifies the operational aspects of the facility, increases the reliability, decreases the time for accelerator setup and recovery. The RFQ with internal bunching does not requires any phase synchronization with up-stream/down-stream structures, and it relaxes the requirements in terms of frequency lock in operation. The trigger for pulsed operation in commissioning or operation will be distributed by LLRF to all the devices. Beam commissioning shall maximize transmission and get the correct beam footprint at the target. For these purposes we will have 3 ACCTs and 2 pair of slit-and-grids in the diagnostic boxes of the line. Beam commissioning will be done at 5 MeV with max 35 mA-40 μs-1 Hz, obtained from < 3 ms pulse from ISRC, to be cut by RFQ RF pulse. In commissioning, the target will be replaced by a copper beam stop. The details and status of the components are described in the next paragraphs.

ISBN: <ask the JACoW BoD> ISSN: <ask the JACoW BoD> doi: 10.18429/JACoW-HB2025-TUCDB02

# ALTERNATIVE DESIGN FOR THE IFMIF-DONES SUPERCONDUCTING HALF-WAVE RESONATOR

M. D'Andrea†, L. Bellan, A. Facco, F. Grespan, A. Pisent, INFN-LNL, Legnaro, Italy

*Abstract*

The IFMIF-DONES facility will irradiate and characterize materials to be used in fusion reactors using a neutron flux produced by the interaction of a deuteron beam with a liquid lithium target. A superconducting radiofrequency linear accelerator will bring the deuteron beam to the final energy of 40 MeV through a series of superconducting half-wave resonators operating at 175 MHz. A prototype cavity for the final acceleration stage (optimized for $\beta$ = 0.18) was designed, fabricated and tested at CEA. Taking this prototype as a starting point, an alternative design of the internal geometry of the cavity was developed at LNL to optimize it from the point of view of production, while maintaining its performance as close as possible to what was observed at CEA. This contribution describes the results achieved in the simulation campaign that led to the definition of this alternative design, the evaluation of its electromagnetic properties and the study of multipacting effects.

## INTRODUCTION

The International Fusion Materials Irradiation Facility – DEMO Oriented Neutron Source (IFMIF-DONES) [1-3] is a crucial part of the European roadmap to fusion-generated electricity. This facility, currently under construction in Granada (Spain), will serve as a fusion-like source for the assessment of material damage in conditions comparable to those of the first wall of the DEMO fusion reactor. A neutron flux of $10^{18}$ $cm^{-2}s^{-1}$ is produced by the interaction of a deuteron beam of unprecedented intensity with a liquid lithium target. A complex accelerator system was designed to achieve the required deuteron beam parameters of 40 MeV energy and 125 mA CW current (for a total power of 5 MW) [3,4]. A superconducting radiofrequency (SRF) linac, shown in Fig. 1, brings the deuteron beam to the final energy through 46 superconducting half-wave resonators. The cavities are divided into two sets optimized for different deuteron velocities: the first set includes the first 19 cavities, which are housed in the first two cryomodules and are optimized for $\beta$ = 0.115 (thus they are called "low-$\beta$ cavities"), while the second set includes the remaining 27 cavities, which are housed in the final three cryomodules and are optimized for $\beta$ = 0.18 (thus they are called "high-$\beta$ cavities"). All resonators are made of Nb and operate at the frequency of 175 MHz.

The design and qualification of the low-$\beta$ cavities were carried out in the Engineering Validation and Engineering Design Activities (IFMIF/EVEDA) framework [5]. A prototype resonator for the high-$\beta$ cavities was designed, fabricated and tested by the French Alternative Energies and Atomic Energy Commission (CEA) [6]. An alternative design was developed at the Legnaro National Laboratories (LNL) using the CEA prototype as a starting point.

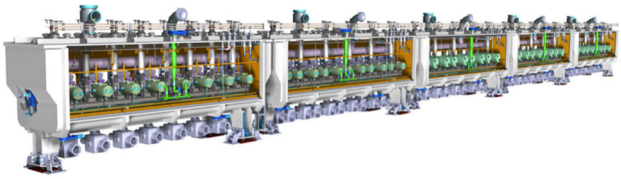

Figure 1: Model of the IFMIF-DONES SRF linac [3].

## CAVITY DESIGN AND ELECTROMAGNETIC PROPERTIES

The definition of this alternative design was motivated by the goal of simplifying the manufacturing of the internal conductor. The general geometry of the LNL design is very similar to that of the CEA prototype, i.e., a cylindrical half-wave resonator (HWR) with toroidal endcaps. The main difference between the two designs is the shape of the inner conductor. The CEA prototype features an oval shape around the beam drift, which needed to be machined out of a solid Nb block [6]. On the other hand, in the LNL design the inner conductor is instead shaped like a cylinder flattened on the sides where the beam drift openings are located (similarly to the cavities developed for FRIB [7,8]) and can be manufactured from a Nb sheet. This design was modelled with CST Studio Suite [9] and is shown in Fig. 2. The dimensions of the cavity needed to be adjusted with respect to the CEA prototype, to recover the resonating frequency of 175 MHz and the optimal $\beta$ of 0.18. As a result, the height of the cavity was increased by about 60 mm, while the accelerating gap was increased by about 0.15 mm. Additionally, the maximum radius of the inner conductor was increased by 20 mm to keep the peak magnetic field under control.

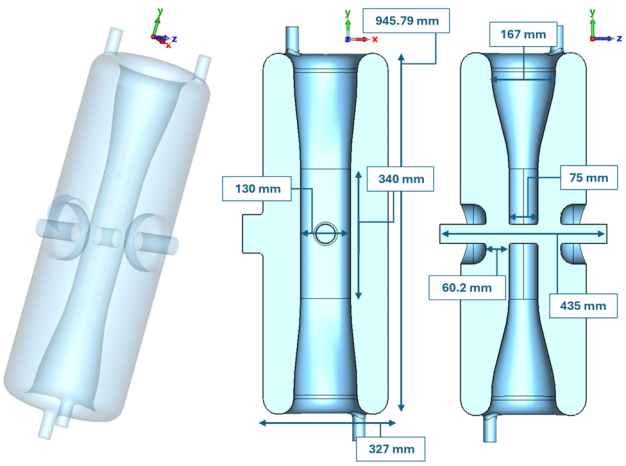


Figure 2: 3D model of the LNL design with section views. The relevant dimensions are shown.

† marco.dandrea@lnl.infn.it

ISBN: <ask the JACoW BoD> ISSN: <ask the JACoW BoD> doi: 10.18429/JACoW-HB2025-TUCDB04

# RESEARCH AND DEVELOPMENT OF THE TIMING SYSTEM FOR CSNS-II ACCELERATOR

Peng Zhu *[1,2,3], Sinong Cheng[2,3], Wei Long[2,3], Yuliang Zhang[2,3], Ge Lei[2,4], Gongfa Liu[1], Mingyang Huang[2,3,4], Xiaohan Lu[2,3,4]

[1] NSRL, University of Science and Technology of China, Hefei, China
[2] Institute of High Energy Physics, Chinese Academy of Sciences, Beijing, China
[3] Spallation Neutron Source Science Center, Dongguan, China
[4] University of the Chinese Academy of Sciences, Beijing, China

*Abstract*

A novel event-based timing system has been developed for CSNS-II, utilizing the MicroTCA.4 hardware architecture and Zynq System-on-Chip technology. This system coordinates beam processes and protection systems throughout the entire accelerator complex and beamlines. The design facilitates precise generation and distribution of timing signals while integrating control logic, communication protocol stacks, and Input/Output Controller functionality within a single platform. By merging programmable logic with embedded processing cores, the system achieves a high degree of hardware-software co-design, enhancing both flexibility and real-time performance. This paper presents a significant advancement in accelerator timing system design and marks a new direction in the evolution of hardware platforms for large-scale scientific facilities.

## INTRODUCTION

The China Spallation Neutron Source (CSNS) is China's first and the world's fourth pulsed spallation neutron source. Officially completed and opened for user operation in September 2018 [1,2]. To meet the escalating demand from the user community and to enhance China's international competitiveness in neutron science, the CSNS-II project has been officially launched. The primary objectives of CSNS-II are to increase the proton beam power from 100 kW to 500 kW and to construct and upgrade multiple neutron spectrometers, as shown in Figure 1. The primary function of the timing system is to deliver precisely synchronized trigger signals to various subsystems within the facility including the linear accelerator (LINAC) and rapid cycling synchrotron (RCS), ensuring their coordinated and orderly operation. Figure 2 illustrates the schematic of the LINAC beam delivering to three different accelerators.

## REQUIREMENTS OF THE TIMING FOR ACCELERATOR

Due to differences in operational principles, each subsystem exhibits a distinct time delay between receiving a trigger signal and initiating its actual response. To compensate for these inherent delays, the timing system applies calibrated timing offsets to the trigger signals, thereby aligning the

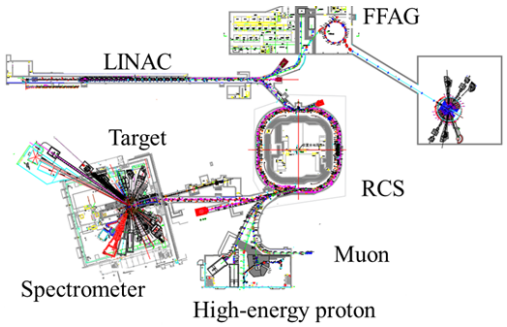


Figure 1: Schematic layout of the CSNS-II and FFAG (envisioned facility).

effective operation times of all subsystems as required [3]. To ensure long-term stability and reliable operation, Table 1 summarizes the key design specifications of the CSNS-II timing system. Meanwhile, to improve beam delivery efficiency, the faulty beamline can be isolated at the ion source upon failure, ensuring uninterrupted beam supply to the other accelerators, as depicted in Figure 3.

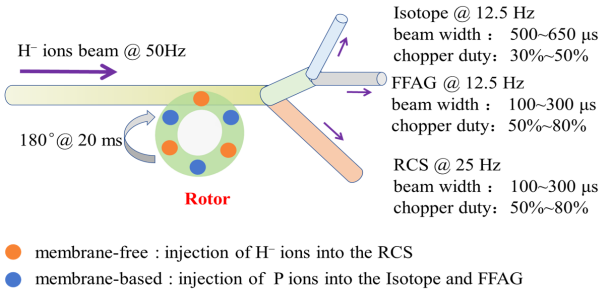


Figure 2: Schematic of the LINAC beam delivering to three different accelerators.

## DESIGN AND DEVELOPMENT

### *Overall Layout and Architecture Design*

Figure 4 illustrates the overall layout of the CSNS-II timing system. Distributed timing technologies, particularly Event Timing and White Rabbit (WR), are widely employed in large-scale particle accelerator facilities [4,5]. Event Timing, being more mature and extensively applied than WR, will be retained in the current system to ensure compatibility

* zhup@ihep.ac.cn

ISBN: <ask the JACoW BoD> ISSN: <ask the JACoW BoD> doi: 10.18429/JACoW-HB2025-WEIAB01

# THREE YEARS OF SPIRAL2 SC LINAC OPERATION AT GANIL: CHALLENGES AND FUTUR

A. K. Orduz*, J-M. Lagniel, A. Leduc, G. Normand
Grand Accélérateur National d'Ions Lourds (GANIL), Caen, France

*Abstract*

GANIL (Grand Accélérateur National d'Ions Lourds) started the operation of the SPIRAL2 superconducting linac in 2022. Experiments in the Neutron For Science (NFS) room, specific beam dynamics studies, and various technical improvements were carried out during its operation in the second half of each year, after the run of the cyclotrons in the first half. In 2024, a first period of operation with both linac and cyclotrons was successfully performed. So far, most experiments in the NFS room have been performed using $D^+$ beams, and in some cases with $^4He^{2+}$ and $H^+$, at energies ranging from 0.75 to 33 MeV/A. Linac tunings with $^{18}O^{6+}$ and $^{40}Ar^{14+}$ ion beams, at energies between 5 and 14.5 MeV/A, were also carried out. Furthermore, the first Super Separator Spectrometer ($S^3$) experimental room milestone was reached, with the successful delivery of a $^{40}Ar^{14+}$ beam up to the first target station.

This paper presents a summary of the beam time sharing during the first three years of operation, preliminary results of beam dynamics studies, and the future plans of GANIL.

## INTRODUCTION

The Grand Accélérateur National d'Ions Lourds (GANIL) is operating since 1983, initially with a cyclotron-based facility and several experimental rooms dedicated mainly to fundamental nuclear physics research but also for atomic and condensed matter physics, radiobiology and industrial applications. In 2022, the SPIRAL2 superconducting linear accelerator became fully operational, significantly expanding GANIL's capabilities by providing high-intensity pulsed or CW beams to the user community.

During the SC linac commissioning conducted between 2019 and 2021, nominal energy acceleration was successfully demonstrated for $H^+$, $D^+$, and $^4He^{2+}$ beams. Afterwards, those beams were transported to the NFS experimental room, where they served for initial validations and pilot experiments [1]. Since 2022, SPIRAL2 is operating in the second part of the year, providing beams not only for physics experiments - predominantly at NFS - but also for dedicated studies of beam dynamics, diagnostics, and other accelerator subsystems. In this context, particular emphasis has been placed on heavy-ion tuning for the Super Separator Spectrometer ($S^3$) commissioning and on linac operation strategies in scenarios involving cavity failures [2].

This article is divided in three sections to present the results of SPIRAL2 operation. Section 1 gives a summary of the first three years of operation and reports the first $S^3$ milestone. Section 2 discusses the preliminary results of a cavity failure compensation study and the pressure fluctuations observed in the warm sections of the linac when accelerating heavy-ion beams. Finally, in section 3, the ongoing projects at GANIL are discussed.

## THREE YEARS OF SPIRAL2 OPERATION

During its three years of operation, SPIRAL2 has been in service for approximately three months per year, typically from late August to early December. The beam availability (beam time for physics, machine studies and beam in standby) in 2022 and 2024 was above 72 %, but only 65 % in 2023 due to some issues with the linac reference phase and damage to the NFS rotary converter (Fig. 1) [2, 3].

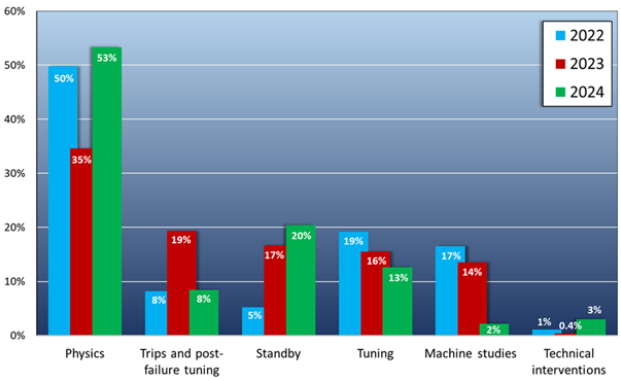


Figure 1: SPIRAL2 beam time sharing from 2022 to 2024.

During three years of operation, nineteen physics experiments and seven beam dynamics studies were successfully conducted. $H^+$, $D^+$, and $^4He^{2+}$ beams were accelerated from 0.75 MeV/A up to their nominal energies. More than 80 % of the physics program at the NFS experimental hall was carried out with $D^+$ beams, delivered intensities between 9 µA to 47 µA on target, using the Single-Bunch Selector (SBS) operating at 1 bunch/100. In parallel, the first test within the REPARE project was conducted, aiming at *R&D* into the production of innovative radioelements and, in particular, the accurate measurement of $^{211}$At yields [4]. In addition to physics experiments, dedicated beam time was allocated to RF studies, diagnostics developments, and beam dynamics investigations.

Two main methods have been developed and implemented to tune the linac [5]. The "advanced method" tunes the voltage and phase of each cavity using an improved phase-scan method to limit errors in phase measurement [6]. The "with reference method" uses the cavity phase and voltage obtained during a "reference tuning" to find the new parameters using the phase measured on the BPM located just before the

* angie.orduz@ganil.fr

ISBN: <ask the JACoW BoD> ISSN: <ask the JACoW BoD> doi: 10.18429/JACoW-HB2025-WEIAC03

# HIGH POWER BEAM IMAGING FOR MACHINE PROTECTION

C.A. Thomas*, H. Kocevar, R. Kuriakose,
M. Mohammednezhad, K. Rosengren[1], A. Takibayev, ESS ERIC, Lund, Sweden
E. Adli, H. Gjersdal[2], K. Sjobak, University of Oslo, Oslo, Norway
E. Hansen, Centre for Mathematical Sciences, Lund University, Sweden
[1] also at Advenica, Malmo, Sweden
[2] also at Inventas, Oslo, Norway



*Abstract*

Optical imaging systems have been designed and installed upstream of the European Spallation Source (ESS) tuning dump (TD) and the ESS spallation target to provide machine protection and beam tuning support functionality. The ESS accelerator delivers a high-power, low-emittance proton beam that must be carefully controlled. In the TD, the optical imaging systems remotely view the beam profile using light from a luminescent chromia alumina ceramic screen. The images of the beam 2D profiles are processed in real-time to detect any potential beam properties that can lead to machine component damage. This paper reports on the commissioning of the imaging instrument during the ESS linac commissioning period. Studies of the system show its performance, assuring robust protection. The system sensitivity allows detection of the very first beam on TD, and an appropriate chosen light attenuation system permits operation over 7 orders of magnitude, mapping the TD beam pulses from 5 µs (1 mA) to 3 ms (65 mA).

## INTRODUCTION

High-power accelerators such as the European Spallation Source (ESS) operate with intense proton beams that can damage intercepting components if not properly controlled [1]. Materials interacting with the beam can undergo melting or high thermal stress, leading to fatigue and mechanical failure. Ensuring reliable protection of accelerator components therefore requires accurate monitoring of beam properties, particularly the transverse size and peak current. While current monitors safeguard against over-current conditions, complementary imaging diagnostics are essential to measure the beam profile and trigger interlocks when errant conditions arise [2].

To address this challenge, dedicated optical imaging systems have been developed at ESS upstream of both the TD and the spallation target [3]. These instruments rely on luminescent screens coupled with high-performance optics and cameras, with real-time image processing implemented in FPGA-based hardware. This setup provides both machine protection and operational support, enabling detection of hazardous beam conditions within microseconds while offering valuable diagnostic information during commissioning and tuning.

* cyrille.thomas@ess.eu

This paper reports on the design, commissioning, and performance of the ESS imaging system for the TD. We describe its architecture, optics, and detector characteristics, and the implemented machine protection function. Experimental results from linac commissioning are presented, highlighting the system's sensitivity, dynamic range, and robustness in ensuring safe operation under a wide range of beam conditions.

## BEAM DAMAGE

Damage to components intercepting the beam occurs when the energy deposition raises the temperature above the material stress limit. Depending on the maximum temperature reached, the material can be subjected to melting or high thermal-stress leading to fatigue. The local material temperature induced during the passage of a proton pulse in a material slice can be expressed as:

$$\Delta T = \frac{\Delta P}{\rho C_p}\delta t, \tag{1}$$

where $\Delta P = \rho \delta E_z J_b$ represents the beam-induced power density, with $\rho$ the material density, $\delta E_z$ being the material stopping power and $J_b$ the local beam current density; $C_p$ is the material specific heat capacity; $\delta t$ is the pulse duration.

The maximum temperature can be used to evaluate the local potential damage to a material. For instance, one can look at two examples: the ESS tuning dump (TD), which is made essentially of copper, and the luminescent screen in front of the TD, which is chromia alumina. Both components present a flat surface orthogonal to the beam. The proton beam pulses traversing the screen and the TD have a 2D-Gaussian distribution, so the maximum beam current density is expressed as:

$$J_b = \frac{I_b}{2\pi\sigma_x\sigma_y}, \tag{2}$$

with $I_b$ the peak current, $\sigma_{x,y}$ the transverse rms beam size in the horizontal and vertical axes respectively.

The material stopping power can be accurately calculated with the Bethe formula. However, it can be retrieved from NIST PSTAR [4], or by using codes such as SRIM [5] or MCNP [6]. It is dependent on the material, but also on proton energy. Table 1 shows the stopping power and maximum heat using Eq. 1 normalised to the beam parameters: $\sigma_x\sigma_y$ =1 cm$^2$, $I_b$ =1 mA, and $\delta t$ =1 s. The nominal ESS beam on TD is 3.75 cm$^2$, 62.5 mA and 2.86 ms, which corresponds to a multiplication factor of 0.047 to the temperature

ISBN: <ask the JACoW BoD> ISSN: <ask the JACoW BoD> doi: 10.18429/JACoW-HB2025-WEIAC04

# SUPER-RESOLUTION RECONSTRUCTION ALGORITHM APPLIED TO THE RECONSTRUCTION OF ELECTRON BEAM TRANSVERSE PHASE SPACE BASED ON THE SCANNING SLIT METHOD

H. Hu*, B. Zhou*, Y. Xia, D. Lu, Y. Zeng, Y. Wang, K. Liu, T. Hu†
Huazhong University of Science and Technology, Wuhan, China

*Abstract*

Electron beam injectors, critical to advanced light sources and ultrafast diffraction systems, require precise transverse phase space diagnostics to optimize beam quality. Conventional slit-scanning combined with computed tomography (CT) enables non-presumptive phase space reconstruction but faces resolution limitations under sparse sampling. This study introduces a deep learning framework to achieve super-resolution reconstruction from minimal scan data. By integrating beam transport physics with neural networks, the method overcomes resolution degradation in low-data regimes. The proposed algorithm, coupled with beam dynamics simulations, forms a systematic engineering solution for high-fidelity diagnostics. This approach enhances phase space characterization efficiency, supporting accelerator commissioning with reduced experimental overhead.

## INTRODUCTION

Accurate transverse phase space diagnostics are essential for optimizing beam quality in electron beam injectors, which are critical components of advanced light sources and ultrafast electron diffraction systems. The slit-scanning method combined with computed tomography [1,2] (CT) enables non-presumptive phase space reconstruction, allowing full distribution characterization without assuming a prior beam model. However, achieving high resolution requires dense angular sampling, which increases measurement time and demands high mechanical and beam stability.

In practical commissioning and tuning, constraints on beam time and stability often force operation in sparse sampling regimes, leading to severe resolution degradation in conventional algebraic reconstruction techniques. This limits the ability to resolve fine phase space features and accurately determine beam parameters such as emittance, thus impacting both diagnostic reliability and accelerator optimization efficiency.

To overcome these limitations, we propose a physics-informed deep learning framework [3] for super-resolution [4] phase space reconstruction from minimal slit-scan data. Trained on synthetic datasets from beam dynamics simulations, the network learns to recover high-frequency details lost in undersampled measurements while ensuring physical consistency. Numerical studies on a low-energy injector test platform demonstrate significant resolution gains and robustness over traditional methods, offering a promising approach for efficient, high-fidelity beam diagnostics.

## PRINCIPLE OF SLIT-SCANNING PHASE SPACE MEASUREMENT

### *Principle*

As defined in Eq. (1), the transverse geometric emittance characterizes the phase space area of an electron bunch. However, in practical measurements the particle angles cannot be directly accessed. Instead, the slit-scanning method is commonly employed as an indirect diagnostic of beam emittance [5].

$$\varepsilon \equiv \sqrt{\langle x^2\rangle\langle x'^2\rangle - \langle xx'\rangle^2}. \tag{1}$$

The principle of this method is illustrated in Fig. 1. A typical slit-scan system consists of a transversely movable slit, a downstream fluorescent screen, and a drift section in between. By sampling the beam with a sufficiently narrow slit, a fraction of the bunch is transmitted through and subsequently drifts to the screen. The transverse position of the transmitted beamlet on the screen, together with the drift length, allows the reconstruction of its divergence angle. Repeating this process while incrementally shifting the slit provides a series of beamlets with measured positions and divergences [6]. From these scanning data, the transverse geometric emittance of the main bunch can be approximated. The statistic in Eq. (1) can be derived from Eqs. (2)-(4) [7].

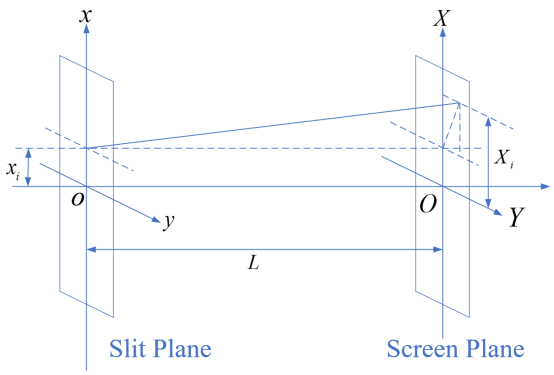


Figure 1: Principle of Slit-Scanning Phase Space Measurement

$$\langle x^2\rangle = \frac{1}{N}\sum_{i=1}^{N}(x_i - \bar{x})^2 \tag{2}$$

* equal contribution
† TongningHu@hust.edu.cn

ISBN: <ask the JACoW BoD> ISSN: <ask the JACoW BoD> doi: 10.18429/JACoW-HB2025-WEIBB01

# OPERATIONAL EXPERIENCE DURING COMMISSIONING OF ESS

A. Gorzawski*, E. O'Brien[1], M. Munoz, Y. Levinnsen,
European Spallation Source ERIC, Lund, Sweden
[1]also at the LTH, Lund, Sweden

*Abstract*

The European Spallation Source (ESS) is a neutron research facility based in Lund, Sweden. Its linear accelerator will operate with a high peak current of 62.5 mA and a long pulse length of 2.86 ms at a repetition rate of 14 Hz, enabling it to deliver 2 MW of beam power to the target. In the first half of 2025, accelerator commissioning was completed with the achievement of a beam energy exceeding 870 MeV, establishing ESS as a 2 MW-capable installation. For the first time, the entire linac was operated using both normal-conducting and superconducting cavities. The operational challenges during commissioning included coordinating installation and work activities, daily planning, and maintaining beam delivery to the tuning beam dump for the studies planned in this phase. In addition to these challenges, this contribution will present an overview of major operational incidents that impacted the commissioning timeline.

## INTRODUCTION

The European Spallation Source (ESS), currently under commissioning, is a spallation neutron source driven by a superconducting proton linac [1]. In the spring of 2025, the main activities related to the beam commissioning were held at the ESS. After several years of commissioning periods related to upstream accelerator sections [2, 3], the larger, almost full-scale Linac scope (see Fig. 1) was commissioned in the first half of 2025. The remaining part that allows transport of the beam towards the target will be commissioned on the occasion of the Beam On Target (BoT) commissioning, currently planned for early 2026. The Beam Commissioning to the Tuning Beam Dump (TBD) from the beginning was a full organization effort profiting from the operation division's availability and expertise.

One of the goals of the beam commissioning activities was to accelerate the protons to 870 MeV, making one of the steps needed to provide 2 MW operating beam power for the later neutron production. Also, within the scope of the commissioning, beam dynamics [4] and RF-related studies were performed to enable higher beam current (nominal 62.5 mA), longer and more frequent beam pulses. However, current commissioning phases were focused on beam pulses below 50 µs and 1 Hz [5].

The ESS MCR (Main Control Room) is administratively part of the Operations Division under the Operations and Machine Directorate (OMD). MCR has operated in the 24h/7 mode since November 2024, when the first Linac and CDS (Cryogenic Distribution Line) cool-down was performed. Shortly after that, the so-called RF Conditioning phase was started for both: normal and superconducting parts [6] of the ESS Linac. All 91 cavities (and related RF systems) were conditioned, verified, and prepared for the Beam Operation later in the year. The MCR team works in the two crew member pattern, on the 8h shift rota, in the 24h/7 patterns. The entire team consisted of 6 Shift Leaders (SL) and 6 Operators (OP), and was supported by an additional 2 SLs and almost a dozen OPs trained across the organization.

## WORK SCOPE AND PLANNING

The initial commissioning plan consisted of planned 10 weeks of Beam Commissioning to the TBD, hereafter in the text referred to often as Beam On Dump (BoD). It was later extended by an additional few weeks (until June 27), providing a total of 13 weeks (308 shifts) available for the commissioning of accelerator systems.

For the work of the remaining hardware scope needed for the Beam On Target (BoT), extra days with larger accesses for the installations and regular maintenance were planned on every second Tuesday. During the run, few additional extra days were introduced.

The scope for the MCR overseeing and activities has been continuously enlarging since 2023. Main areas where MCR currently provides support, assistance, and performs work are listed below.

*Beam and RF Operation* that includes support for the commissioners, daily work coordination, and off-office-hours support in execution of the prepared tests and experiments.

*Conventional Facilities* including Electrical, Water cooling, and HVAC systems. The support is based on monitoring of abnormal processes and invoking OnCall support (see later).

*Cryogenics* support for the off-office hours operation based on monitoring of abnormal processes and invoking OnCall support (see later). The main workforce for that part is within the Cryogenics group based in the Accelerator Division, also under the OMD directorate.

*Emergency Response Team* Support for the on-site First Responders and Crisis Management Team when needed.

*Work Coordination* Daily support with access for planned and approved work in the overseen areas, which expand as ESS projects get towards the end. The Work Order Office is administratively part of the Operations Division, hence in close collaboration with the MCR.

## DAILY OPERATIONAL ROUTINES

*Logbook:* Keeping it up to date is not only a legal requirement from the authorities, but also a source of information about the timeline of actions, issues, and possible solutions.

* arek.gorzawski@ess.eu

ISBN: <ask the JACoW BoD> ISSN: <ask the JACoW BoD> doi: 10.18429/JACoW-HB2025-WEIBC01

# BEAM HALO LOSSES REDUCTION WITH SIMULATION CONSTRAINED BAYESIAN OPTIMIZATION

J. Hyun*, A. De Franco, T. Akagi, K. Hirosawa, K. Kondo, K. Masuda, A. Mizuno[1]
QST, Aomori, Japan
Y. Carin, F. Cismondi, D. Gex, F. Scantamburlo, F4E, Garching, Germany
H. Dzitko, IFMIF/EVEDA Project Team, Aomori, Japan
[1]also at JASRI, Hyogo, Japan

*Abstract*

The Linear IFMIF Prototype Accelerator (LIPAc) is designed to demonstrate continuous wave (CW) acceleration of a 125 mA deuteron beam up to 9 MeV using a radio-frequency quadrupole (RFQ) and a superconducting radio-frequency (SRF) linac. Prior to SRF linac installation, beam commissioning was conducted with a 5 MeV deuteron beam. Attempts to increase the duty cycle revealed a significant rise in vacuum pressure, as detected by sensors, thus limiting the operational duty cycle to about 3%. Simulation studies indicated that the pressure increase was likely attributable to beam halo formation. To address this issue, Bayesian optimization was applied to the beam optics—specifically, four quadrupole magnets and four steerers—with the objective of minimizing halo-induced losses by monitoring vacuum pressure while constraining core beam losses. This approach successfully reduced the sector vacuum pressure by approximately 67 %. Further simulations verified that beam halo formation driven by nonlinear space-charge forces was effectively mitigated by relaxing beam focusing in specific regions, consistent with theoretical predictions. As a result, the duty cycle was increased to 8.7 %. These findings demonstrate that machine learning techniques, such as Bayesian optimization, can effectively support beam optics tuning in high-current accelerator systems. This paper presents a comparative analysis of the beam optics before and after optimization, highlighting the improvements in halo suppression.

## INTRODUCTION

The International Fusion Materials Irradiation Facility (IFMIF) is a proposed accelerator-based neutron source designed to characterize candidate materials for future energy-producing fusion reactors. IFMIF intends to generate a high-intensity neutron flux via deuterium-lithium stripping, producing around 14 MeV neutron spectrum closely resembling the first wall of a fusion reactor. This facility plays a critical role in assessing the radiation resistance and long-term performance of structural materials under fusion-relevant conditions. The IFMIF accelerator system consists of two 125 mA/40 MeV deuteron beams operated in continuous-wave (CW) mode, but its accelerator technologies have to be established. Therefore, the realization of IFMIF requires verification of equipment compatibility and beam handling for a 125 mA beam in CW mode—particularly in the low-energy section where space-charge effects are dominant. This validation is essential to ensure stable beam transport and minimize particle losses under conditions representative of the full-scale facility.

The Linear IFMIF Prototype Accelerator (LIPAc), which constitutes the low-energy section of IFMIF, is currently under installation and undergoing stepwise commissioning in Japan. This work is being carried out within the framework of the Broader Approach agreement between the Government of Japan and the European Atomic Energy Community (EURATOM), as part of the IFMIF/EVEDA project [1]. The objective of LIPAc is to validate the acceleration of a 125 mA deuteron beam up to 9 MeV in CW mode, while maintaining particle losses below 1 W/m [1, 2].

The LIPAc beamline consists of five sections: a low energy beam transport line (LEBT) equipped with an ECR ion source, a radio frequency quadrupole (RFQ) that accelerates the beam to 5 MeV, a medium-energy beam transport line (MEBT) containing five identical quadrupole magnets (quads), a superconducting RF (SRF) linac that further accelerates the beam to 9 MeV, and a high-energy beam transport line (HEBT) comprising eight quads of three different types and a beam dump.

Prior to the installation of the SRF linac, a temporary beam transport line was installed as a substitute using four identical quads, referred to as the MEBT extension line (MEL). Beam commissioning was conducted until June 2024 with the goals of characterizing beam properties, validating diagnostic devices, and increasing the duty cycle. This commissioning stage is referred to as Phase B+. Figure 1 shows the beamline configuration for Phase B+.

During the initial stage of Phase B+, conducted at a low duty cycle, discrepancies were observed between the measured beam sizes and simulation results. A matched beam was eventually achieved by revising the simulation model and the quad's excitation formulas, referred to as a *gtoI* method [3, 4]. In the subsequent step, efforts were made to increase the duty cycle. Although particle-tracking simulations optimized the beam optics and minimized particle losses along the beamline, vacuum degradation in the MEL section, caused by residual losses, was still observed. Simulation studies suggested that part of the transverse beam halo was lost. It should be noted that reliable halo simulations for a newly built machine are inherently difficult, as they require precise knowledge of the input particle distribution

* hyun.jibong@qst.go.jp

ISBN: <ask the JACoW BoD> ISSN: <ask the JACoW BoD> doi: 10.18429/JACoW-HB2025-WECBC01

# A ROBUST AND REDUNDANT DESIGN OF THE FAST PROTECTION SYSTEM FOR CSNS-II

Peng Zhu*[1,2], Lei Zeng[1,2], Jianmin Tian[1,2], Yuliang Zhang[1,2], Renjun Yang[1,2,3], Weiling Huang[1,2,3], Xiaohan Lu[1,2,3], Yongcheng He[1,2], Kangjia Xue[1,2], Xuan Wu[1,2], Lin Wang[1,2,3], Mingtao Li[1,2,3], Sinong Cheng[1,2], Dapeng Jin[1,3]

[1] Institute of High Energy Physics, Chinese Academy of Sciences (CAS), Beijing, China
[2] Spallation Neutron Source Science Center, Dongguan, China
[3] University of the Chinese Academy of Sciences, Beijing, China

*Abstract*

To ensure the long-term stability and reliability of the hardware platform under continuous operation, a key innovation is the custom design and implementation of a high-performance architecture, specifically, the "FPGA + Rocket IO + ATCA" solution, tailored for the Fast Protection System (FPS) of CSNS-II. This in-house-developed cooperative architecture integrates backplane and front-panel functionalities, enabling functional decoupling and modular design while significantly enhancing system scalability and maintainability. By minimizing transmission delays and mitigating signal degradation typically associated with intermediate logic components and shared bus topologies, the architecture improves timing determinism and signal integrity in inter-board communications. This paper presents a comprehensive analysis demonstrating that the proposed system is particularly well-suited for fast protection and real-time control applications requiring nanosecond-level synchronization accuracy. The design not only simplifies hardware expansion but also enhances overall system maintainability and adaptability.

## INTRODUCTION

The China Spallation Neutron Source (CSNS) is the fourth large-scale pulsed high-intensity proton accelerator globally. Since its inception in 2018, CSNS has consistently improved beam power and operational stability, achieving stable beam delivery exceeding 100 kW and progressively advancing towards a target of 170 kW [1]. To further enhance neutron yields and expand experimental capabilities, CSNS Phase II (CSNS-II) has officially approved in 2024. Among the most crucial upgrades in CSNS-II, a new superconducting (SC) segment is introduced following the initial 80 MeV radio frequency quadrupole (RFQ) and drift tube LINAC (DTL) sections [2]. This upgrade employs high-efficiency Spoke cavities and elliptical cavities, increasing the output beam energy from 80 MeV to 300 MeV, as shown in Figure 1. This advancement enhances injection and overall transmission efficiency, enabling the achievement of beam powers up to 500 kW.

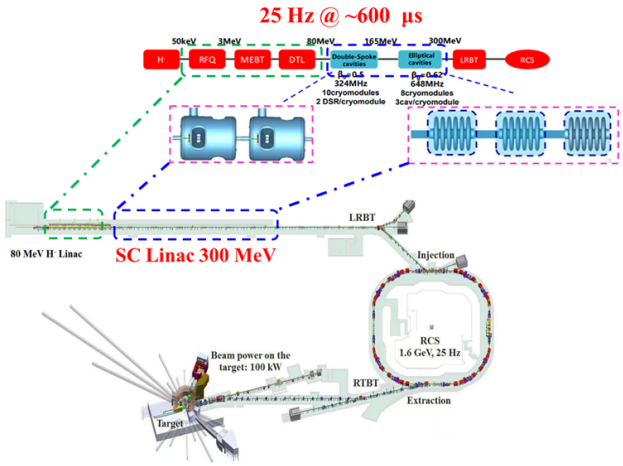


Figure 1: Overall layout of the CSNS-II LINAC.

## REQUIREMENTS OF THE FPS

### *The Response Time*

The FPS is required to accurately detect abnormal operational conditions and to terminate the beam within microsecond-level response times, thereby preventing equipment damage and safety hazards associated with uncontrolled beam loss [3–5]. Consequently, the development of an FPS with high reliability, ultra-fast response, and intelligent diagnostic capabilities represents a key technological challenge for ensuring the long-term stable, safe, and reliable operation of CSNS-II.

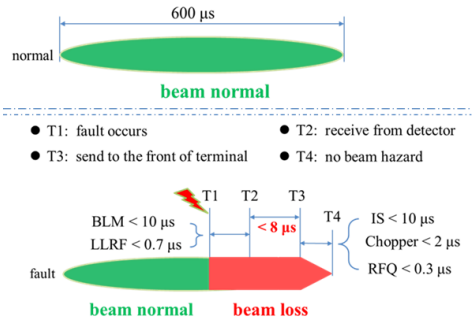


Figure 2: Schematic diagram of the response time.

* zhup@ihep.ac.cn

ISBN: <ask the JACoW BoD> ISSN: <ask the JACoW BoD> doi: 10.18429/JACoW-HB2025-WEICB01

# UPDATE DESIGN FOR THE MUON COLLIDER PROTON COMPLEX*

S. Johannesson†, N. Milas, M. Sörqvist[1], J. Holmberg[1], M. Eshraqi
ESS, Lund, Sweden
[1]also at Lund University, Lund, Sweden

*Abstract*

The proton complex is the first piece in the Muon Collider. It comprises a high power acceleration section, a compressor and a target delivery system. For the International Muon Collider Collaboration (IMCC) we are investigating two possibilities: a 5 GeV (2 MW) and a 10 GeV (4 MW) final energies. In this work we present the updated design for the proton complex, including chopping schemes for the LINAC, an investigation on the use of a Rapid Cycling Synchrotron for reaching the final energy and a refinement of the simulations for the accumulator and compressor sessions.

## INTRODUCTION

Both the European strategy for particle physics and the American Particle Physics Project Prioritization Panel (P5) have identified the need for particle accelerators reaching >10 TeV. A promising alternative to reach this goal is a Muon Collider. A Muon Collider consists of a complex of accelerators starting with a proton complex producing a short and intense proton pulse to generate muons from a fixed target. The muons are then cooled, accelerated, and collided in a series of different accelerator structures and rings [1].

The aim of the proton complex is to produce one short and intense proton bunch with a certain frequency for the target to produce pions, which decay to muons. The parameters for two design options can be seen in Table 1.

Table 1: Parameters

| Parameter | Option 1 | Option 2 |
|---|---|---|
| Beam Power | 2 MW | 4 MW |
| Beam energy | 5 GeV | 10 GeV |
| Accumulated bunch length | 120 ns | |
| Final Bunch Length | 2 ns | |
| Repetition Rate | 5 Hz | |
| # protons on target | $5 \times 10^{14}$ | |

An overview of the current design of the proton complex can be seen in Fig. 1. All acceleration is carried out in a LINAC. The accumulator stacks short pulses from the LINAC until the desired bunch intensity is achieved. Once this intensity is reached, a compressor shortens the bunch. A recombiner can then be used to merge several bunches together. Finally, the protons are directed through a transport line toward the target.

* Work supported by the European Union
† sofia.johannesson@ess.eu

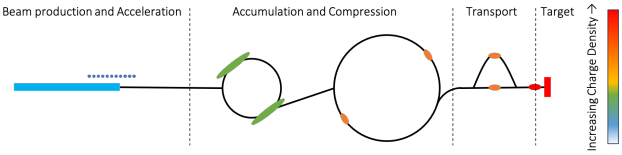


Figure 1: The current baseline for the proton complex consists of a LINAC, an accumulator ring, a compressor ring, a transport to target, including recombination of two bunches.

The design is a compromise between the challenge of maintaining an intense bunch, experiencing strong space charge effects, with the challenge of bunch recombination. The current baseline designs include a recombination of two bunches, however, alternative designs are under exploration.

Each part of the proton complex will be explored in more detail in the following sections using mainly the simulation code Xsuite [2], as well as some alternative considerations.

## LINAC

We updated the LINAC design presented in [1]. The superconducting part of the LINAC is divided into four main sections. The first section is composed of Spokes cavities working at 352 MHz and with a geometric beta $\beta_g = 0.5$. The second and fourth sections are composed of elliptical cavities with $\beta_g = 0.67$ and with $\beta_g = 0.86$ respectively, and with a transverse focusing section every four cavities. The last section has the new cavities with a $\beta_g = 1$ and a double periodicity compared with the previous, namely eight cavities in between transverse focusing sections. The final length for the LINAC with an energy of 5 GeV is 680 m long (accounting for the normal conducting front-end) and 1150 m for the 10 GeV case.

Figure 2 shows the transverse and longitudinal envelopes in the superconducting LINAC for both final energy options. For the 5 GeV case, we also recalculated, see Fig. 3, the $H^-$ stripping losses due to intra-beam stripping, showing that we are well below the limit of 1 W/m, currently used in high power facilities like ESS in order to allow hands-on maintenance and machine protection [3].

## ACCUMULATOR

The accumulator consists of a 180 m ring in option 1 or a 300 m ring in option 2, but is in both cases a fairly simple ring consisting of a FODO-lattice without any RF-structures present.

The current simulations show no major showstoppers for either option. The final tune footprint of the 5 GeV option, as well as the 10 GeV option, can be seen in Fig. 4. The tune

ISBN: <ask the JACoW BoD> ISSN: <ask the JACoW BoD> doi: 10.18429/JACoW-HB2025-WEICB03

# SPACE CHARGE EFFECTS DURING HALF-INTEGER RESONANCE CROSSING IN THE PSB

T. Prebibaj*, F. Asvesta, H. Bartosik, CERN, Geneva, Switzerland
G. Franchetti, GSI Helmholtzzentrum für Schwerionenforschung, Darmstadt, Germany

*Abstract*

Space charge effects are the main performance limitation for the beam brightness in the CERN Proton Synchrotron Booster (PSB). Operating at higher vertical tunes, near or above the vertical half-integer resonance $2Q_y = 9$, offers more space in the tune diagram to accommodate the large space charge tune spread, potentially allowing for brighter beams. In this context, an experimental campaign was performed to characterize the space charge dynamics during the controlled crossing of the half-integer resonance. This contribution summarizes the main results. The scaling of beam degradation with the space charge detuning and resonance crossing rate is analyzed, which could be relevant to any high-intensity synchrotron operating near a half-integer resonance. Finally, the achievable beam brightness in the PSB for injection above the half-integer resonance was tested experimentally and first results are reported here.

## INTRODUCTION

The proton beams that collide at CERN's Large Hadron Collider (LHC) are prepared by a chain of accelerators: Linac4, the Proton Synchrotron Booster (PSB), the Proton Synchrotron (PS), and the Super Proton Synchrotron (SPS). The High-Luminosity LHC (HL-LHC) project [1] aims to significantly increase the collision rate at the LHC, which sets stronger demands on the beam performance delivered by the injectors. A key performance parameter is the beam brightness, defined as the ratio between the beam intensity and the average transverse emittance:

$$B = \frac{N_b}{(\epsilon_x + \epsilon_y)/2}. \quad (1)$$

Higher brightness beams result in higher luminosity and thus more collisions at the LHC.

At the PSB injection energy, space charge effects determine the achievable brightness performance. The space charge induced tune spread can shift particles onto the integer tunes ($Q_{x,y} = 4$), where they interact with the 4$^{\text{th}}$ order systematic resonances $4Q_{x,y} = 16$, which are strongly excited by the space charge potential due to the lattice periodicity of 16 [2]. In bunched beams, the modulation of the space charge detuning leads to periodic resonance crossing [3], which can increase the emittance and reduce the achievable brightness.

To mitigate these limitations, the PSB was upgraded within the LHC Injectors Upgrade (LIU) project [4]. The most important changes were the replacement of the existing proton linac (Linac2) with a new H$^-$ linac (Linac4), which raised the injection energy from 50 MeV to 160 MeV, and the implementation of the corresponding charge-exchange injection system. These upgrades enabled higher-intensity, higher-brightness beams with lower injection losses for the same space charge tune spread as before the upgrade. Figure 1 shows the measured brightness before and after the upgrades.

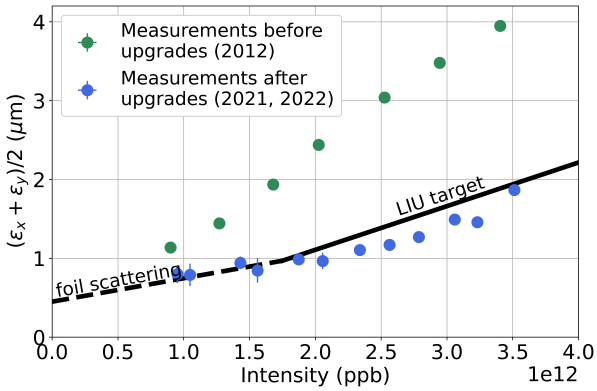


Figure 1: Measured average transverse emittance as a function of the beam intensity for ring 3 of the PSB before (green) and after (blue) the LIU upgrades. The LIU brightness target (black solid line) and the limits coming from scattering effects on the injection foil (black dashed line) are drawn.

While the upgrades allow reaching the LIU target brightness, space charge remains one of the main limitations when pushing beyond these targets for exploring the ultimate brightness reach. The machine is typically operated with high working points at injection, i.e. $4.35 < Q_{x,y} < 4.45$, far from $Q_{x,y} = 4$, to minimize the emittance growth. Previous studies have shown that operating with even higher working points at injection, closer but below the vertical half-integer resonance $2Q_y = 9$, could further improve the brightness [5]. This raises the question of whether injecting above the half-integer resonance and crossing it during acceleration could provide an additional brightness gain.

Crossing the half-integer resonance is particularly challenging, as it is strongly excited by residual quadrupole-like errors and can cause significant beam degradation. In this context, a series of studies were launched in order to improve the resonance compensation and to investigate the dynamics of the crossing under space charge effects for different beam and machine configurations. The objective is to evaluate whether a controlled crossing could provide operational benefits for the PSB or any other high-intensity accelerator

* tirsi.prebibaj@cern.ch

ISBN: <ask the JACoW BoD> ISSN: <ask the JACoW BoD> doi: 10.18429/JACoW-HB2025-WEICB04

# IMPEDANCE OF CERAMIC CHAMBERS AND ITS IMPACT ON BEAM STABILITY

Liangsheng Huang†,1, Li Rao[1], Mingyang Huang[1], Shouyan Xu[1], Biao Tan[1], Haibo Li[1], Shengyi Chen[1], Renhong Liu[1], Lirui Zeng[1]
Institute of High Energy Physics, Chinese Academy of Sciences, Beijing, China
[1]also at Spallation Neutron Source Science Center, Dongguan, China

*Abstract*

A striped ceramic vacuum chamber is used in the Rapid Cycling Synchrotron (RCS) of the China Spallation Neutron Source (CSNS) to maintain required vacuum of beam. Earlier analyses suggested that the beam-coupling impedance of this structure would be negligible. Recent measurements, however, revealed a low-frequency resonant mode in the chamber, and subsequent studies identified it as the driver of transverse coupled-bunch instability. This paper presents the impedance characterization of the ceramic chamber, quantifies its contribution to the transverse coupled-bunch instability.

## INTRODUCTION

The accelerators of China Spallation Neutron Source (CSNS) comprise an 80 MeV H− linac and a 1.6 GeV rapid-cycling synchrotron (RCS) [1]. The RCS accumulates the 80 MeV H− beam via multi-turn charge-exchange injection and accelerates it to 1.6 GeV at a repetition rate of 25 Hz. The facility operates at 100 kW beam power with $1.56\times10^{13}$ protons per pulse. Given the high intensity and rapid cycling, beam losses must be kept to very low levels.

The RCS is a four-fold structure [2]. Figure 1 displays the layout of RCS. Each superperiod comprises two straight sections and one arc. Consequently, four uninterrupted 11 m straight sections accommodate the injection and extraction systems, RF cavities, and the transverse collimation system. The main parameters are summarized in Table 1. The lattice comprises triplet cells around a 227.92-m circumference and includes 24 dipole and 48 quadrupole magnets, excited by a 25 Hz DC-biased sinusoidal current waveform [3]. The 48 quadrupoles are powered by five power-supply families. The nominal tune is (4.86, 4.78), and the natural chromaticity is (−4, −9). Although chromaticity correction is not required below transition energy, DC sextupoles are employed to improve chromaticity control, particularly at low beam energy. The transverse acceptance of the RCS is designed as 540 π·mm·mrad. In the longitudinal plane, the RF voltage is ramped to shrink the bucket and maximize capture, accumulation, and acceleration efficiency. The maximum RF voltage is 165 kV with a synchronous phase of 45°.

RCS beam commissioning [4] commenced in 2017. In 2019, an instability in the horizontal plane was first detected as the beam power increased from 20 to 50 kW, and it intensified at higher power. Under certain conditions, a similar effect was observed in the vertical plane. Since then, beam-based diagnosing and mitigating this instability became a principal focus of commissioning. A dedicated measurement campaign established that the phenomenon is a transverse coupled-bunch instability (TCBI). Targeted impedance measurements revealed a narrow-band resonance originating from the RF shield of the ceramic vacuum chambers. Calculation and simulation confirmed that this impedance drives the instability [5]. To address the instability, an optimized tune curve and chromaticity were implemented, successfully achieving the designed beam power of 100 kW.

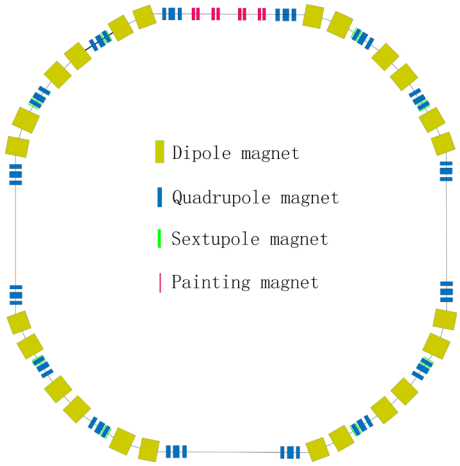


Figure 1: The layout of RCS.

Table 1: Main RCS Parameters

| Parameter | Unit | CSNS |
|---|---|---|
| Circumference | m | 227.92 |
| Energy (Inj./Ext.) | GeV | 0.08/1.6 |
| Repetition rate | Hz | 25 |
| Bunch number | | 2 |
| Beam intensity | $10^{13}$ | 1.56 |
| Nominal tune (H/V) | | 4.86/4.78 |
| Chromaticity (H/V) | | -4/-9 |

This paper reports the identification and quantification of the RF-shield–induced beam-coupling impedance in the ceramic vacuum chamber, presents observations of beam instabilities, and details the mitigation strategies deployed. We conclude with a summary of the impedance and instability results and an outline of future directions.

† huangls@ihep.ac.cn

ISBN: <ask the JACoW BoD> ISSN: <ask the JACoW BoD> doi: 10.18429/JACoW-HB2025-WEICC01

# RFQ BEAM DYNAMICS DESIGN USING AI TECHNIQUES

M. Comunian*, L. Bellan, A. Pisent
INFN-LNL, Legnaro, Italy



*Abstract*

An optimization toolkit named VeRDe (Venetian RFQ Design) has been developed at the Legnaro National Laboratories for the design of Radiofrequency Quadrupoles (RFQs). It builds on well-established RFQ design methodologies and is based on the Los Alamos codes: PARMTEQM, PARI, RFQuick, and CURLI. The toolkit enables detailed control over the evolution of key RFQ cell parameters, like voltage etc... The RFQ design process, involving many cells (ranging from tens to hundreds), results in a high number of degrees of freedom. While theoretical guidelines help reduce this complexity, final-stage optimization often requires evaluating hundreds to thousands of candidate designs. To address this, VeRDe now incorporates advanced optimization techniques based on evolutionary and swarm intelligence algorithms, specifically: Particle Swarm Optimization (PSO), Improved Stochastic Ranking Evolutionary Strategy (ISRES), Genetic Algorithm (GA), and others. These enhancements aim to significantly accelerate and improve the optimization process.

In this article, a description of the toolkit is presented, along with a comparison between the IFMIF RFQ and a proposed upgrade for the DONES RFQ.

## INTRODUCTION

The beam dynamics group has a well-established experience in the RFQ design [1–3]. The core of the simulations is given by the Los Alamos RFQ codes [4]: PARMTEQM, PARI, RFQuick and CURLI. The design is an iterative process between the above codes where: RFQuick estimates the longitudinal capture efficiency, given the current limit by CURLI, through the study of the buncher section characteristics; PARI designs the RFQ cells based on the RFQuick output (that uses the Crandall tables to estimate the multipoles of the cells); PARMTEQM performs the simulations based on the PARI output.

The number of parameters needed for each RFQ cell definition may vary, but at least four parameters are required: the transverse focusing term, the voltage, the modulation and the synchronous phase. Considering that the RFQ is composed by a number of cells that can vary from several tens to hundreds, it is straightforward to understand that the degree of freedom of the process is very large. In general, there are several theories that help the designer to reduce the degree of freedom of the design process. However, at the final stage of the optimization, where small changes of the parameters are involved, from hundreds to thousands of RFQ candidates may be produced. Therefore, it is useful to explore this range with an automatic tool that helps to manage this very large amount of information.

## OPTIMIZATION TOOLKIT: VeRDe

Several design features such as voltage/transverse focusing ramps are not included in the Los Alamos software and therefore needed to be implemented manually. At this goal an optimization toolkit VeRDe (Venetian RFQ Design), written in Python, has been developed. It allows to:

- Interface to the Los Alamos RFQ design software, giving a manageable input parameter page, where the user can choose several parameters such as the ion type, the charge, the current, etc.;
- supply voltage, $R_0$, $B$, $m$ and $\Phi_s$ [4] ramp laws based on the benchmarked type used for the IFMIF/EVEDA RFQ design [5]. For a defined voltage shape, it also calculates the relative frequency detuning and power dissipation, both quantities being useful for the subsequent design stages, i.e., radiofrequency and mechanical;
- supply $B$ law for the low $B$ type RFQ, using as formula a fix distance between $\sigma T0$ and $\sigma L0$ at the RFQ begin;
- collect and calculate the required data and supply the plots and analysis;
- translate the PARI format onto the TOUTATIS [6] rfq input file.
- save all the generated RFQs for further analysis.

In this working framework, two routines can be chosen:

1. the single run mode where the software adds the above features and integrates the Los Alamos software;
2. the parametric run mode which allows the study of several cases given a certain range of parameters.

### *Extension of Multipoles Tables*

We extended the original Crandall tables of multipoles [7] to include a larger set of modulation and $L/R_0$ by means of full 3D electrostatic FEM simulations, in total more than 5000 simulations has been done. A generic Electrical fields in a cell of a RFQ is reported in Fig. 1 as finite element calculation results.

This new set is now fully integrated on the LANL codes.

The multipoles considered is up to the $A_{nm}$ with n+m=5, this order is enough to made RFQs with equivalent to two term modulation or sin like modulation. But this order is not sufficient for trapezoidal RFQ modulation.

The runs of VeRDe are with this new set of multipoles. This permit a study with larger set of parameters in the RFQ accelerator section.

In Fig. 2 is reported, as color scale, the multipole $A_{10}$ for the old set of $L/R_0$ vs modulation and for the new set up to 5 as modulation and covering RFQ with low $L/R_0$.

* michele.comunian@lnl.infn.it

ISBN: <ask the JACoW BoD> ISSN: <ask the JACoW BoD> doi: 10.18429/JACoW-HB2025-WECCC03

# BEAM DYNAMICS AND LINAC DESIGN FOR THE 200 MEV ENERGY UPGRADE AT KOMAC *

S.H. Moon †, S. Lee, S.-B Park, D.-H Kim, H.-S Kim, H.-J Kwon
Korea Atomic Energy Research Institute, Gyeongju, Republic of Korea

*Abstract*

Since 2013, the Korea Multi-purpose Accelerator Complex (KOMAC) has been operating a 100 MeV linear proton accelerator. Designed from its inception with the long-term vision of upgrading to a high-power spallation neutron source, KOMAC's proton accelerator aims to achieve a final energy of 1 GeV. As an intermediate milestone toward this goal, a 200 MeV energy upgrade is currently being planned.

To support this upgrade to 200 MeV, comprehensive linac designs and beam dynamics simulations have been carried out, adopting a Separate-type Drift Tube Linac (SDTL). This presentation discusses the beam dynamics design of the linac and the user-side beamline for the proposed upgrade. Additionally, error analysis simulations were performed based on the initial design calculations. These simulations have validated the robustness and stability of the linac design, confirming its feasibility for stable operation at 200 MeV linac.

## INTRODUCTION

The Korea Multi-purpose Accelerator Complex (KOMAC), operated by the Korea Atomic Energy Research Institute (KAERI) in Gyeongju, houses a 100 MeV pulsed proton linear accelerator commissioned in 2013 as part of the Proton Engineering Frontier Project (PEFP). The facility comprises a 50 keV microwave ion source, a 3 MeV four vane radio frequency quadrupole (RFQ), and a drift tube linac (DTL) accelerating the proton beam up to 100 MeV.

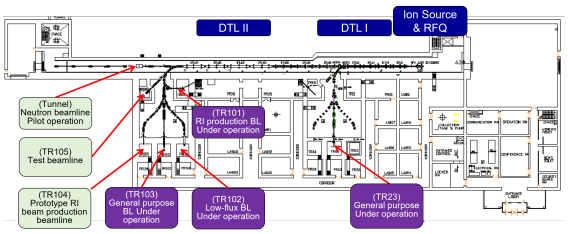


Figure 1: Current layout of KOMAC accelerator.

The Fig. 1 shows the current layout of KOMAC. One beamline utilizing protons accelerated up to 20 MeV is installed, and five beamlines using 100 MeV protons have been constructed and are currently in operation.

### *Energy Upgrade Plan*

KOMAC's energy upgrade plan is divided into short-term and long-term phases. The short-term plan involves upgrading the current proton energy from 100 MeV to 200 MeV. The reason for setting 200 MeV as the target in the short-term plan is that, depending on future expansion strategies, this energy level allows flexibility: it can serve as an injector for a rapid cycling synchrotron (RCS) if a circular accelerator is adopted, or additional accelerating structures can be installed downstream if a linear accelerator is selected. The long-term plan aims to increase the proton beam energy up to 1 GeV, with the goal of utilizing it as a spallation neutron source.

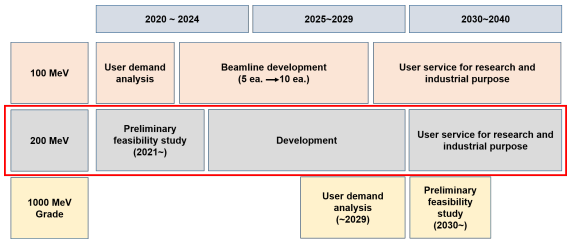


Figure 2: Roadmap of KOMAC.

The Fig. 2 presents the roadmap for KOMAC's energy upgrade plan mentioned earlier. The section highlighted in red represents the short-term plan, which involves upgrading the proton energy to 200 MeV.

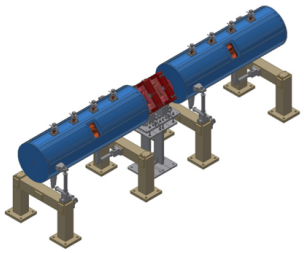

Figure 3: Separated Drift Tube Linac type cavity.

Two types of accelerating structures were considered for the 200 MeV energy upgrade. The first option was a superconducting HWR cavity, and the second option was a normal-conducting SDTL type cavity as shown in Fig. 3. After evaluating various scenarios and requirements, the decision was made to proceed with the SDTL design, and the detailed engineering of that structure was carried out accordingly [1, 2].

## BEAM DYNAMICS SIMULATION

### *Linac Design*

After extensive discussion and consideration, the cavity structure was finalized as the SDTL type. Research is currently being conducted on two types of SDTL: the 5-cell type

* Work supported by KOMAC operation fund of KAERI by MSIT (Ministry of Science and ICT)
† msh3069@kaeri.re.kr

ISBN: <ask the JACoW BoD> ISSN: <ask the JACoW BoD> doi: 10.18429/JACoW-HB2025-WECCC04

# BEAMLINE PHYSICS DESIGN AND HIGH-BRIGHTNESS BEAM OPTIMIZATION FOR THE CSNS-II*

Yanliang Han†, Huachang Liu, Jun Peng, Zhiping Li
IHEP, CAS, Beijing, 100049, China
Spallation Neutron Source Science Center, Dongguan 523808, China

*Abstract*

Commissioning of the China Spallation Neutron Source (CSNS) commenced in 2018, with the facility reaching a neutron production beam power of 100 kW. An upgrade program, known as CSNS-II, was launched in 2024 with the goal of increasing output to 500 kW in the coming years. Alongside these developments, several multidisciplinary application facilities have been deployed or are in planning stages. These include the Associated Proton Beam Experiment Platform, Back-n White Neutron Source Station, High Energy Proton Experiment Station, Muon Station for Science, Technology and Industry (MELODY), and the Isotope Production Platform. This paper presents the upgrade and these application stations and discusses the design of their associated physics beam lines.

## INTRODUCTION

The China Spallation Neutron Source (CSNS) is an accelerator-based pulsed neutron source situated in Guangdong Province, China. Construction of the CSNS began in 2011 and was completed in 2018 [1,2]. The facility achieved its designed beam power of 100 kW in 2020.

In 2024, an upgrade of CSNS had been started with the main goal of beam power 500 kW, whose layout is shown in Fig. 1. The beam energy at the end of linac will be increased from 80 MeV to 300 MeV and the peak current will be increased from 10 mA to 40 mA. The main parameters about the upgrade are summarized in Table 1. To achieve the higher beam energy at the linac, superconducting cavities will be installed after the Drift Tube Linac (DTL). The ion source has been replaced with a new RF-type ion source, capable of providing the required peak current negative hydrogen beam with high stability. The Rapid Cycling Synchrotron (RCS) injection system has also been upgraded to support future high beam power operation. In the RCS, several Magnetic Alloy Cavities will be installed to enhance longitudinal beam dynamic performance, and octupole magnets are positioned to mitigate potential beam instability. For the neutron target, all reserved beamlines will be utilized, and the number of spectrometers will increase to 20.

In addition to the main facility, several other platforms have been established at the CSNS site. At the end of the linac, the Associated Proton Experiment Platform (APEP) is located. A dedicated back-n experiment station is deployed at the main neutron target. For the future CSNS-II, several additional platforms are planned. One such platform is the High Energy Proton Experiment Station (HPES), designed to provide low-current protons for the calibration of particle detectors. A muon production platform, which will facilitate scientific research related to muons, will also be constructed. At the end of the linac, the beam energy will reach 300 MeV, making it suitable for the production of certain isotope elements. On campus, a research platform is currently under development.

In the remainder of this paper, we first discuss some aspects of the physics design for the CSNS-II linac and then provide an overview of the platforms related to the CSNS facility.

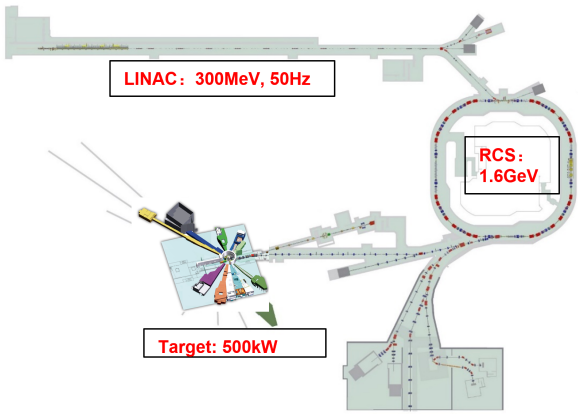


Figure 1: The layout of the CSNS-II facility.

Table 1: The Main Parameters of the CSNS and CSNS-II

| Parameters | CSNS | CSNS-II |
|---|---|---|
| Beam Power [kW] | 100 | 500 |
| Beam Energy [GeV] | 1.6 | 1.6 |
| Peak Current@linac [mA] | 10 | 40 |
| Beam energy @linac [MeV] | 80 | 300 |
| Duty factor [%] | 1.06 | 1.56 |
| Number of Targets | 1 | 1 |
| Number of spectrometers | 3 | 20 |

## THE LINAC OF CSNS-II

The linac of CSNS-II comprises an RF $H^-$ source, a Radio-Frequency Quadrupole (RFQ), a Medium Energy Beam Transfer line, four drift tube normal conducting linacs (DTL), a superconducting linac with spoke and elliptical cavities, and a transfer line connecting the linac to the RCS ring. The layout of the linac is depicted in Fig. 2. The beam

* Work supported by Basic Research Foundation of SAPS pre-research, CAS (E02971U6)
† Email: ylhan@ihep.ac.cn

ISBN: <ask the JACoW BoD> ISSN: <ask the JACoW BoD> doi: 10.18429/JACoW-HB2025-WEIDB01

# BEAM DYNAMICS STUDIES ON THE ISIS RCS WITH A NEW ASSESSMENT OF NON-LINEAR DRIVING TERMS AND MOTION

E. Ahmadi, C. M. Warsop, H. V. Cavanagh, H. Rafique, R. E. Williamson
Rutherford Appleton Laboratory, Oxfordshire, UK



*Abstract*

ISIS is the pulsed muon and neutron source at RAL in the UK. Its operation centres on an 800 MeV rapid cycling synchrotron (RCS) running at 50 Hz, delivering $3\times10^{13}$ protons per pulse (ppp) and 0.2 MW average beam power to targets.

Current studies are aiming to improve the measurement, modelling, and control of ISIS ring beam dynamics, with the goal of optimizing operational setup and benchmarking beam loss studies for ISIS and the proposed MW upgrade, ISIS-II. This paper gives a brief overview of transverse beam dynamics studies at ISIS, as well as beam measurement and modelling. The paper then focuses on non-linear beam dynamics studies in the low-intensity regime.

Measured beam loss maps in tune space have been used to identify non-linear resonance lines. To better characterize individual resonance lines and improve the non-linear lattice model, comparisons are made between loss maps from experiment and results from extended particle tracking, Frequency Map Analysis (FMA) simulations, and analytical calculations. Detailed investigations of the third-order resonance lines $3Q_x=13$ and $Q_x+2Q_y=12$ are outlined.

## INTRODUCTION

The ISIS machines centre on a 50 Hz, 163 m circumference, rapid-cycling synchrotron. This accelerates protons from 70 to 800 MeV, delivering ~$3\times10^{13}$ ppp, or 0.2 MW, to muon and neutron targets. The machine employs 130-turn charge-exchange injection and single-turn vertical extraction. The nominal tunes are $(Q_x, Q_y)=(4.31, 3.83)$, and are varied through the 10 ms acceleration cycle via families of programmable trim quadrupoles [1].

Beam loss at high intensity imposes limits on machine performance, and studies are underway to improve beam modelling, measurement and control. These studies cover most aspects of transverse and longitudinal dynamics, and are summarised below. Benchmarked studies of losses at high intensity will be valuable groundwork for designs of the MW upgrade, ISIS II [2].

The main focus of this paper is non-linear transverse dynamics. Of ultimate interest is the effect of non-linearities on high intensity performance, i.e. the effect of low intensity non-linear fields plus those of space charge and wakes. This work addresses the low intensity non-linear dynamics, as a basis for future high intensity study.

Of particular interest for ISIS is the $3Q_x=13$ line near the working point, which we study here with low intensity coasting beams to understand in detail the basic transverse beam dynamics. Later, this work will be linked with high intensity effects relevant for the operational, bunched RCS beam. The effect of a coupling resonance $Q_x+2Q_y=12$, near the working point is also studied. Finally, work on Q vs. loss measurement surveys of all resonance lines are summarised, along with analysis via Dynamic aperture and FMA tracking.

## ISIS RING R&D WORK

User demand for higher beam intensity, with the same or better availability, is a key motivator for the current R&D programme at ISIS. The availability of modern modelling tools also plays an important role. In addition, a systematic approach to activation and loss is needed to reduce the long-term maintenance burden and risk. All these factors contribute to the direction of the current R&D efforts at ISIS. In addition, im-proved operational fault finding and the need to bench-mark models to de-risk and inform ISIS-II underpin the R&D activities. In the following, we will highlight R&D studies related to transverse beam dynamics

### *Machine Alignment and Orbits*

We are reassessing the ring's mechanical alignment relative to the original 1980s design, combining historical schematic data with new comprehensive surveys to quantify time-dependent drifts and the efficacy of realignment. The calculated misalignments are translated and applied to lattice models in transverse planes, enabling direct interpretation of their expected effect on the closed orbits [3].

### *Magnet Modelling*

A significant challenge in developing an accurate machine model is the limited availability of direct, comprehensive magnetic measurements for the installed ring magnets. To overcome this, computational modelling was employed to create detailed representations of each magnet type. The modelling process involved matching 3D electromagnetic simulations performed in OPERA to the existing, albeit limited, measurement data [4].

### *Linear Lattice Measurements*

A detailed low-intensity study of the vertical $2Q_y = 7$ resonance was performed by ramping the tune and measuring beam loss while systematically varying the resonance driving term using trim quadrupoles. The observed shift and width of the stopband matched expectations, indicating good experimental understanding and enabling accurate correction of the important linear resonances [5].

## 3RD INTEGER STUDY $3Q_X=13$

### *Theoretical Background*

For the third-order horizontal resonance $3Q_xN$ (here $N$=13), the single-resonance Hamiltonian provides compact, operationally useful scalings between the resonance

ISBN: <ask the JACoW BoD> ISSN: <ask the JACoW BoD> doi: 10.18429/JACoW-HB2025-WEIDC01

# ACCELERATOR DESIGN FOR THE HIGH BRILLIANCE NEUTRON SOURCE (HBS)

K. Kümpel*, M. Droba, S. Lamprecht, O. Meusel, N. F. Petry, H. Podlech[1], J. Storch, S. Wagner
Institute of Applied Physics (IAP), Frankfurt, Germany
T. Gutberlet, A. Lehrach, P. Zakalek, JCNS, Forschungszentrum Jühlich GmbH, Jülich, Germany
C. Zhang, Schwerionenforschung, Campus Frankfurt, Frankfurt, Germany
[1]also at Helmholtz Research Academy Hesse for Fair (HFHF), GSI Helmholtzzentrum für

*Abstract*

The High Brilliance Neutron Source (HBS) is a new High Current Accelerator-driven Neutron Source (HiCANS) project, planned and to be realized at the Forschungszentrum Jülich, Germany. The project represents a promising alternative for expanding neutron availability in Europe by using a high-current, low-energy proton accelerator and state-of-the-art technologies to deliver thermal neutron fluxes comparable to medium to high flux reactor sources, supporting both scientific and industrial applications. The driver accelerator is designed to reliably accelerate a 100 mA proton beam to 70 MeV, which will then be distributed pulse-by-pulse via a multiplexer to three different neutron targets, each operating with a distinct time structure. The planned linear accelerator (LINAC) consists of an ECR source, a LEBT section, two RFQs, and more than 45 normal-conducting CH drift tube structures. This talk will present the layout of the proposed normal-conducting HBS accelerator, with a particular focus on the challenges in the design of the resonators and the beam dynamics of the CH drift tube section.

## THE HBS LINAC

With a beam current of 100 mA the High Brilliance Neutron Source (HBS) belongs to the so-called High Current Accelerator-driven Neutron Sources (HiCANS) [1] [2]. A new class of compact neutron sources that could be used both for scientific and industrial applications. The normal conducting linear accelerator (LINAC) will accelerate a proton beam to a final energy of 70 MeV before it is divided in a multiplexer, that is part of the High Energy Beam Transfer (HEBT), and send to three different target stations that can be used simultaneously [3]. Each of the three beams has its own time structure depending on the instruments used in the different experiments. Table 1 sums up the required specifications of the HBS LINAC.

The design philosophy for the LINAC as shown in Fig. 1 aims at high reliability and availability, high efficiency, and risk minimization [4].

One of the most fundamental decisions during the design of a linear accelerator is whether it will be built consisting of normal- or superconducting cavities or at which beam energy you switch from normal- to superconducting. The decision of building the HBS LINAC completely with normal conducting technology is based - among others - on the following three aspects: [5]

Table 1: Required Specifications for the HBS LINAC

| Required | Specifications |
|---|---|
| Particle type | Protons |
| Accelerator type | RF LINAC |
| Beam current | 100 mA |
| Final energy | 70 MeV |
| Beam duty factor | 6 (up to 20) % |
| RF duty factor | 8 (up to 25) % |
| Pulse length | 208/208/833 µs |
| Repetition rate | 96/96/24 Hz |
| Average beam power | 420 (1400) kW |
| Peak beam power | 7 MW |
| Availability | > 95 % |
| Maintainability | Hand-on |
| Life time | > 25 |

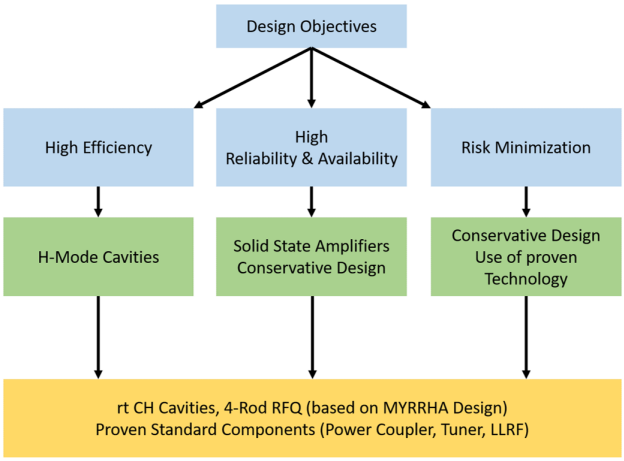


Figure 1: Design philosophy driven by obtaining high availability, risk minimization, high efficiency and cost reduction. [4]

- **Beam Current** The HBS LINAC has a high beam current of 100 mA. The higher the beam current, the more the total power consumption of a cavity is dominated by the beam loading compared to the losses of the cavity which reduces the advantages of using a superconducting LINAC for the HBS Project.

* kuempel@iap.uni-frankfurt.de

ISBN: <ask the JACoW BoD> ISSN: <ask the JACoW BoD> doi: 10.18429/JACoW-HB2025-WECDB02

# SIMULATIONS OF BEAM-COUPLING IMPEDANCE TO GUIDE MODEL-BASED MITIGATIONS IN HADRON RINGS

E. de la Fuente*,[1], C. Zannini†, C. Antuono, G. Rumolo, L. Sito[2], CERN, Geneva, Switzerland
[1]also at Universidad Politecnica de Madrid, Madrid, Spain
[2]also at University of Naples Federico II, Naples, Italy

*Abstract*

Beam coupling impedance is a fundamental performance limitation in high-intensity hadron rings, affecting both beam stability and the thermal load on accelerator components. As beam intensity increases, impedance-driven collective effects—such as transverse mode coupling and longitudinal coupled-bunch instabilities—become more pronounced, while beam-induced power losses can cause local overheating and hardware damage. Accurately evaluating these effects remains challenging due to complex accelerator geometries, realistic electromagnetic material modelling, and the wide frequency ranges involved. Accurate impedance modelling is essential for predicting instability thresholds and quantifying power deposition in current and future hadron accelerators, such as the LHC and FCC-hh. In this contribution, an impedance-driven workflow, supported by recently developed Python open-source tools, allows effective understanding and mitigation of operational limitations. Examples are discussed showing how the proposed workflow enabled impedance mitigation solutions in different hadron rings.

## INTRODUCTION

The determination of beam-coupling impedance and its impact on accelerator performance is a longstanding challenge in high-intensity accelerators, often requiring a multiphysics approach [1] ranging from beam instabilities to device thermo–mechanical stress. To identify mitigations for impedance-limited scenarios and guide device design, an impedance assessment workflow has been established with the development of modern Python open-source tools.

### *The Impedance Assessment Workflow*

Developing a robust impedance model for each device is central to the workflow. In practice, analytical methods provide accurate impedance predictions for simplified structures, while for realistic accelerator components with complex geometries, the numerical solution of Maxwell's equations is required.

To accurately simulate the full-wave impedance response of a device, we have relied on the commercial CST Wakefield solver. However, the first open-source alternative, `Wakis` [2], is currently under development at CERN. Built with modularity in mind, several of its functionalities are already integrated in the impedance workflow. For instance, the `IDDEFIX` module allows for characterization of impedance modes via the resonator formalism $\{f_r, R_s, Q\}_{\mathrm{mode}}$, fitted using differential evolution [3] even for partially decayed (short-wakelength) simulations.

To evaluate beam-induced heating due to impedance, the `BIHC` module was developed to provide total and—pairing with `IDDEFIX`—mode-by-mode power loss values. The beam-induced heating of the device in the single beam scenario can be estimated by:

$$P = 2(f_0 e N_{beam})^2 \cdot \sum_{p=0}^{+\infty} |\Lambda(p\omega_0)|^2 \Re[Z_{\parallel}(p\omega_0)], \quad (1)$$

where $f_0$ is the revolution frequency of the machine, $e$ is the charge of the particle, $N_{beam}$ is the total number of particles in the beam, and $\Lambda$ is the normalised beam spectrum. For devices located in a collider common chamber, the two-beam formalism [4] is applied. To account for frequency uncertainties in narrow resonances, `BIHC` provides a statistical analysis by rigidly shifting the impedance curves by integer multiples of the revolution frequency to cover the full spectral line spacing, reporting min/avg/max (and occurrence) of $P_{\mathrm{loss}}$ at key cycle points (e.g. flat-top) [5], when the bunch length shrinks and the beam spectrum interacts with the impedance over a broader range of frequencies.

By extracting the electric **E** and magnetic **H** field distributions at each resonant mode's frequency $f_r$, the fraction of power dissipated in each material can be computed. Each mode's field distribution is then weighted by the mode power loss to provide a 3D power loss map. Using `Wakis` geometry processing capabilities, the 3D power loss map can be interpolated to the device's STL geometry to analyze sources of localised heating. The power loss map is given to the component owner to perform thermo-mechanical simulations in order to ensure the device's integrity and guide possible design changes.

To assess the impact on beam stability, the transverse $Z_{\perp,x}, Z_{\perp,y}$ impedance of every accelerator component, weighted by the local beta-functions, is gathered to build an impedance model of the accelerator, used as an input for beam-dynamic studies. Macroparticle tracking simulations (e.g. with `Xsuite` [6]) or semi-analytical Sacherer predictions are used to determine beam instability limits and optimise operational knobs.

In this contribution, four case-studies that followed the presented workflow are discussed, showing how the methodology enabled the understanding and mitigation of impedance-driven limitations.

* elena.de.la.fuente.garcia@cern.ch
† carlo.zannini@cern.ch

ISBN: <ask the JACoW BoD> ISSN: <ask the JACoW BoD> doi: 10.18429/JACoW-HB2025-WECDB03

# OPTIMIZATION OF BEAM PERFORMANCE BY CORRECTION OF IMPEDANCE DRIVEN TUNE SHIFTS AT THE CERN SPS

I. Mases Sole*,[1], F. Asvesta, H. Bartosik, K. Li, C. Zannini, CERN, Geneva, Switzerland
G. Franchetti[1], GSI, Darmstadt, Germany
[1]also at Goethe University Frankfurt, Frankfurt, Germany

*Abstract*

High-intensity multi-bunch beams in the CERN Super Proton Synchrotron (SPS) experience significant coherent and incoherent tune shifts due to the transverse beam coupling impedance. Studies with LHC-type beams have been performed to optimize the working point along the extended SPS injection plateau to enhance beam performance and beam brightness. The initial tune correction approach focused on adjusting the coherent tunes at each injection. We report here about measurements of emittance growth and beam losses for various working points and tune correction approaches in the multi-bunch scenarios. The results indicate that maintaining the incoherent tunes constant effectively mitigates emittance growth by avoiding resonances in the presence of space charge. These findings highlight the critical role of incoherent tunes in optimizing high-brightness beams in the SPS.

## INTRODUCTION

Following the implementation of the LHC Injector Upgrade (LIU) project [1] from 2019 to 2021, the intensity of LHC-type beams in the CERN SPS has been progressively increased from $1.3 \times 10^{11}$ p/b to $2.3 \times 10^{11}$ p/b. These high-intensity, multi-bunch beams are subject to significant collective effects during the long SPS injection plateau, which is needed for accommodating several batches from the pre-injectors, typically from three to five depending on the LHC filling pattern. Alongside space-charge effects that induce maximum incoherent vertical tune shifts of approximately $\delta Q_y^{\mathrm{SC}} \approx -0.2$ , the beams also experience tune shifts of comparable magnitude originating from the SPS beam coupling impedance. These impedance-driven tune shifts accumulate along the bunch trains (the bunches are grouped in a relatively small part of the ring circumference), leading to bunch-to-bunch tune variations [2]. Properly accounting for these variations is essential when setting the machine working point during the injection plateau, and understanding how the working point influences the beam brightness is the primary focus of this study.

Furthermore, high chromaticity and a strong bunch-by-bunch damper are needed for ensuring beam stability in the transverse planes [3, 4]. In the longitudinal plane, strong beam loading and instabilities need to be managed [5]. Achieving the LIU target beam parameters [6] with the tight budgets on losses (10 % total) and emittance blow-up (10 % from injection to extraction) has proven to be challenging. In particular, the beam suffers from losses on the injection plateau as well as transverse emittance degradation.

In 2024–2025, dedicated studies targeted the mitigation of these effects for high-intensity LHC beams in the SPS using the Q20 optics [7]. It was found that moving to higher vertical tunes than the nominal operational point tends to enhance losses, while the transverse emittances evolution was also affected. This paper presents the approach used to maximize beam brightness by fine-tuning both coherent and incoherent tunes along the SPS injection plateau.

## BEAM PARAMETERS

In this study, we focus on two beam variants: the so-called BCMS (Bunch Compression Merging and Splitting) beam and the Standard beam. Both have a bunch spacing of 25 ns, but the BCMS beam has higher brightness due to the way it is produced in the CERN pre-injectors (PSB and PS) [8]. Table 1 summarizes the main LIU target beam parameters for both variants at SPS injection and extraction. These parameters correspond to the requirements that the SPS needs to achieve for the HL-LHC [9].

For the BCMS beam, each injection from the PS consists of 48 bunches. On the long injection plateau of the SPS, 5 batches from the PS are accumulated, with 3.6 s between consecutive injections. This results in a train of $5 \times 48$ bunches (240 bunches) injected into the LHC. For the Standard beam, the PS provides batches of 72 bunches. In this case, 4 batches are accumulated and accelerated, leading to a total of 288 bunches transferred to the LHC.

Table 1: Target Parameters at SPS Injection and Extraction

| | **BCMS injection / extract** | **Standard injection / extract** |
|---|---|---|
| $N$ ($10^{11}$ p/b) | 2.57 / 2.32 | 2.57 / 2.32 |
| $\epsilon_{x,y}$ (µm) | 1.50 / 1.65 | 1.89 / 2.08 |
| $p$ (GeV/c) | 26 / 450 | 26 / 450 |
| $B_l$ (ns) | 3.0* / 1.65 | 3.0* / 1.65 |

* bunch length after filamentation

## CORRECTION OF COHERENT TUNES

Due to the beam coupling impedance, the beam particles in the SPS experience a coherent and incoherent tune shift. These tune shifts depend, among other parameters, on the bunch intensity, the filling scheme, and the total beam intensity [2]. With each successive batch injection, the tune

* ingrid.mases.sole@cern.ch

ISBN: <ask the JACoW BoD> ISSN: <ask the JACoW BoD> doi: 10.18429/JACoW-HB2025-WECDC01

# AI TECHNIQUES AND STRATEGIES FOR LINAC TUNING AT LNL

L. Bellan*, F. Grespan, D. Bortolato, M. Comunian, E. Fagotti, M. Montis, Y. K. Ong[1], A. Pisent
INFN-LNL, Legnaro, Italy
[1]also at University of Sapienza, Rome, Italy
N. Milas, R. Miyamoto, D. Nicosia, ESS, Lund, Sweden



*Abstract*

Based on the operational experience on the superconducting heavy ion linac ALPI, we introduced Machine Learning techniques to improve the performances and speed up the tuning of the ion linac at LNL. The technique proved to be particularly effective to overcome issues on the longitudinal matching. The algorithm has been adapted to be compatible with high intensity linacs, in terms of transverse and longitudinal acceptance, available diagnostics and machine protection prescriptions. After a detailed preparatory simulation work, the algorithm has been tested during the 2025 commissioning shift of the ESS linac. In this paper the results obtained in the ALPI and ESS campaigns.

## INTRODUCTION

Online tuning techniques are playing a pivotal role in supporting the operation of accelerators. Because of the ability to optimize high-dimensional parameter systems, they are a natural framework for such optimization. One of not trivial online optimization regards the longitudinal beam dynamics. In order to perform it efficiently, we present the studies and the approach followed for the tuning of two types of ion linac accelerators: the LNL heavy ion linac ALPI and the high intensity proton linac of ESS.

ALPI (Acceleratore Lineare Per Ioni) Fig. 1 is the last stage of acceleration of the heavy ion facility of Legnaro National Laboratories. It is CW folded independent cavities linac, equipped with 77 superconductive quarter waves (QW) cooled down at 4 K, divided in three groups (low-$\beta$ 0.055 at 80 MHz, medium-$\beta$ 0.11, high-$\beta$ 0.13 at 160 MHz both). One of ALPI injector is PIAVE, a superconductive 80 MHz RFQ (Radio Frequency quadrupole) PIAVE, which delivers the stable heavy ions.

The ESS accelerator (Fig. 1) is designed [1] to operate at a duty cycle of 4 % (a beam pulse of 2.86 ms, 14 Hz repetition rate) and will accelerate a proton beam of 62.5 mA pulse peak to 2 GeV energy. The warm linac is composed by a 4-vane RFQ and a DTL at 352.21 MHz, connected by a MEBT. The MEBT is equipped with 10 quadruples and three bunchers. It ensures the transverse and longitudinal matching at the DTL input which is critical for the appropiate beam input into SRFs. The superconductive section is composed by three families of cavities the spokes, the medium beta and high beta cavities (elliptic type), cooled down at 2 K by liquid helium. There are several diagnostics along the linac; of particular interests for this article are the BLoMs [2] (Beam Loss Monitors) along the linac and the Beam Dump ACCTs at the end of the line.

* luca.bellan@lnl.infn.it

## STRATEGY AND RESULTS

### *PIAVE-ALPI Studies*

From the beam dynamics point of view, the main weak point of ALPI is given by its lattice: it is composed by 3 normal conductive quadrupoles (for transverse focusing) and by 8 QWs cavities. This very long period impacts the longitudinal phase advance, transverse RF defocusing, and the QWs magnetic steering coming from the residual magnetic field on axis. The net result is a rather small longitudinal and transverse acceptance. as shown in Fig. 2. The input beam is equivalent to the input beam from PIAVE.

On one hand, there is no margin at all if any variation such as input baricenters change occurs. On the other hand, the changes are instantaneously translated in current loss at the FC (Farady Cup) placed after the high beta cavities. This charateristics was used as observable for the objective function of the algorithm. As a matter of fact, because of the old linac engineering and beam dynamics design, we observed several phase shifts of the baricenter of the input beam coming PIAVE during shifts, which could led to severe losses of the beam (> 70 %). For such cases, a complete retuning of the linac was necessary, which required several hours to be completed. A possible solution came from AI algorithms: we first tested in simulation the ability of AI algorithms to tune the phases of the cavities looking at the FC [3] in simulation (thorugh PSO algorithm), and then we decided to apply the ML learning ARBO [4, 5] (which is a modified Bayesian [6]) algorithm on the online machine to the absolute phases (of a maximum of $\pm$10 deg, in order to avoid to exit from the synchronicity) of each QW cavity of the low beta (24 cavities), looking at the FC after a magnetic bending. We ensure that the energy remains the same through the optimization setting the magnetic bending at the end of the accelerator chain as dispersive. In this way the current at FC becomes susceptible to the possible changes of the $B\rho$ of the beam induced by the possible phase cavities configurations explored by the ML algorithm.

The difference in energy resulted contianed within maximum $\Delta W/W = 0.2$ %. In June 2024 we attempted a full optimization of the linac. The beam accelerated was a $^{129}Xe^{25+}$ @ 4.9 MeV/u, 1 μA. Figure 3 shows the simulation analysis of the results obtained during the optimization of the phases.

The red area shows the longitudinal acceptance after optimization (see Fig. 4). The longitudianl acceptance was re-shaped in order to cover the new position of the beam

ISBN: <ask the JACoW BoD> ISSN: <ask the JACoW BoD> doi: 10.18429/JACoW-HB2025-WECDC03

# EXPLORING THE POTENTIAL OF $H_3^+$ FOR HIGH-INTENSITY APPLICATIONS

L. G. Zhang*, Y. N. Rao, H. W. Koay, P. Jung[1], T. Planche†,[1], TRIUMF, Vancouver, Canada
[1]also at University of Victoria, Victoria, Canada

*Abstract*

The use of $H_3^+$ (triatomic hydrogen ions) presents a promising alternative to the more conventional $H^-$ ions in high power proton accelerators. In this work, we examine the advantages of $H_3^+$ beams with respect to extraction efficiency, Lorentz dissociation, and space charge limits. The physical properties of $H_3^+$ enable it to overcome the injection/extraction energy and intensity limits, while still supporting charge exchange based injection and extraction with minimal beam loss. To further illustrate its potential, a conceptual design of a superconducting $H_3^+$ cyclotron is briefly presented, demonstrating both its technical feasibility and performance advantages.

## INTRODUCTION

High intensity proton accelerators are essential for applications such as spallation neutron sources, neutrino factories, and isotope production. The performance of these facilities is fundamentally constrained by space charge and beam loss limits. Most of these proton driven facilities rely on $H^-$ acceleration followed by charge exchange injection or extraction. [1–7] However, the use of $H^-$ limits the achievable injection/extraction beam energy and intensity. This is primarily due to two factors: Lorentz stripping in the high magnetic fields and the reduction of the stripping efficiency at higher energies.

The molecular ions $H_2^+$ [8] and $H_3^+$ [9] have emerged as attractive alternatives for $H^-$. In particular, $H_3^+$ (triatomic hydrogen ion) combines high binding energy with a stable symmetric structure, potentially overcoming key challenges faced by $H^-$ beams. This paper examines the fundamental properties and accelerator physics implications of $H_3^+$, highlighting its potential for high intensity applications.

## STRIPPING EFFICIENCY IN CARBON FOIL

For charge exchange stripping, bound electrons (for $H^-$) or molecular bonds (for $H_3^+$) are removed by interaction with a thin carbon foil. The efficiency of this process depends strongly on the ion's velocity and the corresponding stripping cross section, which varies differently for $H^-$ and $H_3^+$. In this section we will compare the stripping efficiency of these 2 ions as a function of energy.

### *Stripping of $H^-$*

The process occurs through two successive electron-loss collisions as the ion traverses the foil of thickness $T$ (in atoms/cm$^2$). The fractions of the beam in the three charge states ($H^- \equiv N_{-1}$, $H^0 \equiv N_0$, $H^+ \equiv N_1$) are governed by a set of rate equations

$$\frac{dN_{-1}}{dx} = -(\sigma_{-1,0} + \sigma_{-1,1})N_{-1}, \quad (1)$$

$$\frac{dN_0}{dx} = \sigma_{-1,0}N_{-1} - (\sigma_{0,1} + \sigma_{0,-1})N_0 + \sigma_{1,0}N_1, \quad (2)$$

$$\frac{dN_1}{dx} = \sigma_{-1,1}N_{-1} + \sigma_{0,1}N_0 - (\sigma_{1,0} + \sigma_{1,-1})N_1, \quad (3)$$

where $x$ is the path length (in atoms/cm$^2$) and $\sigma_{i,j}$ is the cross section for a particle to change from state $i$ to state $j$. In high energy beam, electron capture cross sections ($\sigma_{0,-1}, \sigma_{1,0}, \sigma_{1,-1}$) are typically small and often neglected for thin foils. The two dominant electron loss processes are

1. Single electron loss: $H^- \rightarrow H^0$ (cross section $\sigma_{-1,0}$)
2. Second electron loss: $H^0 \rightarrow H^+$ (cross section $\sigma_{0,1}$)

For a $H^-$ beam incident on a foil of thickness $T$ (in μg/cm$^2$), the final proton fraction, or stripping efficiency $\eta$, is given by the expression

$$\begin{aligned}\eta = N_1 &= 1 - N_{-1} - N_0 \\ &\approx 1 - \frac{\sigma_{0,1} \cdot e^{-\lambda_{-1}T'} - \sigma_{-1,0} \cdot e^{-\lambda_0 T'}}{\sigma_{0,1} - \sigma_{-1,0}},\end{aligned} \quad (4)$$

where $N_{-1}(T)$ and $N_0(T)$ are the solutions for the $H^-$ and $H^0$ fractions calculated by solving the Eqs. (1) and (2). $\lambda_{-1} = \sigma_{-1,0} + \sigma_{-1,1}$ and $\lambda_0 = \sigma_{0,1}$. The term $T'$ is the foil thickness in atoms/cm$^2$.

The dependence on the ion's kinetic energy $E$ is embedded in the cross sections ($\sigma_{i,j}$). For high projectile velocities, the $H^-$ electron-loss cross sections follow the scaling predicted by the Bethe-Born Approximation

$$\sigma_{i,j}(E) \propto \frac{1}{\beta^2}, \quad (5)$$

where $\beta = v/c$ is the relativistic velocity factor. Gillespie derived the cross section of $H^-$ stripping [10] based on Bethe's model and the scaling in his formula has also been verified by experimental data in carbon [11].

To calculate the efficiency $\eta(E)$ at a high energy $E$, one typically uses reference cross sections ($\sigma_{\text{ref}}$) measured at a lower energy $E_{\text{ref}}$ and scales them

$$\sigma_{i,j}(E) = \frac{\sigma_{i,j}(\infty)}{\beta(E)^2}, \quad (6)$$

* lzhang@triumf.ca
† Corresponding author, tplanche@triumf.ca

ISBN: <ask the JACoW BoD> ISSN: <ask the JACoW BoD> doi: 10.18429/JACoW-HB2025-THIAC02

# HIGH INTENSITY ION SOURCE ACTIVITY AT CEA

B. Bolzon†, M. Barant, V. Calvelli, O. Delferrière, A. Dubois, G. Ferrand, Y. Gauthier, D. Minenna, R. Penavaire, Y. Sauce, O. Tuske
Université Paris-Saclay, CEA Paris-Saclay, France



*Abstract*

CEA Paris-Saclay has been engaged for over three decades in developing high-intensity proton and deuteron sources, from the SILHI ECR ion source to large-scale projects such as FAIR, SPIRAL2, and LIPAc. Although these sources meet the required beam performance, continuous operation is limited by BN disk degradation. To enhance compactness, ease maintenance, and reduce beam emittance, a new family of sources, ALISES, has been developed. Design differences between SILHI-like and ALISES sources are presented, along with simulations highlighting the role of non-resonant cavities and evanescent-wave coupling in plasma ignition and sustainment. Experiments revealed similar BN disk degradation patterns in ALISES v3 and LIPAc sources, leading to hypotheses on the underlying mechanisms. Mitigation strategies under study include an improved RF ridged waveguide design to reduce breakdown risk and better match the plasma impedance. Tests with ALISES v3 of a solid-state amplifier replacing the magnetron demonstrated enhanced frequency stability, reduced current ripple and rise time, and precise RF control, offering more favourable operating conditions. These ongoing developments open promising perspectives for improving the long-term reliability of high-intensity ion sources.

## INTRODUCTION

CEA Paris-Saclay has been involved in the development of high-intensity Electron Cyclotron Resonance (ECR) proton and deuteron sources since the early 1990s, beginning with the High Intensity Light Ion Source (SILHI) [1] [2]. ECR ion sources were chosen due to their simplicity to produce light ion beams of high intensity, low divergence and emittance, and meeting robustness and relatively low maintenance requirements. Based on the success of SILHI, CEA has developed SILHI-like type sources for different projects such as the Facility for Antiproton and Ion Research (FAIR) [3], the second-generation On-line RAdioactive Ion beam Production Facility (SPIRAL2) [4] and the Linear IFMIF Prototype Accelerator (LIPAc) [5].

The LIPAc and SPIRAL2 ion sources operate in continuous mode (100% duty cycle), delivering deuteron beams of 100 keV/140 mA and 40 keV/5 mA, respectively, in terms of energy and current. In both facilities, Boron Nitride (BN) disks exhibit unfortunately rapid degradation, which can be attributed to the fact that a higher duty cycle leads to longer plasma exposure time and consequently faster wear. Located at both ends of the plasma chamber, BN disks play an essential role as their high Secondary Electron Yield (SEY) enhances the plasma electron density. Their degradation therefore represents a major concern for facilities demanding continuous operation and high availability, as maintenance must be performed more frequently than initially planned.

The physics behind these observations is not yet understood. However, despite BN disks degradations, SILHI-like type sources have showed that they can successfully deliver beams with parameters under project requirements.

Following these achievements, a campaign of R&D has been conducted since 2010 at CEA Paris-Saclay with the aim of simplifying the design of ECR ion sources in order to win in compactness, to ease maintenance and to lower beam emittance. A new source family was born, named ALISES for Advanced Light Ion Source Extraction System, with the two first versions named ALISES v1&2 and the last version, ALISES v3 [6]. While ALISES v3 source shows very promising performance [7], it was observed also BN disks degradation when operating this source with a continuous beam.

This paper first outlines the key design differences between SILHI-like type sources and the ALISES family, describes extraction system simulation tools and reports the beam commissioning results on ALISES v3.

Next, simulations of particle dynamics on ALISES v3 are presented, providing insights into the mechanisms governing plasma ignition and sustainment in non-resonant cavities.

Subsequently, BN disk degradation is analysed for both the LIPAc (SILHI-like) and ALISES v3 sources, revealing similar patterns. Preliminary studies aimed at understanding and mitigating this degradation are then discussed.

Finally, first tests performed on ALISES v3 with a Radio Frequency (RF) Solid-State Amplifier (SSA), used as a replacement for the conventional magnetron, are reported. The objective is to assess the potential of this new RF chain to enhance the reliability of high-intensity ion sources.

## DESCRIPTION OF CEA SOURCES

### *SILHI-Like Type Sources vs ALISES Family*

Both SILHI-like type sources and ALISES family are based on ECR heating, with the 87.5 mT iso-surface, corresponding to the ECR zone, located inside the plasma chamber. Microwave injection is achieved via a three-step ridged waveguide, focusing the RF field onto the source axis. Plasma heating is provided by a 2.45 GHz, 2 kW industrial magnetron (SAIREM), driven by an analog pulse generator. The plasma chamber ends are closed with BN disks. Their high SEY increases plasma density, while BN sputtering gradually coats the chamber walls, further enhancing plasma performance. Beam extraction is performed through a five-electrode, water-cooled column

† benoit.bolzon@cea.fr

ISBN: <ask the JACoW BoD> ISSN: <ask the JACoW BoD> doi: 10.18429/JACoW-HB2025-THCAB01

# THE EFFECT OF MAGNET ALIGNMENT ON CLOSED ORBITS IN THE ISIS RAPID CYCLING SYNCHROTRON

H. Rafique*, H. V. Cavanagh, B. Kyle, C. M. Warsop, ISIS Neutron and Muon Source, UK

*Abstract*

The ISIS Rapid Cycling Synchrotron (RCS) operates at a repetition rate of 50 Hz and delivers high-intensity proton beams of up to $3 \times 10^{13}$ protons per pulse at 800 MeV to two neutron and one muon production targets. Maintaining control over the closed orbit is essential to optimal performance. Magnet alignment surveys are now regularly carried out during accelerator shutdowns, translated into misalignments, and applied to a cpymad model of the RCS. The model is used to identify realignment candidates and infer the bare (uncorrected) orbit. This paper includes comparison of inferred and measured bare orbits, and the operational implications of realignment based on the model. The approach demonstrates the value of integrating magnet alignment survey data with beam dynamics modelling to inform machine setup and improve operational performance in high-intensity synchrotrons.

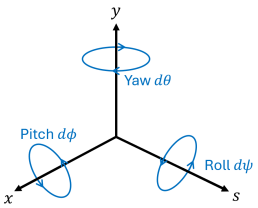


Figure 1: Definition of angular misalignments using MAD-X convention, note that pitch $d\phi$ about the horizontal axis is left-handed, whereas yaw and roll are right-handed [5].

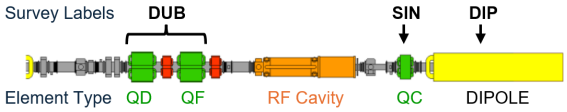


Figure 2: Single super-period magnet layout of the ISIS RCS with magnet types and survey labels.

## INTRODUCTION

To optimise operations and inform ISIS II design the Accelerator Physics Group at ISIS is currently engaged in combining benchmarked accelerator models with measurement based setup [1]. Previous work has reported on improvements in loss from realignment of single magnets [2], but there has not been a detailed investigation of magnet misalignment and the resulting effects on closed orbit distortion since commissioning. Understanding of the bare orbit is fundamental to model-based operational optimisation. The goal of this study is to define misalignments from first principles, suggest realignment candidates, and quantify the contribution of misalignments to the bare orbit.

Misalignments are defined by comparing original design data to survey data taken in shutdown periods. The effect of misalignments on the closed orbit is inferred by applying individual magnet misalignments to a MAD-X [3] lattice model, where the bare tune and the effect of individual corrector magnets has been benchmarked against measurements. The model-inferred orbits are compared to measurements, providing further insight into the effect of magnet alignment on the closed orbit in the ISIS RCS.

## DEFINING MISALIGNMENTS

Whereas the lattice model in MAD-X format uses the curvilinear co-ordinate system $(x,\ y,\ s)$, design and survey measurements are in Cartesian $(X,\ Y,\ Z)$ [4]. We consider the six MAD-X alignment errors for a magnet, namely offsets in the curvilinear axes $(dx,\ dy,\ ds)$, and rotations about these axes $(d\phi,\ d\theta,\ d\psi)$ representing pitch, yaw, and roll, as defined in Fig. 1.

The ISIS RCS has a decagonal layout of 10 repeating super-periods, each consisting of four main magnets as shown in Fig. 2. The main sector dipole provides 36° of bending, and has two fiducial points, labelled C and D, one at each end, separated by a chord length of 4350 $\pm$ 4 mm [4]. A quadrupole doublet sits on a single frame downstream of the main dipole. First, a defocussing quadrupole (QD) followed by a focussing quadrupole (QF) with centroids 3410 mm and 4846 mm from dipole fiducial point D respectively. The doublet quadrupoles each have two fiducial points, DUB A and DUB B on the QD are separated by 739 mm, DUB C and DUB D on the QF are separated by 722 mm [4].

A set of trim quadrupoles are placed immediately after each doublet quadrupole, these are not surveyed. The super-period straight ends with a defocussing singlet QC quadrupole which has no fiducial points. Since January 2025, in order to support this work, singlet quadrupole positions are measured using a bespoke alignment jig. As there are two fiducial points for each main magnet, one at each end, it is not possible to define the roll angle $(d\psi)$.

For each magnet, a vector is defined as that between the two fiducial points. Design vectors are those defined using the design positions, and survey vectors are those defined using the measured survey positions. The Cartesian vertical $Z$ and curvilinear vertical $y$ are equivalent, thus $d\phi$ and $dy$ misalignments are defined as the difference between design and survey vectors for each magnet.

In the curvilinear horizontal plane $x$, the design vector in the Cartesian $(X,\ Y)$ plane for each magnet is translated to a local co-moving frame $(\hat{s},\ \hat{x})$ such that it is centred on $(\hat{s},\ \hat{x}) = (0, 0)$ and aligned along the $\hat{s}$ axis. As a first approach the same transformation is performed on the corre-

* haroon.rafique@stfc.ac.uk

ISBN: <ask the JACoW BoD> ISSN: <ask the JACoW BoD> doi: 10.18429/JACoW-HB2025-THCAC01

# LINAC4 ION SOURCE: STATUS, PERFORMANCE AND OPERATION

J. B. Lallement[†,1], G. Bellodi[1], S. Bertolo[1], F. Di Lorenzo[1], A. M. Lombardi[1], A. Mamaras[1,2], C. Mastrostefano[1], M. O'Neil[1], E. Pasino[1], E. Sargsyan[1]
[1]CERN, Geneva, Switzerland
[2]Aristotle University of Thessaloniki, Thessaloniki, Greece

*Abstract*

The Linac4 H⁻ ion source plays a vital role for the CERN operation and experimental users. Its performance and availability have a direct and critical impact on the CERN's proton accelerator chain and the physics programs it supports. This paper presents an overview of the system, the operational experience and the lessons learned during the full five years of official running. Key topics as installation and maintenance strategy, spare parts management, cesiation procedure, automated RF power regulation and recent upgrade and improvements are discussed together with current performance metrics and availability figures.

## INTRODUCTION

Since 2021, Linac4 is the proton beam injector for CERN's accelerator complex, including the Large Hadron Collider (LHC). It accelerates negative hydrogen ions, H⁻, to 160 MeV and transfers them to the Proton Synchrotron Booster (PSB). The ions are stripped of their two electrons during the PSB charge exchange injection process. Linac4 is an 80 m-long normal conducting linac consisting of a 45 keV cesiated RF ion source, a low-energy beam transport (LEBT), a 3 MeV radio-frequency quadrupole (RFQ) resonating at 352 MHz, a medium-energy beam transport (MEBT) with a beam chopper and 3 buncher cavities, 3 drift-tube linac (DTL) tanks up to 50 MeV, 7 cell-coupled drift-tube linac (CCDTL) modules to 102 MeV, and 12 pi-mode structure (PIMS) cavities reaching 160 MeV. The beam chopper modulates the beam pulse time structure to limit beam losses during PSB beam injection and capture processes and when switching between its 4 superimposed rings. The peak beam current from the source is 40 mA, resulting into 32 mA out of the RFQ and 30 mA peak current at the PSB injection with pulse length modulated between 0 and 600 µs, depending on user's beam requests, at 0.83 Hz repetition rate.

The ion source is composed of a ceramic (Al2O3) plasma chamber with an external five-turn RF antenna. Hydrogen gas is injected via a pulsed solenoid valve and a 2 MHz RF amplifier can provide up to 100 kW power to ignite and sustain the plasma. The source is operated in surface H⁻ production mode, with a continuous caesium injection. In routine operation, the ion source produces 850 µs beam pulses requiring about 35-40 kW of forward RF power. The first part of the beam pulse (250 µs) is affected by two transient processes; the source current rise time and space charge compensation build up time. It is sent through the RFQ but fully dumped at 3 MeV, in the MEBT.

† jean-baptiste.lallement@cern.ch

## DESIGN AND PERFORMANCE IMPROVEMENTS

From 2017 until the end of the run in 2022, Linac4 was operated using the ion source version IS03 [1], which was producing H⁻ ion beam with a current of 35 mA, resulting in 27 mA at 3 MeV. During that period, attempts to run with higher current from the source did not result in a higher intensity out of the RFQ. This limitation was mainly due to the extracted beam emittance exceeding the RFQ transverse acceptance. The IS03 extraction design, which included a puller-dump electrode at an electric potential of 10 kV, could withstand a high co-extracted electron current, which allowed the source to operate with or without caesium. Over the years, the cesiation process was better managed and finally routinely used for surface H⁻ production. A new geometry of the source extraction electrodes could therefore be developed and optimised, assuming a reduced co-extracted electron current, for higher beam currents of up to 50 mA [2]. The new IS04 source extraction system has a simplified design with only three electrodes: plasma, puller, and ground. The puller-dump and Einzel lens of the previous source version causing undesired emittance growth were eliminated. Having one power supply less also proved to be beneficial for the reliability and the availability of the source and consequently of the linac. Co-extracted electrons are now disposed of at 45 keV onto a dedicated dump after deflection by a permanent dipole magnet housed at the base of the dump. The dump can be biased with a voltage of up to +1 kV to contain secondary electrons produced on the dump and create a potential barrier for the positive compensation particles collected in the beam in the low-energy beam transport section. Beam extraction simulation of the two versions of the ion source are shown in Fig. 1.

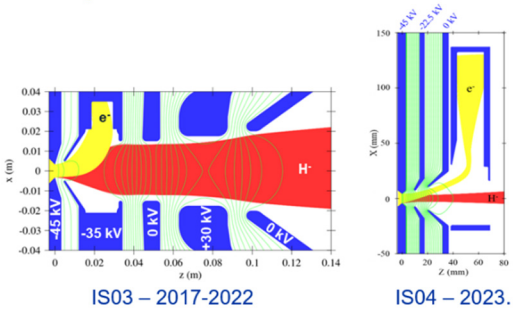


Figure 1: IS03 and IS04 extraction systems and beam envelopes (red H⁻, yellow e⁻). The electrons are dumped at energies of 10 keV and 45 keV respectively.

The new source extraction system has been thoroughly tested at the Linac4 test stand [3] in 2022 to characterize

ISBN: <ask the JACoW BoD> ISSN: <ask the JACoW BoD> doi: 10.18429/JACoW-HB2025-THCBB02

# STATUS AND FUTURE OF THE BEAM GAS CURTAIN: A NON-INVASIVE PROFILE AND EMITTANCE MONITOR FOR HIGH-INTENSITY HADRON MACHINES

H. D. Zhang*,[1], M. Patel[1], O. Stringer[1], C.P. Welsch[1], University of Liverpool, United Kingdom
D. Butti, T. Lefevre, C. Pasquino, G. Schneider, R. Veness
CERN, Geneva, Switzerland
P. Forck, S. Udrea, GSI, Darmstadt, Germany
[1]also at Cockcroft Institute, Warrington, United Kingdom

*Abstract*

High-intensity hadron machines host beams with destructive power, and traditional beam profile monitors, such as scintillating screens and wire scanners, suffer a short lifetime under such severe conditions. The application of the beam gas curtain monitor (BGC) in the LHC, along with 3 years of successful operation, fills the gap in such measurements in a minimally invasive manner for high-intensity hadron machines. By using a supersonic gas curtain with a tailored shape and gas density, the monitor satisfies the requirements of vacuum, resolution, and machine protection. In this contribution, the operational experience of BGC in the LHC will be discussed, as well as the development plan in the phase of HLLHC, and the possible halo monitor for hadron machines.

## INTRODUCTION

The beams in Hadron machines, especially those in spallation sources and colliders, typically have high energy and intensity, which poses a destructive power to accelerator components. Without good control and monitoring, the power deposited on the accelerator systems could cause magnet quench, beam dump, unexpected nuclear activation, and even machine damage. With those concerns, accelerators sometimes have to be operated at reduced intensities or luminosities, which limits the machine's full potential.

Online beam profile measurement and emittance monitoring associated with better beam control are the keys to preventing those unwanted events and pushing the boundary of the machine operation. However, due to the same destructive power of the beams, few methods are available. Wire scanners [1] are the most popular ones used in most hadron facilities. Since the wires directly interact with the beam, their durability is an issue, and thus they normally work in a reduced intensity. Residual gas-based methods such as ionisation beam profile monitors (IPM) [2] or beam-induced fluorescence monitors (BIF) [3] were also used in Hadron machines and are intrinsically non-invasive. A dipole system was required in an IPM system when secondary electrons are collected from the ionisation by the beam to achieve a required resolution. Electrodes that provide a high voltage channel to collect the secondary particles also make the device very complicated and suffer from heating due to impedance. Meanwhile, the BIF monitor requires only a simple optical system, but due to the low cross-section and limited solid angle to collect fluorescent photons, a local pressure bump is usually required to increase the signal level.

The usage of a supersonic gas curtain [4, 5] provides an alternative way to introduce a pressure bump in a controllable manner. By generating a gas curtain, it also provides a screen for two-dimensional detection by using either IPM or BIF modes. The beam gas curtain (BGC) monitor, based on this concept and using fluorescence detection, was applied in the Large Hadron Collider (LHC) and has been operated for almost three years. Based on the experience gained from the operation, the device can be adapted to other high-intensity hadron machines as well.

## PRINCIPLE

As shown in Fig. 1, a supersonic gas curtain was generated through a molecular beam generating system. It started from a 30 µm nozzle and three stages of skimmers. A fourth skimmer was used for the molecular beam to flow through, but to prevent the molecular beam from flowing back. Those skimmers separate the whole system into chambers to allow differential pumping and help preserve the vacuum conditions in the main accelerator channels. The third skimmer with a slit oriented in 45° makes a screen-like gas curtain allowing for a two-dimensional measurement. Simulation tools [6] were developed to design and optimise the curtain generating system with respect to the target curtain shapes, density, and background pressure to satisfy the application.

Two modes, both IPM and BIF, can be used to operate the gas-curtain-based profile monitor. The former one collects secondary particles from the interaction between the gas curtain and the beam. Those particles can be electrons or ions. Because the ionisation process features a stronger signal due to a larger cross-section and the efficiency of collecting secondaries, the associated gas curtain monitor should allow for measurement with a short integration time [4] or even bunch-to-bunch [7]. So far, only ions have been collected for detection due to their large mass and low velocity spread from supersonic molecular beams, resulting in less distortion due to space charge and any other stray fields. If electrons are collected, a dedicated dipole magnet needs to be implemented to achieve the desired resolution. This has not been

* haozhang@liverpool.ac.uk

ISBN: <ask the JACoW BoD> ISSN: <ask the JACoW BoD> doi: 10.18429/JACoW-HB2025-THCBC01

# OVERVIEW OF PRESENT AND FUTURE HADRON BEAM COLLIMATION*

S. Redaelli for the LHC Collimation Teams, CERN, Geneva, Switzerland

*Abstract*

The collimation system of the Large Hadron Collider (LHC) at CERN represents the state of the art of multi-stage collimation systems for high-intensity hadron beams. It provides an excellent cleaning performance that has so far ensured safe and efficient operation of the LHC with beam stored energies well above 400 MJ. However, further improvements are needed in view of the High-Luminosity upgrade of the LHC (HL-LHC) that will start operation in 2030. The performance of the LHC beam collimation is reviewed, addressing in particular a first-phase upgrade that was deployed for the LHC Run 3 (2022-2026). The remaining challenges for the HL-LHC and the solutions being implemented are then reviewed. Applications to future colliders under study are also discussed.



## INTRODUCTION

The Large Hadron Collider (LHC) at CERN is a 27 km-long circular proton and heavy-ion collider [1]. The machine is currently in the penultimate year of Run 3 (2022–2026), which will be followed by LS3 (Long Shutdown 3, 2026–2030) to implement the High-Luminosity LHC (HL-LHC) upgrade [2]. This upgrade will nearly double the beam current and increase the peak luminosity by a factor of five, imposing stringent requirements on the collimation system [3]. Substantial upgrades during previous shutdowns have already improved the collimation performance and validated key HL-LHC design solutions. Run 3 therefore represents a transition toward HL-LHC operating conditions. As illustrated in Fig. 1, the stored beam energy at 6.8 TeV now routinely exceeds 400 MJ, with a record of 458 MJ achieved in October 2025.

The current performance of the LHC collimation system is a key asset for the physics programme and provides a strong foundation for the upgrades planned for LS3. It also serves as a test bed for future hadron accelerators, such as the FCC-hh [4]. This paper reviews the LHC collimation design and performance, outlines the HL-LHC upgrade strategy, and introduces the preliminary FCC-hh collimation concepts.

## LHC BEAM COLLIMATION IN RUN 3

Collimation systems [5] are designed to control beam losses and protect accelerator components, with performance goals defined by machine-specific loss scenarios and operational constraints. For the LHC, their primary role is to clean betatron and off-momentum halos, intercepting halo particles before they reach sensitive equipment and ensuring that losses remain below the quench limits of superconducting magnets. Collimators also provide passive machine protection as the first line of defense against abnormal losses and failure scenarios, keeping energy leakage below damage thresholds. In colliders, dedicated devices intercept collision products and reduce radiation to critical components, thereby enabling efficient high-luminosity operation. Additional objectives include minimizing detector backgrounds, localizing radiation in controlled areas to facilitate maintenance, shielding equipment to extend its lifetime, and enabling active halo scraping.

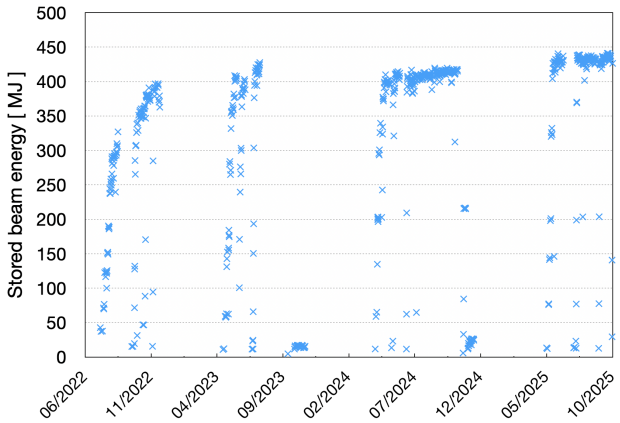


Figure 1: LHC beam stored energy in Run 3.

The LHC collimation system [6] fulfills each design criterion listed above. Halo collimation in the LHC is achieved through a multistage system comprising primary (TCP), secondary (TCS), and active absorber (TCLA) collimators in IR3 (momentum cleaning) and IR7 (betatron cleaning). Tertiary collimators (TCTs), made of tungsten alloy, intercept remaining halo particles by protecting the inner triplet magnets and detectors in all collision points. Physics debris collimators (TCLs), are installed downstream of ATLAS and CMS to intercept collision debris; and injection- and dump-protection collimators are installed at IR6, IR2, and IR8. The hierarchical collimator settings ensure that each device intercepts only the halo fraction for which it is designed, maintaining optimal performance and protection.

The main LS2 collimation upgrades [7] include: (1) twelve new low-impedance collimators in IR7 for betatron cleaning—four TCPs and eight TCSs—using molybdenum-graphite (MoGr) jaws, with TCPs in bulk MoGr and TCSs coated with 5 µm of Mo (Mo-MoGr) [8]; (2) two TCLD collimators in the dispersion suppressor (DS) regions around ALICE [9] to dispose of losses from heavy-ion collisions; (3) four crystal primary collimators (TCPCs) in IR7 to enhance betatron cleaning of heavy-ion beams [10]; (4) two passive absorbers (TCAPM) in IR7 to reduce radiation wear on warm quadrupoles [11]. All new TCP, TCS, and TCLD collimators

* Work supported by the HL-LHC project.

ISBN: <ask the JACoW BoD> ISSN: <ask the JACoW BoD> doi: 10.18429/JACoW-HB2025-THCBC02

# LOW-FREQUENCY TRANSVERSE RESONATOR IMPEDANCES ON THE ISIS PROTON SYNCHROTRON

D. W. Posthuma de Boer*,[1], C. M. Warsop, R. E. Williamson
ISIS Neutron and Muon Source, Rutherford Appleton Laboratory, Harwell, UK
[1]also at John Adams Institute, Oxford, UK



*Abstract*

ISIS is the pulsed, spallation neutron and muon source at the Rutherford Appleton Laboratory in the UK. Its rapid cycling synchrotron accelerates $3 \times 10^{13}$ protons-per-pulse from 70 to 800 MeV at 50 Hz, delivering a mean beam power of 0.2 MW to its two target stations. The intensity of ISIS is beam-loss limited, so increasing its neutron and muon output requires beam-loss mechanisms to be well understood and alleviated.

Despite mitigation efforts, a vertical head-tail instability is often one of the main sources of beam-loss during high-intensity operations at ISIS. Finite-element simulations and probe-coil measurements have identified a series of low-frequency resonator impedances from the RF screens in the AC magnets. New bench measurements of RF screens will be presented that provide further evidence of them being responsible for the beam instability, and have been used to inform an update to the impedance model. A comparison between this model and beam-based impedance measurements will be presented, as well as analytical predictions for beam stability at ISIS. A possible method to mitigate the RF screen resonator impedances will also be introduced.

## INTRODUCTION

The ISIS Neutron and Muon Source has successfully operated for 40 years. Key parameters of the rapid cycling synchrotron (RCS) which drives the facility are listed in Table 1. Its dual harmonic RF system accelerates up to $3 \times 10^{13}$ protons to 800 MeV with a repetition rate of 50 Hz, producing a mean beam power of 0.2 MW. Its proton beams collide with one of two fixed targets to produce spallation neutrons for various experiments, and also produce muons from an intermediate target.

ISIS has reported a vertical head-tail instability around 2 ms through its 10 ms RCS cycle for over three decades. It was originally attributed to resistive-wall impedances [1], but its intra-bunch structure and growth rate did not match predictions [2]. More recently, beam-based impedance measurements hinted at a large 85 kHz narrowband impedance [3], but common sources of low-frequency resonances such as kicker magnets could not explain the observation [4]. A possible source of this low-frequency resonator impedance was identified on the RF screens used inside the AC magnets at ISIS, which make up > 50 % of its circumference [4]. The same structures were also found to be candidate drivers of the 2 ms instability.

* david.posthuma-de-boer@stfc.ac.uk

Table 1: Key ISIS Synchrotron Parameters

| Property | Value |
|---|---|
| Kinetic Energy Range | 70 - 800 MeV |
| Number of Bunches ($M$) | 2 |
| Average Radius ($R$) | 26 m |
| No. of Superperiods | 10 |
| Gamma Transition | 5.034 |
| Nominal Tunes ($Q_x, Q_y$) | 4.31, 3.83 (variable) |
| Peak Incoherent Tune Shift | ~ −0.5 [3] |
| Chromaticity ($\xi_x$, $\xi_y$) | −1.1, −1.1 [5] |

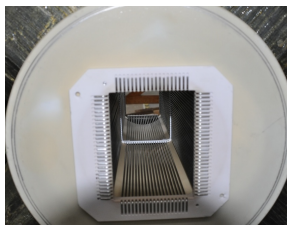

(a)

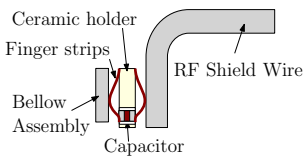


(b)

Figure 1: Photograph of a singlet quadrupoles's RF screen (a) and a schematic view of a capacitive connection (b).

## RF SCREEN IMPEDANCES

Alumina vacuum vessels are used inside all the 50 Hz AC magnets at ISIS, to prevent eddy currents and the associated Ohmic losses which would be induced in a conducting chamber [6]. To prevent the beam's electromagnetic (EM) fields penetrating the ceramic chamber, conducting RF screens are installed in the aperture of each alumina vessel. These are usually formed of 2.3 mm diameter stainless steel wires stretched over the length of the vessel, as shown in Fig. 1(a). To prevent eddy currents from flowing in this screen, a capacitive connection at one end of each wire presents a large impedance at 50 Hz, but a much smaller one to any beam-induced currents; see Fig. 1(b).

CST simulations of these capacitively coupled RF screens predict narrowband vertical driving impedances on the order of some $\mathrm{M\Omega\,m^{-1}}$ per screen for a $\beta = 1$ beam [4]. Figure 2 shows that the resonant frequencies are clustered around ~ 90 and 200 kHz.[1] Peaks in $\Re\left(Z_1^{\perp}\right)$ were fitted to the transverse resonator impedance

$$Z_1^{\perp}(\omega) = \frac{\omega_r}{\omega} \frac{R_{\perp}}{1 + iQ_r\left(\frac{\omega_r}{\omega} - \frac{\omega}{\omega_r}\right)}, \qquad (1)$$

[1] An earlier report of a 300 kHz peak was due to neglecting differences in capacitors used on the dipole RF screens.

ISBN: <ask the JACoW BoD> ISSN: <ask the JACoW BoD> doi: 10.18429/JACoW-HB2025-THCBC03

# LASER-ASSISTED H⁻ STRIPPING INJECTION FOR THE CSNS-II RCS*

Z. X. Pang[1,2,3], M. Y. Huang[†,1,2,3], W. J. Han[1,2], C. D. Dong[1,2,3]
[1]Institute of High Energy Physics, Chinese Academy of Sciences, Beijing, China
[2]Spallation Neutron Source Science Center, Dongguan, China
[3]University of Chinese Academy of Sciences, Beijing, China



*Abstract*

For the China Spallation Neutron Source, the laser-assisted H⁻ stripping is a new essential technology. It can be an alternative to the foil stripping which may be used to solve various difficulties faced by the stripping foils, such as short lifetime, high temperature, large radiation dose, etc. In this paper, based on the phase II of China Spallation Neutron Source (CSNS-II), the laser-assisted H⁻ stripping injection method has been studied in depth. First, the physical principle of laser-assisted H⁻ stripping injection is deeply explored theoretically. The influencing factors of laser and H⁻ beam interaction, Lorentz stripping and other processes are studied. Second, the influences of injection beam parameters on the Lorentz stripping and laser excitation are studied, and the emittance growth of injection beam after stripping is explored. Finally, based on the beam parameters of the CSNS-II, the design scheme of the laser-assisted H⁻ stripping injection has been proposed.

## INTRODUCTION

Negative hydrogen charge exchange injection is an effective method to break the Liouville's theorem and achieve beam accumulation in the multi-turn injection process for the synchrotron. Currently, various carbon foils are commonly employed in high-intensity proton accelerator facilities to realize negative hydrogen stripping injection [1]. However, with the continuous increase in beam power, various difficulty problems have been caused by the method for the operation of the synchrotron, such as: the evaporation phenomenon induced by the peak temperature rise of carbon foils in high intensity beam environments, which leads to reduced foil lifetime [2], large uncontrollable beam loss and radiation dose caused by the foil scattering, and the electron cloud effect resulting from the re-trapping of stripped electrons by the circulating beam[3]. To address the issues, many schemes have been attempted in various laboratories over the past few decades, among which the magnet-laser-based laser-stripping injection scheme exhibits the highest feasibility.

Based on the beam parameters of the accelerator in the CSNS-II, a novel laser-stripping injection scheme is proposed, as shown in Fig. 1 and Table 1. In the first step, a longitudinal high-gradient dipole magnet is used to strip the negative hydrogen beam into hydrogen atoms with only one electron. In the second step, 266 nm and 532 nm lasers are employed to excite the hydrogen atoms to the second excited state in a sequential process. Finally, a 1064 nm laser is utilized to ionize the excited hydrogen atoms into protons. Currently, the development of the first-stage stripping magnet for CSNS-II has been completed. To reduce the implementation difficulty of laser parameters in this project, numerous conceptual attempts are currently experimented.

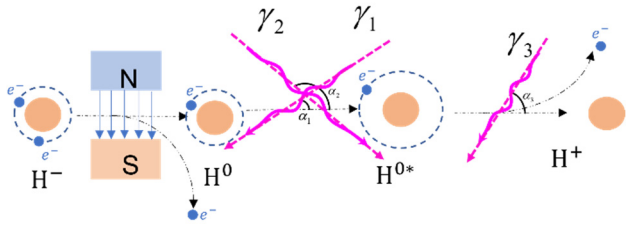


Figure 1: Schematic view of the concept of H⁻ stripping to proton based on CSNS-II.

Table 1: Parameters of CSNS Laser-Stripping Project

| Parameter | Value |
|---|---|
| beam kinetic energy (MeV) | 400 |
| Micro-pulse (ps) | 8.1 |
| Meso-pulse (ns) | 291 |
| Macro-pulse (ms) | 0.5 |
| Emittance-x (mm mrad) | 0.46 |
| Emittance-y (mm mrad) | 0.51 |
| Beta-x (m) | 4.9 |
| Beta-y (m) | 4.4 |
| Energy spread ($10^{-4}$) | 2.0 |
| Frequency (MHz) | 324 |

## LONGITUDINAL HIGH-GRADIENT DIPOLE MAGNET

When a relativistic energy-level negative hydrogen moves in a magnetic field, its neutralization lifetime can be expressed as [4]:

$$\tau = \frac{A_1}{\gamma\beta c B_\perp}\exp\left(\frac{A_2}{\gamma\beta c B_\perp}\right), \qquad (1)$$

$$A_1 = 2.47\times10^{-6}\ sV/m,$$

$$A_2 = 4.49\times10^{9}\ V/m,$$

where β and γ are relativistic parameters of H⁻ particles,

* This work is jointly supported by the Guangdong Basic and Applied Basic Research Foundation (No. 2021B1515120021).
† huangmy@ihep.ac.cn

ISBN: <ask the JACoW BoD> ISSN: <ask the JACoW BoD> doi: 10.18429/JACoW-HB2025-THFA01

# MODELING OF LONG-BUNCH SPACE CHARGE IN CIRCULAR ACCELERATORS WITH UNFIXED CLOSED ORBIT

Kai Zhou, Ming-Yang Huang, Bin Wu, Hanyang Liu, Sheng Wang, Xiao Li
Institute of High Energy Physics, Chinese Academy of Sciences, Beijing, China



*Abstract*

A high-intensity simulation framework named PyFFAG has been developed for modeling beam dynamics in scaling Fixed-Field Alternating Gradient (FFAG) accelerators. The code is written in Python with computational kernels JIT-compiled by Numba. Key capabilities include MPI-based parallel multi-particle tracking, a 2.5D FFT-accelerated particle-in-cell (PIC) space-charge solver and multi-turn painting injection. This paper describes the physical model, numerical solvers, and preliminary benchmarking against other codes.

## INTRODUCTION

Scaling FFAG (Fixed-Field Alternating Gradient) accelerators are promising candidates for high-power pulsed proton drivers because of their fixed magnetic fields, large momentum acceptance, and potential for rapid-cycling operation.

The widely used Zgoubi code is well-suited for single-particle tracking and beam optics calculations for FFAG, but it lacks modules for space charge effects and multi-turn painting injection, which are essential for modeling high-intensity operation [1]. Other simulation frameworks, such as OPAL, include comprehensive 3D space-charge solvers, but these are based on uniform Cartesian meshes and are therefore inefficient for long, arc-shaped bunches typical of scaling FFAG accelerators [2].

To overcome these limitations, we have developed a new simulation code named PyFFAG, written in Python and accelerated using Numba JIT compilation and MPI parallelization. PyFFAG is designed to simulate the full beam dynamics of high-intensity scaling FFAGs, including a 2.5D space-charge model adapted to ring-like long bunches without a fixed closed orbit, and multi-turn painting injection for accumulation studies.

The core solvers employ fourth-order Runge–Kutta and relativistic Boris push algorithms in cylindrical coordinates, using time as the independent variable. The current implementation is still under active development and benchmarking, preliminary results indicate that PyFFAG can serve for modeling intense-beam dynamics in scaling FFAG accelerators.

## FORMULATION AND NUMERICAL METHODS

### *Equations of Motion*

Particle motion is described in cylindrical coordinates $(r, \phi, z)$ with time $t$ as the independent variable. The relativistic Lorentz force equations are:

$$\frac{d\mathbf{p}}{dt} = q(\mathbf{E} + \mathbf{v} \times \mathbf{B}), \qquad \frac{d\mathbf{r}}{dt} = \mathbf{v}. \tag{1}$$

These equations are integrated using either the fourth-order Runge–Kutta (RK4) or the relativistic Boris pusher. RK4 offers high precision for reference orbit and optics calculations, while the Boris algorithm provides symplectic-like stability for long-term multi-particle tracking.

### *Magnetic Field Construction*

Scaling FFAG magnets are characterized by large field gradients and strong nonlinearity, where both the radial and azimuthal field components vary rapidly. Accurate modeling of the mid-plane magnetic field is therefore essential before extrapolating to off-mid-plane regions.

In PyFFAG, the mid-plane field is analytically expressed as:

$$B_z(r, \varphi) = B_0(r)\, F(\varphi - s(r)), \tag{2}$$

where $B_0(r)$ represents the reference radial profile and $F(\varphi)$ describes the azimuthal modulation of the sector magnets.

To represent realistic soft-edge and fringe-field regions, the azimuthal function $F(\varphi)$ is constructed as a product of two sigmoid functions:

$$F(\varphi) = y_{\text{flat}} + (y_{\text{convex}} - y_{\text{flat}})\,[\sigma_k(\varphi - \varphi_0) - \sigma_k(\varphi - \varphi_1)], \tag{3}$$

with

$$\sigma_k(x) = \frac{1}{1 + e^{-kx}}. \tag{4}$$

This analytic representation provides a smooth transition between magnetic sectors and fringe regions. Since all derivatives of the sigmoid function can be obtained analytically, arbitrary high-order derivatives and nonlinear expansion terms are available without numerical differentiation. This feature allows accurate evaluation of field gradients and higher-order multipole components required for beam dynamics calculations.

The magnetic field components outside the mid-plane are obtained from the analytical mid-plane field using a Taylor expansion in the vertical coordinate $z$:

$$B_r = z\frac{\partial B}{\partial r} - \frac{z^3}{6}\frac{\partial}{\partial r}\left(\frac{\partial^2 B}{\partial r^2} + \frac{1}{r}\frac{\partial B}{\partial r} + \frac{1}{r^2}\frac{\partial^2 B}{\partial \theta^2}\right) + \cdots, \tag{5}$$

$$B_\theta = \frac{z}{r}\frac{\partial B}{\partial \theta} - \frac{z^3}{6r}\frac{\partial}{\partial \theta}\left(\frac{\partial^2 B}{\partial r^2} + \frac{1}{r}\frac{\partial B}{\partial r} + \frac{1}{r^2}\frac{\partial^2 B}{\partial \theta^2}\right) + \cdots, \tag{6}$$

$$B_z = B - \frac{z^2}{2}\left(\frac{\partial^2 B}{\partial r^2} + \frac{1}{r}\frac{\partial B}{\partial r} + \frac{1}{r^2}\frac{\partial^2 B}{\partial \theta^2}\right) + \cdots. \tag{7}$$

ISBN: <ask the JACoW BoD> ISSN: <ask the JACoW BoD> doi: 10.18429/JACoW-HB2025-THFA03

# SIMULATION STUDY ON SPACE CHARGE EFFECTS ON TRANSVERSE COUPLED-BUNCH INSTABILITIES

Li Rao[†,1,2,3], Liangsheng Huang[1,2], Hanyang Liu[1,2]
[1]Institute of High Energy Physics, Chinese Academy of Sciences, Beijing, China
[2]Spallation Neutron Source Science Center, Dongguan, China
[3]University of Chinese Academy of Sciences, Beijing, China

*Abstract*

Coupled-bunch instabilities will occur with long-range wakefields. And it's an effective way to adjust the chromaticity to suppress transverse coupled-bunch instabilities. There are some theoretical studies showing that strong space charge can weaken the suppression effect of chromaticity. In this paper, transverse coupled-bunch instabilities with space charge are simulated and analysed using PyHEADTAIL. Results reveal that under strong space charge, the oscillation modes depend solely on the longitudinal position, which weakens the effect of chromaticity, with higher-order modes becoming dominant. When space charge is extremely strong, only the 0 mode remains observable.

## INTRODUCTION

The China Spallation Neutron Source (CSNS) is based on a high-intensity proton accelerator which consisting of a negative hydrogen linac and a rapid cycling synchrotron (RCS) [1]. During the commissioning of the RCS, unexpected transverse instabilities were observed. These are identified as transverse coupled-bunch instabilities through systematic measurements and studies, with the impedance source attributed to ceramic chambers with RF shields [2]. The main parameters of the RCS and impedance are presented in Table 1.

With such low injection energy and high bunch intensity, space charge effects cannot be ignored (the space charge tune shift is about 0.27 at the injection stage). Many methods have been employed to control space charge effects and suppress instabilities such as the optimization of tune curve and chromaticity, achieving the RCS design power of 100kW. In recent years, machine upgrades have been steadily progressing toward the goal of 500 kW for the second phase of the CSNS. By installing two second harmonic cavities to increase the bunching factor [3], beam operation at 170 kW has been achieved. With the continuous increase of beam intensity, space charge effects and wakefield strength are also increasing, which motivates us to study the influence of space charge on instabilities for predicting and mitigating instabilities at higher beam intensities in the future.

## SIMULATION STUDY

We use PyHeadtail, a macro-particle code for simulating beam dynamics in particle accelerators with collective effects developed by CERN [4], to simulate the space charge effects and transverse coupled-bunch instabilities. The parameters of machine used in the simulation are essentially consistent with those in Table 1, except that the horizontal tune is set to 4.80 (which is closer to the actual tune). For simplicity, smooth focusing and DC mode are adopted in the simulation. The energy is the same as the injection energy, the RF voltage is set to 60 kV, in that case the synchrotron tune is 0.01. The bunch initial parameters are set as a single bunch with length of 40 m, transverse emittance of 20 mm·mrad, transverse KV distribution, and longitudinal waterbag distribution. The impedance parameters are also changed (the quality factor is 9 and the resonator frequency is 0.1 MHz). Since the study is at an early stage, our primary goal is to observe clear effects in the simulation rather than to precisely replicate the exact conditions of the real machine.

Table 1: Main Parameters of The RCS and Impedance

| Parameters | Values |
|---|---|
| Circumference [m] | 227.92 |
| Injection energy [GeV] | 0.08 |
| Extraction energy [GeV] | 1.6 |
| Harmonic number | 2 |
| Bunch number | 2 |
| Nominal tune (Hor/Ver) | (4.86/4.78) |
| Natural chromaticity (Hor/Ver) | (-4/-9) |
| Transition gamma | 4.9 |
| Bunch intensity (@100kW) | $7.8 \times 10^{12}$ |
| Shunt impedance [MΩ/m] | 2 |
| Quality factor | 40 |
| Resonator frequency [MHz] | 0.12 |

In the simulation, it was found that under certain parameter conditions (in this case, the chromaticity is $-6$, the shunt impedance is 2 MΩ/m, and the bunch intensity is $5\times10^{12}$), the inclusion of transverse space charge forces leads to two stages of growth in the beam centroid oscillation amplitude, as shown in Fig. 1. It can be seen that with space charge, a larger growth time of beam centroid ($\tau = 0.13$ ms) occurs before the 500th turn, while the growth time without space

† e-mail: raoli@ihep.ac.cn

ISBN: <ask the JACoW BoD> ISSN: <ask the JACoW BoD> doi: 10.18429/JACoW-HB2025-THFA04

# LONGITUDINAL LOCALIZED KICK DRIVEN FAST EXTRACTION METHOD FOR 3D PBS PROTON FLASH DELIVERY*

Y. Xiong[1], H. J. Yao[1], S. X. Zheng†,[1], Key Laboratory of Particle & Radiation Imaging, Tsinghua University, Ministry of Education, Beijing, China
[1]also at Laboratory for Advanced Radiation Sources and Application, Tsinghua University, Beijing, China



*Abstract*

The challenge of delivering FLASH irradiation to large volume targets within 100 ms using 3D pencil beam scanning (PBS) persists. A novel scanning scheme based on a rapid-cycling synchrotron (RCS) is proposed. This work introduces a longitudinal localized kick driven fast extraction method used in the scheme. By applying stripline kicker pulses to specific longitudinal segments of the bunch and dynamically adjusting the kick region based on real-time beam density, accurate spot dose delivery is achieved. Simulations show the results of spot dose accuracy and confirm controlled beam loss (< 10 %) during fall time, demonstrating the method's feasibility for 3D PBS proton FLASH therapy.

## INTRODUCTION

FLASH radiotherapy has demonstrated significant promise in radiation oncology due to its capacity to reduce normal tissue toxicity while maintaining tumor control [1–3]. However, a major challenge in proton FLASH therapy is delivering a sufficient dose rate (> 40 Gy/s) within an irradiation time on the order of 100 ms for large-volume targets. Conventional 3D pencil beam scanning (PBS) techniques, typically employing cyclotrons or synchrotrons, often require over 100 ms for such targets, thus failing to satisfy the FLASH criteria.

To address this timing limitation, we propose a novel irradiation scheme in which the proton beam is parallel to the scanning layers [4]. The scheme brings new requirements for extracting hundreds of beam from one bunch. This is realized by employing longitudinal localized kick driven fast extraction method. The conceptual framework and particle tracking simulation results of spot dose accuracy and beam loss of the approach are presented in this paper.

## LOCALIZED FAST EXTRACTION METHOD

In contrast to the conventional design, our proposed scheme necessitates the extraction of only a fraction of the bunch particles at each scanning point to finish the scanning of hundreds of spots within one layer. This key difference mandates a modification of the fast extraction system, as conceptually illustrated in Fig. 1, which compares the kicker pulse time relative to the bunch length. In conventional method, the flattop of the kick is applied to the entire bunch, with rising and falling edges locates at the longitudinal segments where no particles exists. This will lead to its complete extraction without beam loss. Our method, however, confines the kick to a specific longitudinal segment of the bunch, as shown in Fig. 1. The rising or falling edge will inevitably overlap with the populated part of the bunch and cause beam loss at the septum. The selective kick ensures that only the targeted particles are extracted, enabling the particles stored in a single rapid-cycling period to be distributed across multiple scanning points. Simulation results presented later in this paper will show that the beam loss at septum caused by the rising or falling edge is acceptable for medical use. This technique is termed longitudinal localized kick driven fast extraction.

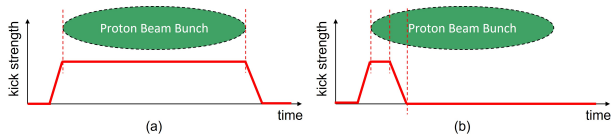


Figure 1: The relationship between the kicker pulse time and bunch length. (a)Conventional fast extraction, the entire bunch is kicked out in a single turn; (b)Fast extraction used in our scheme, the bunch needs to provide particles for hundreds of scanning spots.

Choosing the right type of fast kicker is also crucial. Compact medical synchrotrons typically store bunches with lengths of several hundred nanoseconds, necessitating kicker rise/fall times on the order of nanoseconds. Consequently, the stripline kicker was selected for our design. Since the beam has a larger profile in the $x$-direction, resulting in a latger separation distance and gap between the parallel electrodes, we consider to apply the kick angle to the beam in the $y$-direction in our scheme.

### *Spot Dose Accuracy*

Precise spot dose control is critical in PBS proton therapy and must be carefully integrated into our design. Dose control at each scanning spot translates directly into controlling the number of particles extracted for that spot. As established in the preceding analysis, this extracted particle count varies with the longitudinal segment where the kick field is applied. Therefore, precise particle number control can be achieved by regulating the kicker's pulse time.

Accordingly, we employ a longitudinal current distribution feedback method. This approach involves measuring the

* Work supported by the National Natural Science Foundation of China (No. 12075131).
† zhengsx@tsinghua.edu.cn

ISBN: <ask the JACoW BoD> ISSN: <ask the JACoW BoD> doi: 10.18429/JACoW-HB2025-THFA05

# LONGITUDINAL LIMITATIONS IN THE CERN PROTON SYNCHROTRON BOOSTER

M. Marchi*,[1], S. Albright, F. Asvesta, D. Barrientos, S. Energico, G. Gnemmi, R. Heine[2]
CERN, Geneva, Switzerland
[1]also at Dipartimento di Fisica, Università di Roma La Sapienza, Rome, Italy
[2]also at Technische Universitaet Berlin, Berlin, Germany



*Abstract*

The CERN Proton Synchrotron Booster (PSB) operates at two nominal extraction kinetic energies, 1.4 GeV and 2 GeV, each presenting distinct achievable beam intensities. To mitigate longitudinal instabilities, the PSB RF system employs a combination of double-harmonic voltage and multi-harmonic beam loading compensation system. When operating with single-harmonic voltage and open cavity loops, a fast instability emerges. In contrast, closing the loops suppresses the fast instability but results in gradual longitudinal emittance growth. Longitudinal stability improves significantly when the second harmonic is added in counter-phase at the bunch position, but not in-phase, despite both configurations increasing the synchrotron frequency spread. A new time-domain model of the cavity loops has been incorporated into particle tracking simulations. It allows a more detailed understanding of their influence on beam dynamics. This contribution presents results from a measurement campaign, which have been used to identify present longitudinal limitations and predict future performance.

## INTRODUCTION

The Proton Synchrotron Booster (PSB) is part of the CERN proton injector chain and plays a crucial role in providing high-intensity, high-brightness beams to downstream accelerators. The most demanding beams in terms of intensity are those delivered to the fixed-target experimental facilities. While the PSB can currently supply the intensities required by users, a deeper understanding of its longitudinal limitations is essential to explore its performance potential, particularly following the major RF system upgrade implemented during Long Shutdown 2 (LS2). The RF system now consists of magnetic-alloy cavities, using Finemet material, characterised by a high shunt impedance in a broad frequency window [1]. A direct RF feedback loop located in the power amplifier chain and Low-Level RF (LLRF) digital cavity controllers, deliver wide-band and narrow-band beam loading compensation, respectively [2, 3].

The achievable beam intensity is defined by two main limitations: the hardware capability of the RF power system, and longitudinal beam stability. Both have been studied extensively. The first limitation has been investigated by monitoring the current request of the power amplifiers as a function of bunch intensity, allowing the identification of a clear operational constraint. This relation provides a useful extrapolation tool for predicting the current required at higher intensities.

On the beam dynamics side, longitudinal instabilities have been systematically observed during the acceleration cycle, with the most interesting effects occurring near flat-top energy. Previous studies in Single harmonic RF (SRF) operation have revealed two distinct instability mechanisms that depend strongly on the cavity loop configuration and on the RF voltage program [4]. The present work extends this analysis to the Double harmonic RF (DRF) operation at 2 GeV.

## LONGITUDINAL INTENSITY LIMITATIONS AT 2 GeV IN THE PSB

### *RF System Overview*

The PSB RF system employs Finemet cavities that support multi-harmonic operation, providing broad flexibility for shaping the longitudinal beam parameters [1]. The hardware is modular: each of the four rings hosts three cavities, and each cavity comprises twelve individual cells. An internal direct-feedback loop provides continuous, though modest, beam loading compensation (up to 10 dB). To further suppress impedance at harmonics of the revolution frequency, sixteen parallel LLRF digital cavity controllers implement strong, narrow-band induced-voltage compensation [5].

### *$I_{DC}$ Interlock and Operational Threshold*

When the DC-current exceeds a specified threshold, an interlock in the amplifier power supply activates and inhibits the RF drive. The threshold is an operational setting chosen to meet present requirements and can be raised for studies [6]. To quantify the effect on achievable intensity, dedicated measurements were performed at the nominal threshold (118 A) and with the interlock increased by 25 A (to 143 A), and the resulting intensity reach was compared.

These measurements show a linear dependence of the DC-current with intensity and a steady increase with the energy. At 1.4 GeV, it was possible to reach $1.6 \times 10^{13}$ p/b (protons per bunch) with a DC-current of 148 A [7]. On a 2 GeV cycle the maximum achievable intensity was approximately $1.4 \times 10^{13}$ p/b, requiring 143 A. The extrapolated current needed to sustain $1.6 \times 10^{13}$ p/b at 2 GeV is expected to exceed the present interlock setting, as visible in Fig. 1.

The power supply of the PA is specified to provide up to 200 A DC, although this margin has not yet been fully

* mariangela.marchi@cern.ch

ISBN: <ask the JACoW BoD> ISSN: <ask the JACoW BoD> doi: 10.18429/JACoW-HB2025-THFA07

# SCENARIO OF BEAM-BASED ALIGNMENT WITH NEW BPM SYSTEM FOR FUTURE BEAM COMMISSIONING OF 1.3-MW OPERATION AT THE J-PARC MAIN RING

Y. Saito*,[1], Y. Sato[1], K. Satou[1], T. Asami[1], T. Yasui[1]
The Graduate University for Advanced Studies, SOKENDAI, Tokai, Naka, Ibaraki, Japan
T. Toyama, J-PARC center, KEK & JAEA, Tokai, Naka, Ibaraki, Japan
[1] also at KEK & JAEA, Tokai, Naka, Ibaraki, Japan

*Abstract*

In the main ring synchrotron (MR) of the Japan proton accelerator research complex (J-PARC), ongoing upgrades of the data acquisition system for the BPMs will improve the accuracy from 30 μm to 10 μm in the Closed Orbit Distortion (COD) mode. As a first step to the higher beam intensity with the new equipment, we confirm that the current method of beam-based alignment may cause an orbit offset with respect to the magnetic center of 90 μm and 20 μm precision at most.

## INTRODUCTION

The main ring synchrotron (MR) [1] at the Japan proton accelerator research complex (J-PARC) has supplied the high-intensity proton beam for the neutrino experiment. The MR accelerates the 3-GeV proton beams from the rapid cycling synchrotron (RCS) to 30 GeV. While the present beam power achieved is 830 kW for user operation, the next target is 1.3 MW [2]. To increase the beam intensity, we need to suppress the beam loss, in addition to upgrading the RF system, localizing the beam loss, and shortening cycling period.

To decrease and localize the beam loss for higher intensity, an accurate optics correction is important. For the more precise optics measurements, upgrades of the data acquisition system for the beam position monitors (BPM) is ongoing. The upgrade will improve the accuracy from 30 μm to 10 μm in the Closed Orbit Distortion (COD) mode [2]. Besides the upgrade, we have improved the 3-fold symmetry of optics parameters in MR with correction by the current BPM system, which is effective for decreasing the beam loss [3–5]. After the upgrade of the BPM system, we will pursue further measurements and corrections of optics parameters.

With the upgraded BPMs with better accuracy, there are complexities in determining how to effectively suppress and control the beam loss. First, it is essential to verify whether the current method to determine a BPM offset [6] is reasonable from the perspective of precise beam tuning to 1.3–MW operation. Second, the acceptable range of closed-orbit distortion for achieving the 1.3–MW operation remains to be clarified. Third, a strictly logical strategy for defining the orbit for the operation based on the simulation or analytical discussion has yet to be established. An ideal case is that the orbit passes through all the centers of the magnets. However, the number of the horizontal/vertical steering magnets in MR is 93, while that of the quadrupole magnets is 216. Therefore, the magnet misalignment makes it challenging to realize an orbit through all the centers of the magnets. To find a orbit minimizing the beam loss, it is important to evaluate the offsets of all the magnets from a orbit.

As a first step to deal with those questions and realize the 1.3–MW operation, we calculate the error in the current method for the BPM alignment.

## BIAS ERROR FROM BEAM BASED ALIGNMENT

Beam-based alignment (BBA) is a method for a BPM value of the orbit through the nearest quadrupole magnet center. After the description of BBA, we discuss a possible error in the current method of BBA.

The current method of BBA calculates a BPM value of the orbit through quadrupole magnets as below. It is assumed that the longitudinal position of the BPM is the same as that of the quadrupole magnet. The main idea is that an orbit offset from a quadrupole magnet center causes a dipole field proportional to its field strength and the offset. Therefore, if there is no orbit change depending on the current to the quadrupole magnet, the orbit passes through the center. In BBA, you make a local bump on a quadrupole magnet with the orbit change $x_b$ at the nearest BPM, and change the current $I$ of the nearest quadrupole magnets. Since the orbit change in the quadrupole magnet is not observable, it is assumed that it is approximately same as the change in the BPM. As a definition of the orbit change $\Delta x(I)$ due to changing the current $I$, we use a value of one BPM having best response to $I$ in the straight section. Note that it is able to use several BPMs for better precision, which is not discussed here. Thanks to the linearity of the kick to $I$, linear fit deviates the value of $d\Delta x/dI$ for each $x_b$. The value of $d\Delta x/dI(x_b)$ is proportional to the difference between the orbit and the magnetic center if the nonlinearity effect is ignored. Therefore, linear fit shows that the orbit with $x_b$ where $d\Delta x/dI(x_b) = 0$ passes through the center.

The assumption that the BPM is at the same position as the quadrupole magnet is not strictly valid, which causes a bias error in BBA. In MR, the distance between the BPM and the center of the nearest quadrupole magnet is roughly 1 m. Therefore, the orbit following the result of the BBA

* yoshist@post.kek.jp

ISBN: <ask the JACoW BoD> ISSN: <ask the JACoW BoD> doi: 10.18429/JACoW-HB2025-THFA08

# CONTROLLING INDUCED RADIOACTIVITY IN CSNS-RCS

Yuwen An*,[1,2], Ming-Yang Huang[1,2], Yong Li[1,2], Yue Yuan[1,2], Liangsheng Huang[1,2], Shouyan Xu[1,2], Zhiping Li[1,2], Hanyang Liu[1,2], Jianliang Chen[1,2], Meifei Liu[1,2], Yaoshuo Yuan[1,2], Sheng Wang[1,2]
[1] Institute of High Energy Physics, Chinese Academy of Sciences (CAS), Beijing, China
[2] Spallation Neutron Source Science Center, Dongguan, China

*Abstract*

Controlling induced radioactivity remains crucial for high-intensity proton accelerators. This study analyzes radiation hotspots in a Rapid Cycling Synchrotron (RCS) using extensive dose measurements (2018-2024). We identified hotspots (> 5 mSv/h) exhibiting either transient ("peaking-then-decreasing") or persistent ("increasing-then-stabilizing") behavior. Strategic measures - orbit correction, parameter optimization, and hardware improvements - effectively reduced radiation, exemplified by the dose rate at Kicker01 dropping from over 20 mSv/h. However, persistent hotspots like R1SD03 (10 mSv/h) require further study of local beam loss mechanisms. These findings advance radiation control strategies for safer, more efficient proton accelerators.

## INTRODUCTION

The China Spallation Neutron Source (CSNS) [1, 2] is a major scientific facility comprising an 80 MeV linear accelerator (LINAC) and a 1.6 GeV Rapid Cycling Synchrotron (RCS). Since its commissioning, CSNS has been steadily upgraded to higher beam power, with CSNS-II aiming for 500 kW. As beam intensity increases, radiation-induced activation becomes a significant concern for machine maintenance and personnel safety [3]. High-dose hotspots, defined as localized areas with dose rates exceeding 5 mSv/h, have been observed at various locations in the RCS. Understanding their origins and developing effective mitigation methods are essential for long-term operation.

This paper summarizes dose measurement data from 447 sessions between 2018 and 2024, identifying 24 locations that have exceeded 5 mSv/h. We classify these hotspots into two categories based on their temporal evolution and analyze the underlying mechanisms. Mitigation strategies are discussed and evaluated through case studies. The results offer practical guidance for dose control in high-power proton synchrotrons.

Since its operation began in 2018, CSNS has typically designated Mondays as shutdown periods for maintenance. Approximately half an hour after beam shutdown, strict dose rate measurements are conducted using instruments such as Gamma Survey Meters, performed either at a distance of 30 cm from the equipment surface or directly on the surface. Based on the feedback from these measurements, beam tuning personnel carry out machine adjustments with the aim of reducing the radiation dose generated during the following week's operation.

* anyw@ihep.ac.cn

## DOSE MEASUREMENT OVERVIEW

Dose rate measurements in the Rapid Cycling Synchrotron (RCS) have been regularly conducted since 2018. A total of 447 measurement sessions were recorded, with 24 locations historically exceeding the 5 mSv/h threshold. These identified hotspots are distributed across four regions of the RCS:

Region 1: INBC4[1] outlet, INBH3 inlet, R1QF03 outlet, R1QF07 inlet, R1QF12 inlet

Region 2: Kicker01 outlet, R2MB03 outlet, R2QD11[2] outlet, R2QF06 inlet, R2QF07 inlet, R2QF10 inlet, R2QF12 outlet, R2SD03 outlet

Region 3: LAM[3] inlet, LAM outlet, R3QF07 inlet

Region 4: R4MB03 outlet

To better understand the spatial distribution of these hotspots, it is helpful to refer to the lattice structure of the CSNS-RCS. A schematic of the one-quarter symmetric lattice is shown in Fig. 1. The RCS is a four-fold symmetric ring with a total circumference of 227.92 meters. Each superperiod consists of two mirror-symmetric segments. The basic lattice structure follows a triplet configuration. Taking Region 1 as an example, it contains 12 quadrupole magnets. Each magnet is named according to the convention: Region + Focusing Type + Sequential Number. For instance, R1QF01 denotes the first focusing quadrupole magnet in Region 1. Region 1 also houses 6 bending magnets (MB), which share a common power supply and are named following the pattern: Region + MB + Number (e.g., R1MB01). Regions 2, 3, and 4 are mirror-symmetric to Region 1. The ring features four long straight sections dedicated to housing key components: the injection region, extraction region, RF cavities, and collimators.

Two characteristic patterns have been identified in the evolution of induced radioactivity:

**Type I: Transient Increase:** – A rise in dose rate attributed to suboptimal operational parameters, which promptly decreases in subsequent weekly measurements following parameter optimization. This behavior indicates beam loss that is correctable through routine tuning procedures.

**Type II: Persistent Accumulation** – The dose rate increases and stabilizes at elevated levels, demonstrating limited sensitivity to routine parameter adjustments. This pattern suggests localized beam loss hotspots within the ring,

[1] All INBC and INBH magnets were replaced during the summer maintenance period in 2025.

[2] The dose rate at this location significantly decreased following the vacuum chamber modification in 2021.

[3] LAM refers to the Lambertson extraction magnet.

ISBN: <ask the JACoW BoD> ISSN: <ask the JACoW BoD> doi: 10.18429/JACoW-HB2025-THFA10

# MEASUREMENT AND ANALYSIS OF BEAM INTENSITY FOR THE C-BAND PHOTOTHODE ELECTRON GUN PLATFORM*

F. Li[1,2], W. L. Huang[†,1,2], S. M. Jing[1,2], R. J. Yang[1,2], R. Y. Qiu[1,2], Z. H. Xu[1,2], L. Zeng[1,2], Z. J. Lu[1,2], W. W. Chen[1,2]
[1]Institute of High Energy Physics, Chinese Academy of Sciences (CAS), Beijing, China
[2]China Neutron Spallation Source, Dongguan, China

*Abstract*

This paper presents an overview of the beam intensity measurement system for the C-band photocathode electron gun platform, detailing the observed phenomena during measurements and the associated experimental investigations. The system's design, operational principles, and key components are introduced, followed by an analysis of critical measurement results and unexpected phenomenon, such as dark current interference and beam instability. Corresponding experimental validations and optimization strategies are discussed to enhance measurement accuracy and platform performance, providing insights into the dynamic characteristics and reliability of the electron gun system.

## INTRODUCTION

An RF photocathode injector with a low emittance C-band RF photon gun and C-band high gradient accelerating structures (HGAS) [1] is being developed as the injector of the Southern Advanced Photon Source (SAPS) [2]. SAPS is a 3.5 GeV 4th generation synchrotron which is proposed to be built by the side of the China Spallation Neutron Source (CSNS), located at the Dongguan City, Guangdong Province, China.

As illustrated in Figure 1, the Phase-I system of this C-band RF photoinjector consists of a 266nm laser system and some beam diagnostics devices. In the laser system, the laser beam will be directed to hit the cathode surface of a 3.6-cell C-band RF photocathode electron gun with the help of a reflection lens (RL). The downstream is mainly designed for the beam diagnostics. An integrating current transformer (ICT) is used to measure the charge of the electron beam. The beam emittance and transverse beam profiles are measured by a double-slit emittance monitor and two fluorescent viewscreens. The energy spread can be measured with the help of the bending magnet (BM). The faraday cup (FC) is used as a beam dump and to monitor the bunch charge and the dark current during the operation. The primary beam parameters of C-band Photocathode Gun Exit are summarized in Table. 1.

Figure 2 shows a schematic layout of Phase-II. A 2 m-long C-band travelling wave structure (TWS) will be added to boost the energy to several tens of MeV. The downstream of Phase-I will be replaced to accommodate the beam diagnostics at this energy range.

In this paper, the beam intensity measurement system for the C-band photocathode electron gun platform will be given. The system includes an ICT, an FC, and corresponding electronics and data acquisition systems, the beam charge and the dark current will be measured.

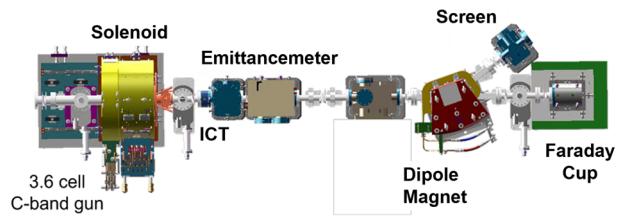


Figure 1: Layout for the C-band test platform (Phase-I).

## DIAGNOSTIC SYSTEM SETUP

At the exit of the photocathode microwave electron gun, precise charge integration measurements for ps-level ultra-short pulse bunches are essential. Compared to interceptive methods like Faraday cups, the beam transformer (ICT) designed by K.B. Unser in 1989 enables non-destructive charge integration and non-intercept absolute current

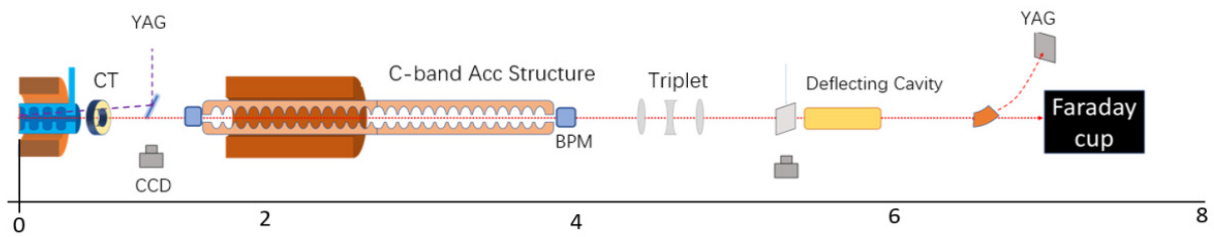


Figure 2: Schematic layout for the C-band test platform (Phase-II).

*Work Supported by National Natural Science Foundation of China (No. 12275294 and No. 12305166), the Natural Science Foundation of Guangdong Province, China, (NO. 2024A1515010016), and Mega Science Project Operation Fund of CSNS
† huangwei@ihep.ac.cn

ISBN: <ask the JACoW BoD> ISSN: <ask the JACoW BoD> doi: 10.18429/JACoW-HB2025-THFA12

# LONGITUDINAL PHASE SPACE RECONSTRUCTION FROM BEAM CURRENT PROJECTIONS USING DEEP CONVOLUTIONAL NEURAL NETWORKS

Y. Luo, H. Yao, Y. Huang, Y. Xiong, P. Fang, C. Li, S. Zheng*
Tsinghua University, Beijing, China

*Abstract*

Longitudinal phase space diagnostics in synchrotrons are crucial for beam dynamics optimization. Although traditional Algebraic Reconstruction Technique (ART) can achieve high reconstruction accuracy, it relies on complex physical computations, making its reconstruction speed inadequate for real-time diagnostic requirements. This paper proposes an end-to-end phase space tomography method based on convolutional neural networks, which establishes a direct mapping from one-dimensional beam current projections to two-dimensional phase space distributions, bypassing the iterative physical simulation process of traditional methods. The network architecture incorporates positional encoding to capture multi-turn temporal dependencies, employs attention mechanisms to weight critical frames, and utilizes convolutional upsampling for spatial reconstruction. Trained and validated on 10,000 simulated datasets generated with XiPAF parameters, this method maintains reconstruction accuracy (KL divergence <0.1, SSIM >0.7, projection discrepancy <0.04) while reducing single reconstruction time from ~3 minutes with ART to ~100 milliseconds, achieving a three-order-of-magnitude acceleration. This paper analyzes the advantages of the proposed network architecture and discusses its promising application prospects for real-time diagnostics in high-intensity hadron beam facilities.

## INTRODUCTION

The longitudinal phase space of a synchrotron is a core dynamical parameter characterizing the longitudinal motion state of the beam, and its accurate diagnosis is of great significance for improving accelerator performance and ensuring stable operation [1]. Traditional measurement methods such as transverse deflection cavities destroy the beam structure, while tomography techniques based on beam current projections provide a non-invasive diagnostic solution.

Existing tomography methods mainly include analytical algorithms (such as filtered back projection), iterative algorithms (such as Algebraic Reconstruction Technique (ART)), and machine learning-based methods. The ART algorithm, by coupling particle tracking with iterative correction, has demonstrated good reconstruction results in several accelerator facilities [2]. However, it relies on complex physical computations, requiring ~3 minutes per reconstruction[1], making it difficult to meet real-time diagnostic needs. Particularly in high-intensity scenarios where nonlinear dynamic effects are significant, traditional methods face challenges in balancing computational efficiency and accuracy.

This paper addresses these issues by proposing an end-to-end phase space reconstruction method based on convolutional neural networks. The main contributions include: (1) demonstrating the network's adaptability to complex beam dynamics environments, particularly its potential for handling nonlinear effects like space charge forces; (2) achieving three orders of magnitude acceleration in reconstruction speed while maintaining comparable accuracy to traditional methods; (3) establishing a foundation for real-time diagnostics in high-intensity hadron facilities while addressing the fundamental challenge of unavailable experimental labels through simulated training.

## PHYSICAL BACKGROUND AND TOMOGRAPHY PRINCIPLES

### *Synchrotron Longitudinal Dynamics*

The longitudinal phase space of a synchrotron uses the phase deviation $\Delta\phi$ and energy deviation $\Delta E$ relative to the synchronous particle as conjugate coordinates. According to Hamiltonian mechanics, the particle trajectory under RF field action corresponds to closed curves of constant Hamiltonian [3]:

$$H = \frac{1}{2}\frac{h\eta\omega_0^2}{\beta^2 E}\left(\frac{\Delta E}{\omega_0}\right)^2 + \frac{eV}{2\pi}\left[\cos\phi - \cos\phi_s + (\phi - \phi_s)\sin\phi_s\right] \quad (1)$$

where $h$ is the harmonic number, $\eta$ is the phase slip factor, $V$ is the RF voltage, and $\phi_s$ is the synchronous phase.

### *Principles of Tomography*

The mathematical foundation of tomography is Radon transform theory. In synchrotrons, each completed revolution of particles produces a slight angular shift in their phase space coordinates, providing natural discrete projection angle sequences for tomography. The signals measured by fast current transformer (FCT) are one-dimensional projections of the phase space distribution on the $\Delta\phi$ axis.

The traditional ART achieves phase space reconstruction through three core steps: first, particle tracking simulation based on dynamical equations generates test particle trajectories in phase space; then, the simulated phase space distribution is projected onto the current signal domain to calculate theoretical projection data; finally, through an iterative correction mechanism, backprojection is performed

* zhengsx@tsinghua.edu.cn

[1] AMD Ryzen Threadripper 3970X 32-Core Processor 3.69 GHz, 96.0 GB RAM

ISBN: <ask the JACoW BoD> ISSN: <ask the JACoW BoD> doi: 10.18429/JACoW-HB2025-THPT06

# BEAM DYNAMICS DESIGN OF A SUPRECONDUCTING RFQ FOR CiADS*

Shilong Gao[1,2], Zhouli Zhang[†,1,2], Chenxing Li[1,2], Weiping Dou[1,2], Yuan He[1,2], Zhijun Wang[1,2]
[1]Institute of Modern Physics, Chinese Academy of Sciences, Lanzhou, China
[2]University of Chinese Academy of Sciences, Beijing, China



*Abstract*

A superconducting radio-frequency quadrupole (SRFQ) is proposed for the future upgrade of the China Initiative Accelerator Driven System (CiADS). The SRFQ is designed to accelerate a 10 mA proton beam to 2.5 MeV within a compact length of 2.9 m. This design achieves 100% transmission efficiency and a carefully controlled output longitudinal emittance, ensuring minimal beam loss in the superconducting cavities. This paper presents the detailed beam dynamics design and its simulated performance.

## INTRODUCTION

Currently, a 162.5 MHz normal conducting (NC) RFQ is employed in the room temperature front end of the CiADS proton LINAC to accelerate the proton beam from 20 keV to 2.1 MeV [1]. It adopts a low surface electric field to ensure long-term stable operation, which results in a length about 5 m. Considering the high RF power losses, stringent thermal management for continuous wave (CW) operation, and potential RF breakdown of a NC cavity, a SRFQ is preferable in the future upgrade of CiADS, which aims to increase the beam current from 5 mA to 10 mA.

Superconducting cavities offer compelling advantages over their NC counterparts [2]. Their low radio-frequency (RF) loss dramatically reduces the demands on the RF power and thermal cooling systems. This makes them exceptionally well-suited for high-duty-factor applications and long-term, stable CW operation. Furthermore, the ability to achieve larger beam apertures and higher accelerating gradients facilitates the acceleration of higher beam currents while simultaneously reducing the overall length of the accelerators.

In addition to considering fabrication with pure niobium, we also explore the use of $Nb_3Sn$ [3]. With a superconducting critical temperature of 18 K, $Nb_3Sn$ significantly surpasses pure niobium (9 K), allowing for a higher operating temperature. For smaller, low-energy accelerators, this approach enables its operation via conduction cooling with compact G-M cryocoolers. This scheme eliminates reliance on large-scale cryogenics, reduces operating costs, and simplifies maintenance. This technological shift opens the door to a new paradigm for SRF accelerators, extending their use beyond large-scale scientific facilities that house large liquid helium cryoplants. The compact superconducting radio-frequency (SRF) system promotes the miniaturization and industrial application of SRF technology in fields such as compact neutron sources and Boron Neutron Capture Therapy (BNCT) [4].

## DESIGN PARAMETERS

The requirements for design parameters of the CiADS SRFQ are summarized in Table 1.

Table 1: Design Requirements

| Parameters | SRFQ | NC RFQ | Unit |
|---|---|---|---|
| $f$ | 162.5 | 162.5 | MHz |
| $I_{peak}$ | 10 | 5 | mA |
| $L$ | < 3000 | | mm |
| $E_{peak}$ | < 40 | < 17.66 | MV/m |
| $W_{in}/W_{out}$ | 0.04 / 2.5 | 0.02 / 2.1 | MeV |
| $T$ | 100 | As high as possible | % |
| $\varepsilon_{out}^{longi.,n.,rms}$ | < 0.03 | < 0.022 | π·cm·mrad |
| $\varepsilon_{out}^{longi.,n.,99.9\%}$ | < 0.54 | < 0.54 | π·cm·mrad |

The operating frequency is set to 162.5 MHz to match the CiADS linac, and the design current is 10 mA, in line with the project's upgrade specifications. A peak surface electric field (Epk) limit of 40 MV/m, comparable to those used in the SRFQ dynamics designs at PKU [5] and KEK [6], was chosen.

A significant decision is to increase the output energy to 2.5 MeV, compared to the 2.1 MeV of the existing NC RFQ. The original 2.1 MeV value was chosen to keep the energy of lost particles below the 2.16 MeV threshold of the 65Cu (p, n) 65Zn reaction, thereby minimizing the activation of the copper structure [7]. The increased energy also enables potential standalone applications for the accelerator, such as serving as a compact neutron source.

Based on the CiADS upgrade requirements, which are informed by the operational experience with the original NC RFQ, the following design objectives for the SRFQ were established:

- **Beam Quality**: For a 10 mA beam, the output longitudinal RMS emittance must be less than 0.03 π·cm·mrad, and the 99.9% longitudinal emittance must be below 0.54 π·cm·mrad [1]. This is crucial for minimizing beam loss in the downstream superconducting sections.
- **Perfect Transmission**: The transmission and acceleration efficiencies must be 100% to prevent any beam loss, which would induce a thermal load and damage the vane surface.

* Work supported by the Large Research Infrastructures China initiative Accelerator Driven System (2017-000052-75-01-000590) and Talent project of Chinese Academy of Sciences (Grant No. E129841YR0)
† zhangzhouli@impcas.ac.cn

ISBN: <ask the JACoW BoD> ISSN: <ask the JACoW BoD> doi: 10.18429/JACoW-HB2025-THPT16

# DESIGN CONSIDERATIONS OF THE BUNCH-BY-BUNCH TRANSVERSE FEEDBACK SYSTEM FOR THE CSNS RCS

W. Chen[1], R. Qiu[1], C. Xie[1], Z. Lu[1], R. Yang*[,1], X. Li[1]
Institute of High Energy Physics, Beijing, China
[1]also at China Spallation Neutron Source, Dongguan, China

*Abstract*

The CSNS RCS (Rapid Cycling Synchrotron) is a proton accelerator designed to achieve a target beam energy of 1.6 GeV, with a typical operating intensity of 140 kW, which is expected to increase to 500 kW after the CSNS II upgrade. However, a significant current instability has been observed during the 100 kW beam operation. To mitigate this instability, techniques such as operational tuning and chrominance modulation were previously used to make the 100 kW beam operate stably. In order to face the subsequent stronger instability, a bunch-by-bunch transverse feedback system is required to mitigate the coherent lateral oscillations caused by instability and injection errors. In this paper, the preliminary design of the feedback system will be presented.

## INTRODUCTION

The China Spallation Neutron Source (CSNS) is a high-intensity proton accelerator facility designed for neutron scattering research, consisting primarily of a linear accelerator (LINAC) and a Rapid Cycling Synchrotron (RCS) [1]. Currently operating at a beam power of approximately 170 kW, CSNS is undergoing an upgrade to CSNS-II, which will increase the beam power to 500 kW by enhancing the LINAC injection energy from 80 MeV to 300 MeV and incorporating additional RF systems [2]. This upgrade aims to support expanded scientific applications, including the addition of more neutron instruments and experimental terminals.

As beam intensity increases in high-power synchrotrons like CSNS, beam instabilities transverse bunch instabilities driven by space charge effects and impedance—become a significant challenge, potentially leading to beam loss and reduced performance. Extensive research has been conducted on these instabilities during CSNS commissioning and operation, revealing their growth with rising intensity and the need for effective mitigation strategies [3, 4]. To address the further intensification of beam instability in the CSNS-II upgrade, various methods are under investigation, including impedance reduction, chromaticity adjustments, and feedback control systems.

Drawing from the experiences of similar high-intensity proton accelerators worldwide—such as the Spallation Neutron Source (SNS) in the United States, the Japan Proton Accelerator Research Complex (J-PARC), and the CERN Proton Synchrotron (PS)—the transverse feedback system has proven to be one of the most effective approaches for damping instabilities and maintaining beam stability. These systems detect beam oscillations bunch-by-bunch and apply corrective kicks to suppress growth, ensuring reliable high-power operation.

Table 1: CSNS RCS Beam Parameters

| Parameters | Value |
|---|---|
| RCS circumference | 227.92 m |
| Repetition rate | 25 Hz |
| Harmonic number | 2 |
| revolution frequency | 1.02 - 2.44 MHz |
| nominal betatron tunes | $Q_x = 4.86$, $Q_y = 4.78$ |
| Bunch length | 600 ns(Inj.)/80 ns(Ext.) |
| BPM signal Voltage | 100 mV - 80 V |

For the specific beam parameters of the CSNS RCS Table 1, the primary requirements for an effective transverse feedback system include: a system bandwidth greater than $f_b/2$ (where $f_b$ is the bunch frequency), a damping time of 0.5 ms, a feedback delay of 1-5 turns, and a maximum output voltage of 5 kV.

This paper presents the design, simulation, and preliminary implementation of such a system tailored to CSNS-II, with the goal of enabling stable operation at the upgraded beam power.

## FEEDBACK SYSTEM OVERVIEW

The transverse feedback system for the CSNS RCS comprises key components: pick-ups, electronics, power amplifier, and kicker, as shown in Fig. 1. To accelerate the development of a functional prototype, an existing tune measurement BPM is repurposed as the pick-up, while the tune measurement exciter functions as the kicker, significantly reducing development time. The electronics subsystem adopts the MTCA.4 architecture, with the AMC module incorporating the commercial SIS8300-KU digitizer board integrated with a self-developed RTM. The SIS8300-KU has Xilinx Kintex Ultrascale FPGA, 10 ADC Channels 125 MS/s-16-Bit or 250 MS/s-14-Bit (depends on assembly/ordering option), 2 DAC Channels 250 MS/s, 16-Bit. The feedback design target is shown as Table 2.

The existing power amplifier for tune measurement operates with a bandwidth of 1 MHz to 8.5 MHz and an output power of 1000 W, which is inadequate for the demands of the transverse feedback system. Based on the CSNS RCS beam parameters—beam energy = 1.6 GeV, the revelotion time $T_0 = 820$ ns, the beam position deviation $\Delta x = 8$ mm, the positions of PU and Kicker $\beta = 8$ m, the damping time

* yangrenjun@ihep.ac.cn

ISBN: <ask the JACoW BoD> ISSN: <ask the JACoW BoD> doi: 10.18429/JACoW-HB2025-THPT17

# DESIGN OF 6D COOLING AND FINAL COOLING CHANNELS FOR A MUON COLLIDER

R. Zhu* [1], J. Yang[1]
Institute of Modern Physics, Chinese Academy of Sciences, Lanzhou, China
[1]also at University of Chinese Academy of Sciences, Beijing, China
C. Rogers, Rutherford Appleton Laboratory, Didcot, United Kingdom

*Abstract*

The muon collider is a promising candidate for exploring new physics at the energy frontier, offering the advantages of lepton collisions at multi-TeV scales. Achieving high luminosity requires reducing the six-dimensional (6D) emittance of the muon beam by several orders of magnitude within the muons' limited lifetime. This is accomplished through ionization cooling, which involves two main stages: initial 6D cooling and final transverse cooling. This paper presents an updated lattice design for both rectilinear 6D cooling and final cooling. The latest design achieves a factor of two reduction in final transverse emittance, marking a significant advancement toward meeting the beam quality requirements of a future muon collider.

## INTRODUCITON

Electron–positron colliders are highly valued for their clean experimental conditions, where collision events are relatively simple and easy to interpret compared with those in hadron colliders. The challenge, however, lies in reaching multi-TeV energies: the small electron mass leads to severe energy losses through synchrotron radiation. Muons, being much heavier than electrons, are far less affected by this limitation while still behaving as fundamental leptons. This combination of properties makes muon colliders a promising candidate for advancing high-energy physics [1].

A major challenge for the muon collider is that the emittance of muon beams from pion decay greatly exceeds the acceptance of downstream accelerators, requiring dedicated cooling to reduce the muon beam emittance. The muon cooling channel consists of two stages: six-dimensional (6D) cooling and final cooling. The 6D cooling stage is divided into two sections: pre-merge, which reduces the emittance to meet the bunch merge requirements [2] ($\varepsilon_T \leq 1.3$ mm, $\varepsilon_L \leq 1.7$ mm), and post-merge, which reduces the emittance that increases during the bunch merge and further lowers it as much as possible to facilitate the design of the final cooling channel. The final cooling channel must further reduce the transverse emittance to 22.5 μm [3], as required for achieving the target collision luminosity. In this paper, we present updated designs for both the 6D cooling and final cooling channels. Compared with previous studies [4, 5], simulations using G4beamline v3.08 [6] demonstrate that the new designs achieve about a factor of two reduction in transverse emittance, while the output longitudinal emittance from final cooling channel remains below the target value of 64 mm [3].

## PRINCIPLE OF MUON COOLING

For muon beams, ionization cooling is the only viable method due to the short lifetime of the muon (2.2 μs in the rest frame). In this process, muons lose both transverse and longitudinal momentum through ionization interactions with atoms in the absorber material. The lost longitudinal momentum is restored in RF cavities, whereas the transverse momentum is not, leading to a reduction in transverse emittance. The evolution of the normalized transverse emittance can be expressed as [7]:

$$\frac{d\varepsilon_T}{ds} = -\frac{1}{\beta^2}\frac{dE_\mu}{ds}\frac{\varepsilon_T}{E_\mu} + \frac{1}{\beta^3}\frac{\beta_T E_s^2}{2E_\mu m_\mu c^2 L_R} \tag{1}$$

where $\varepsilon_T$ is the normalized transverse emittance, $E_\mu$ is the muon beam energy in GeV, $m_\mu$ is the muon mass, $\beta$ is the muon particle velocity, c is the speed of light, $\beta_T$ is the transverse beta value, $dE_\mu/ds$ is the energy loss per unit length, $E_s$ is the characteristic energy and $L_R$ is the radiation length of absorber material. The first term represents cooling, while the second corresponds to heating.

Longitudinal ionization cooling requires dispersion at the absorber, which is typically realized with a wedge-shaped absorber. Dispersion causes higher-momentum particles to traverse thicker parts of the wedge and lose more energy, thereby reducing the longitudinal emittance. In this case, the equilibrium transverse and longitudinal emittances are [7]:

$$\varepsilon_T^{eq} = \frac{\beta_T E_s^2}{2\left|\frac{dE_\mu}{ds}\right|\beta g_T m_\mu c^2 L_R} \tag{2}$$

$$\varepsilon_L^{eq} = \frac{\beta_L m_e c^2 \gamma^2 (1-\frac{\beta^2}{2})}{2g_L \beta m_\mu c^2 [\frac{\ln(K\gamma^2\beta^2)}{\beta^2} - 1]} \tag{3}$$

where $g_T$ and $g_L$ are the transverse and longitudinal partition numbers, defined as

$$g_T = 1 - \frac{D}{2w} \tag{4}$$

$$g_L = \frac{2\gamma^2 - 2\ln[K(\gamma^2-1)]}{\gamma^2 \ln[K(\gamma^2-1)] - (\gamma^2-1)} + \frac{D}{2w} \tag{5}$$

with $D$ the dispersion, $w$ the distance between the beam center and the apex of the wedge, $\gamma$ the Lorentz factor, and $K = 2m_e c^2/I$ with $I$ the mean excitation energy.

* zhuruihu@impcas.ac.cn

ISBN: <ask the JACoW BoD> ISSN: <ask the JACoW BoD> doi: 10.18429/JACoW-HB2025-THPT20

# 162.5 MHz SINGLE-BUNCH SELECTION ULTRA-FAST BIPOLAR CHOPPER POWER SUPPLY DESIGN

Xin Qiao[1,2], Weilong Chen*[,1,2], Zhijun Wang[1,2], Duanyang Jia[1,2], Qi Wu[1,2]
[1]Institute of Modern Physics, Chinese Academy of Sciences, Lanzhou, China
[2]University of Chinese Academy of Sciences, Beijing, China

*Abstract*

Neutron energy spectrum measurement imposes requirements for single-bunch selection and acceleration on the CiADS (China Initiative Accelerator Driven System) superconducting linear accelerator, which operates at a fundamental frequency of 162.5 MHz . Existing chopper power supplies have rise/fall times approaching 20 ns, making them unable to achieve the required 6.15 ns bunch selection via a stable field-free region. To address this issue, an ultrafast bipolar high-voltage pulse power supply with fixed voltage slope control has been designed. This design loads linearly varying ±4 kV voltages (slope ≥180 V/ns) onto the chopper's deflection plates to achieve transverse bunch scanning. The physical aperture restriction at the RFQ (Radio Frequency Quadrupole) entrance is utilized to convert this transverse scan into a time selection window, enabling nanosecond-precision beam bunch selection. This power supply provides crucial technical support for single-bunch selection in the RFQ accelerator. This paper elaborates on the design scheme of the chopper power supply and presents relevant circuit simulation analysis.

## INTRODUCTION

In the CiADS nuclear physics experiment, neutron energy spectrum measurement is a key experiment for analyzing nuclear reaction cross-sections and calibrating system parameters. The beam pulse width in this experiment is the core factor determining the measurement accuracy. The fundamental frequency of the RFQ accelerator in the CiADS superconducting linear accelerator is 162.5 MHz , and the length of a single high-frequency cycle is 6.15 ns . This cycle is the natural single-beam time unit before the beam enters the RFQ. After subsequent acceleration and bunching by the RFQ, the pulse width can be compressed to the ns level, which exactly meets the requirements of neutron energy spectrum measurement. Therefore, screening out a "clean" single beam with a pulse width of 6.15 ns before the beam enters the RFQ is a crucial prerequisite for ensuring the experimental accuracy.

The beam chopper is the core device for single-beam selection. By applying an electric field to the deflection plates, the beam particles within a specific time window are deflected into the RFQ entrance aperture. However, the existing chopper in the CiADS Low Energy Beam Transport section (LEBT) is powered by a conventional constant-voltage power supply, and both the voltage rise and fall times are close to 20 ns, which is much longer than the target beam pulse width of 6.15 ns . The 20 ns edge transition time is equivalent to more than three RFQ high-frequency cycles, resulting in the power supply being unable to form a stable "field-free region". Particles arriving earlier than the selection window are under-deflected because the electric field is not fully established, and particles arriving later than the window are deflected by mistake because the electric field has not completely disappeared. Eventually, the beam entering the RFQ has "front and rear tails" and does not meet the requirement of a "clean" single beam. To solve this problem, this paper proposes a scheme of applying a linearly varying bipolar high voltage to the deflection plates of the chopper. When the DC beam passes through the deflection plates, particles entering at different times are affected by an electric field with varying intensity, resulting in a differential deflection integration effect and forming a transverse deflection difference. After subsequent beam transmission, the particles exhibit a "time - position" corresponding transverse scan at the RFQ entrance. Combining with the 10 mm physical aperture limitation of the RFQ entrance, the spatial constraint can be transformed into a 6.15 ns time selection window to achieve precise single - beam screening. Among them, the central beam experiences a symmetric voltage change of "negative high voltage → zero potential → positive high voltage", and the positive and negative deflections cancel each other out, leaving only the transverse displacement, so it can be normally transmitted to the RFQ. Particles earlier than the central beam are subject to a net negative deflection, and particles later than the central beam are subject to a net positive deflection. Both are finally blocked by the RFQ entrance aperture, and only the particles within the target time window can enter the RFQ. From the derivation of technical parameters, the chopper adopts the electrostatic deflection principle. For a 20 KeV proton beam, combined with the layout parameters of the low - energy section of the CiADS superconducting linear accelerator prototype II and the single - beam selection window (corresponding to a 6.15 ns pulse width), the required voltage change rate of the deflection plates is finally calculated to be 201.8 V/ns [1]. Based on the above principles and parameter requirements, this paper designs an ultra - fast bipolar chopping power supply with fixed voltage slope control.

## DESIGN SCHEME OF ULTRA-FAST BIPOLAR CHOPPER POWER SUPPLY

To meet the single-bunch selection requirement of "bipolar output for deflection cancellation, linear voltage for stable

* chenweilong@impcas.ac.cn

ISBN: <ask the JACoW BoD> ISSN: <ask the JACoW BoD> doi: 10.18429/JACoW-HB2025-THPT21

# DEVELOPMENT OF READOUT SYSTEM FOR TARGET MULTI-WIRE SCANNER BEAM PROFILE MEASUREMENT OF CSNS-II*

Z. H. Xu[1,2], Z. J. Lu[1,2], R.Y. Qiu[1,2], F. Li[1,2], L. Zeng[1,2], W. L. Huang[1,2], M. Liu[1,2], R. J. Yang†[,1,2]
[1]Institute of High Energy Physics, Chinese Academy of Sciences (CAS), Beijing, China
[2]China Neutron Spallation Source, Dongguan, China

*Abstract*

Target Multi-Wire Scanner is a beam diagnostics device in the CSNS-II accelerator, designed to measure the pre-target beam profile. This paper details the hardware composition, software architecture, and beam-target interaction test results of the CSNS-II front-end multi-wire scanner readout system. In contrast to the CSNS predecessor, the upgraded system employs a hybrid software architecture combining a LabVIEW-based signal acquisition platform with a standardized EPICS Input/Output Controller developed in C. The LabVIEW software handles signal acquisition and front-end electronics control, while processed data is transmitted to the EPICS IOC for standardized data publishing. This architecture enhances system stability and ensures reliable EPICS-based data interaction, demonstrating an optimized instrumentation framework for high-precision beam diagnostics in high-power proton accelerators.

## INTRODUCTION

The Target Multi-Wire Scanner (TargetMWS) is a critical beam diagnostics device in the accelerator of CSNS-II [1], used for real-time monitoring of the beam profile. The scanner consists of wire arrays arranged in the X and Y directions, containing 81 and 41 wires respectively. Positioned upstream of the target, when the beam strikes the target, it directly interacts with the wires, generating electrical signals. By collecting signals from each wire and correlating them with their installed coordinates, the beam profile at the target can be reconstructed. The readout system is a vital component of the Target Multi-Wire Scanner system. Its hardware configuration comprises an NI chassis, controller, and multifunction data acquisition cards. The readout system software is developed using LabVIEW and MSYS2. The multi-wire scanner is located in front of the neutron target, with its specific position illustrated in Fig. 1.

## HARDWARE SYSTEM DESIGN

### *Structure and Signal Generation Mechanism of the TargetMWS*

The wires employed in the multi-wire scanner are precision-engineered from tungsten-rhenium alloy, selected for its exceptional thermal stability, mechanical robustness, and radiation resistance under intense beam conditions. The wires are systematically arranged along two orthogonal orientations， horizontal and vertical to facilitate comprehensive transverse beam profiling. The vertical array comprises 81 wires, dedicated to measuring the horizontal beam profile, while the horizontal array consists of 41 wires, designed to capture the vertical beam profile. Signal generation originates primarily from secondary electron emission and ionization phenomena induced by beam-wire interactions. When the high-energy beam particles strike the wire surfaces, charged particles are ejected, producing an electrical current signal proportional to the local beam intensity. The amplitude of this signal is influenced by factors including beam particle type, energy, wire material properties, and the spatial overlap between the beam and the wire. The maximum signal amplitude occurs when the beam centroid aligns precisely with a wire, enabling accurate determination of the beam center and facilitating high-resolution profile reconstruction. The structure of TargetMWS detector is shown in Fig. 2.

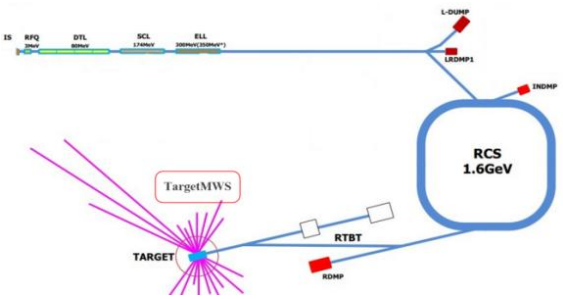


Figure 1: The position of TargetMWS.

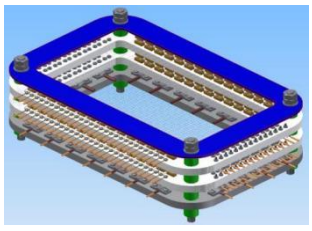

Figure 2: The structure of TargetMWS detector.

### *Hardware System*

Since the signal output from the TargetMWS detector is a current signal, it first requires front-end analog electronics for I-V conversion. After signal filtering, it is then fed into the acquisition system for signal acquisition.

*Work Supported by National Natural Science Foundation of China (NO. 12305166) and the Natural Science Foundation of Guangdong Province, China, (NO. 2024A1515010016)
†yangrenjun@ihep.ac.cn

ISBN: <ask the JACoW BoD> ISSN: <ask the JACoW BoD> doi: 10.18429/JACoW-HB2025-THPT25

# DYNAMIC APERTURE TRACKING FOR HIGH-INTENSITY PROTON ACCELERATORS

J. Tan, L. Huang, J. Chen, L. Rao, M. Huang,
Institute of High Energy Physics, Chinese Academy of Sciences, Beijing, China
Spallation Neutron Source Science Center, Dongguan, China



*Abstract*

Dynamic aperture tracking is an widely employed and effective method in the design of circular accelerators. However, in high-intensity proton accelerators, the pronounced space charge effect induces substantial tune shifts, which can severely compromise the accuracy of nonlinear dynamics analysis. In this study, we present a novel dynamic aperture tracking code tailored for high-intensity proton accelerators, which explicitly accounts for space charge-induced tune shifts. The CSNS/RCS synchrotron serves as a case study to validate the code's efficacy.

## INTRODUCTION

Dynamic aperture (DA) tracking is a fundamental tool in the study and optimization of nonlinear beam dynamics for circular accelerators. It provides quantitative insight into the stable region in transverse phase space and is crucial for maintaining beam quality and minimizing losses during operation. For electron storage rings and low-intensity proton machines, single-particle tracking with multipole field errors is generally sufficient to describe the nonlinear behavior of the beam.

However, in high-intensity proton accelerators, collective effects, particularly the space charge effect, introduce significant complications. The space charge force generates a substantial tune spread across the particle distribution, with the maximum tune shift even reaching several tenths. Such a large tune spread makes particles interact with many resonance conditions, which are not well represented in standard single-particle nonlinear dynamics analysis. As a result, conventional DA tracking tends to misestimate beam stability and fails to reflect the actual loss mechanisms in high-intensity machines.

To address this issue, it is essential to incorporate space charge effects into the dynamic aperture tracking framework. Full self-consistent multi-particle simulations can achieve this, but they are computationally expensive and not well suited for systematic nonlinear optimization studies. Therefore, a simplified yet representative model that accounts for the influence of space charge on the tune distribution is highly desirable.

In this work, we develop a dynamic aperture tracking code specifically designed for high-intensity proton accelerators, in which the space charge–induced tune shifts are included analytically. The method allows efficient evaluation of the nonlinear dynamics under realistic space charge conditions. The Rapid Cycling Synchrotron (RCS) of the China Spallation Neutron Source (CSNS) [1] is used as a practical example to validate the approach and demonstrate its potential applications for the CSNS-II upgrade and similar high-intensity machines.

## METHOD

In conventional DA tracking, particle motion is evaluated under the influence of static magnetic fields, including multipole components, while collective effects are neglected. This approach assumes that each particle follows a fixed tune, determined by the linear optics and magnetic nonlinearities. However, in high-intensity proton accelerators, strong space charge forces cause tune shifts and spreads that vary with particle amplitude and longitudinal position. These effects significantly alter the resonance structure and must be incorporated into the analysis.

To efficiently include space charge effects in DA studies, we applied a simple model that modifies the particle tunes according to their transverse amplitudes and the instantaneous beam current. The model assumes a Gaussian beam distribution and computes the incoherent tune shift using the linearized space charge formula:

$$\Delta Q_{x,y} = -\frac{r_p N_b}{2\pi\beta^2\gamma^3\varepsilon_{x,y}} F_{x,y},$$

where $r_p$ is the classical proton radius, $N_b$ is the number of particles per bunch, $\beta$ and $\gamma$ are the relativistic factors, $\varepsilon_{x,y}$ are the transverse emittances, and $F_{x,y}$ are form factors depending on the beam aspect ratio. The tune shifts are then mapped to each tracked particle based on its action variables, effectively generating an amplitude dependent tune spread.

This modified tune distribution is embedded into the DA tracking algorithm. At each integration step, particle motion is updated with the effective tune shift corresponding to its instantaneous amplitude. The resonance driving term (RDT) analysis is also adapted to include the space charge induced tune modulation, enabling a consistent evaluation of resonance strength and location under collective effects.

The calculation code is based on the code in [2]. The resulting code maintains computational efficiency comparable to traditional single-particle tracking, while providing a more realistic estimation of the stable phase space region in high-intensity machines.

## RESULTS

The developed DA tracking code has been tested using the RCS of the CSNS as a representative case study. The CSNS/RCS accelerates protons from 80 MeV to 1.6 GeV at a repetition rate of 25 Hz, corresponding to a beam power

ISBN: <ask the JACoW BoD> ISSN: <ask the JACoW BoD> doi: 10.18429/JACoW-HB2025-THPT26

# THE IMPACT OF INTRA-BEAM SCATTERING ON THE SCHOTTKY NOISE OF THE BUNCHED BEAM

M. Abed, V. Lebedev†
Joint Institute for Nuclear Research, Dubna, Russia

*Abstract*

Schottky noise arises from statistical fluctuations in the beam current due to the discrete nature of charged particles and is widely used as a non-invasive diagnostic in circular accelerators. For bunched beams, the longitudinal Schottky spectrum consists of synchrotron satellites around revolution harmonics, with line widths primarily determined by synchrotron tune spread and growing linearly with harmonic number. When intra-beam scattering (IBS) or similar diffusion mechanisms are taken into account, an additional broadening appears, and the line width grows quadratically with harmonic number. In this work, we present an analytical model for the impact of pure diffusion on longitudinal Schottky noise. The results of this work are important for accurate interpretation of Schottky diagnostics and for improving understanding of the stochastic cooling of bunched beams.

## INTRODUCTION

The discreteness of charged particles in a beam leads to statistical fluctuations of the beam current, known as Schottky noise. It is widely used as a non-invasive diagnostic in circular accelerators. The Schottky noise spectrum is used to estimate key beam parameters such as tune, chromaticity, momentum spread, and emittance. It is also rich in valuable information about the beam's internal dynamics. In particular, it reflects the influence of different diffusion and damping mechanisms such as intra-beam scattering and beam cooling. Characterizing their impact on Schottky noise is essential for understanding beam stability and improvement of accelerator performance.

The Schottky noise spectrum depends on the beam structure. For coasting beams, it appears as a continuous distribution around each harmonic of the revolution frequency, with shape determined by the beam momentum distribution. For bunched beams, synchrotron lines are observed around the revolution harmonics, reflecting the longitudinal synchrotron oscillations. The widths of these lines, in the absence of diffusion, grow linearly with the harmonic number. Diffusion accounting yields additional broadening of the spectral lines.

In storage rings and colliders, several diffusion mechanisms are present. Typically, the intra-beam scattering (IBS) makes the largest contribution. IBS has two components, diffusion and friction, which affect Schottky noise differently and can be considered separately. In this article, we investigate how diffusional kicks from multiple IBS modify the shape and width of the longitudinal Schottky spectrum. Although developed model was built to account IBS, it remains valid for any "pure" diffusion where kicks of different particles are independent.

## SYNCHORTRON MOTION

Throughout this article we consider a harmonic RF system but assume linear longitudinal motion with accounting dependence of synchrotron frequency on the amplitude. For a linearized RF voltage, the longitudinal particle motion under random diffusional kicks $f(t)$ is described by the Langevin equations:

$$\dot{s} = -\eta\beta c\delta, \qquad \dot{\delta} = \frac{\Omega_s^2}{\eta\beta c} s + f(t), \tag{1}$$

where $s$ denotes the longitudinal deviation from the synchronous particle, $\delta$ is the relative momentum deviation, $\Omega_s$ is the synchrotron frequency, $\eta = a_c - 1/\gamma^2$ is the slip-factor, $\alpha_c$ is the momentum compaction, and $\beta c$ is the velocity of the reference particle. The random force $f(t)$ describes a stationary, Gaussian Markov process. Its statistical properties are defined by $\overline{f(t)} = 0$ and $\overline{f(t_1) f(t_2)} = D\delta(t_1 - t_2)$, where $D$ is the longitudinal diffusion.

The solution of the Langevin equations is :

$$\begin{aligned} s(t) &= \hat{s}\, cos(\Omega_s t + \psi) - \frac{\eta\beta c}{\Omega_s} \int_0^t \text{in}\big(\Omega_s (t - t')\big) f(t')\, dt', \\ \delta(t) &= \frac{\hat{s}\, \Omega_s}{\eta\beta c}\, sin(\Omega_s t + \psi) + \int_0^t \text{os}\big(\Omega_s (t - t')\big) f(t')\, dt', \end{aligned} \tag{2}$$

where $\hat{s}$ and $\psi_o$ are the amplitude and the initial phase of the synchrotron oscillation, respectively. The solution consists of two parts: a deterministic component, set by the initial particle phase and amplitude, and a stochastic component arising from $f(t)$. Averaging the solution over all realizations of the random kicks one obtains:

$$\begin{aligned} \overline{s(t)} &= \hat{s}\, cos(\Omega_s t + \psi) \\ \overline{\delta(t)} &= \frac{\hat{s}\, \Omega_s}{\eta\beta c}\, sin(\Omega_s t + \psi), \end{aligned} \tag{3}$$

which represents the average deterministic trajectory of a particle motion, equivalent to the synchrotron trajectory in the absence of diffusive random kicks.

The diffusive IBS kicks lead to spreading the particle trajectories determined by:

$$\begin{aligned} \overline{\Delta s(t)^2} &= \overline{s(t)^2} - \overline{s(0)}^2 = \frac{\eta^4 \beta^4 c^4 D}{\Omega_s^2} \left( \frac{t}{2} - \frac{\sin(2\Omega_s t)}{4\Omega_s} \right), \\ \overline{\Delta\delta(t)^2} &= \overline{\delta(t)^2} - \overline{\delta(0)}^2 = D \left( \frac{t}{2} + \frac{\sin(2\Omega_s t)}{4\Omega_s} \right). \end{aligned} \tag{4}$$

The time dependence of the spreading reflects the diffusive nature of the random force, leading to a non-stationary process gradually enlarging the particle phase-space distribution. Typically, the synchrotron frequency is small

† email address: valebedev@jinr.ru

ISBN: <ask the JACoW BoD> ISSN: <ask the JACoW BoD> doi: 10.18429/JACoW-HB2025-THPT28

# ELECTRON COOLING USING LONGITUDINAL HOLLOW ELECTRON BEAM*

X. D. Yang†, H. Zhao, Institute of Modern Physics, CAS, Lanzhou, China

*Abstract*

The intra-beam scattering in high charge state intense heavy ion beams is a problem worth considering. By controlling the longitudinal distribution of the ion beam, it may be possible to alleviate the ion beam loss and improve the lifetime of the ion beam caused by intra-beam scattering. Unlike the traditional cooling process of direct current electron beams or longitudinal uniform distribution electron bunch beams, a longitudinal hollow electron beam is used to cool heavy ion beams. Ions at the edge of the ion beam will receive stronger cooling, while ions at the center of the ion beam will receive weaker cooling, avoiding overcooling at the center of the ion beam. This paper discusses the generation, measurement, and related issues of longitudinal hollow electron beams. Corresponding solutions and suggestions have been proposed for the problems and challenges that may be encountered in the research. The cooling process of longitudinal hollow electron beams will be simulated and experimentally studied in the future, with the hope of obtaining beneficial effects.

## INTRODUCTION

Intra-beam scattering is one of the main reasons of reduction of the beam intensity and shortening of stored lifetime in the collider, light source and storage ring, especially in the case of the high energy high intensity heavy ion beam with high charge state. The intra-beam scattering presents dissimilar influence in the different facilities. It can be counteracted partially by the synchrotron radiation damping in the lepton machine. It also can be suppressed by the wiggler. But there is no similar damping in the hadron machine.

The intensity and quality of ion beam in an accelerator are the most important parameters, and they are often asked to increase and improve according to the requirements of various physics experiments. High intensity beam of heavy ion with high charge state and short bunch length was expected to store in a storage ring with long lifetime and less loss.

Intra-beam scattering has become a bottleneck for maintaining the optimal performance of the accelerator. In this case, intra-beam scattering becomes the primary cause of emittance growth in the six-dimensional phase space. Particles with large amplitudes will escape the bucket and be lost in the ring. As a result, the lifetime of the ion beam in the storage ring decreases.

In order to increase the lifetime of ion beam and decrease the loss, the behavior of intra-beam scattering in the high intensity heavy ion storage ring with short bunch should be investigated completely and systemically. Electron cooling was chosen to suppress the effect of intra-beam scattering, another unexpected effect happened during the cooling.

From the perspective of beam dynamics, and based on understanding the mechanism of intra-beam scattering in high-density beams in heavy ion storage rings, more effective methods to suppress intra-beam scattering should be explored and attempted.

Under electron cooling, the distribution of ion beams quickly deviates from the initial Gaussian type, forming a denser core and a longer tail. The ions standing in the tail of the beam will be lost soon due to large amplitude [1].

A new idea was introduced in this paper. A novel solution was proposed. This novel method will be attempted to suppress intra-beam scattering. The feasibility and validity of this method was verified in this study. This idea will focus on the investigation on the suppression of intra-beam scattering in the high intensity heavy ion beam in the storage ring with the help of longitudinal hollow electron beam.

The traditional DC electron beam in the electron cooler was modulated into an electron bunch with different longitudinal distributions. The stronger cooling was expected in the tail of the ion beam and the weaker cooling was performed in the tail of the ion beam. The particle on the outside will experience stronger cooling and will be driven back into the center of the ion beam. The ion loss will be decreased and the lifetime will be increased. The intensity of the ion beam in the storage ring will be maintained for a longer period. Two functions will be combined into one electron cooler. The shorter the pulse, the higher intensity and lower emittance heavy ion beam was expected in the cooler storage ring. In the future, the results of this project will be constructive to the upgrade and improvement of existing machines and also be helpful to the design and operation of future storage and high-energy electron coolers.

## MOTIVATION

From the previous experimental results [2] indicated that the partially transverse hollow electron beam has an advantage in beam accumulation. The optimal ratio Ugrid/Uanode is near 0.2 in the electron gun of electron cooling device. In this case, the centre density is 2 times less than the edge density in the electron beam.

The transverse hollow electron beam is beneficial for accumulating ion beams with higher current intensity.

The electron cooling will be expected to serve as a knob to control the longitudinal distribution of the ion beam in the storage ring.

The longitudinal hollow electron beam is expected to obtain benefits in the following aspects.

- Suppress intra-beam scattering.
- Control the longitudinal distribution of the ion beam.
- Make the beam bunch contain as many particles as possible.

* Work supported by NSFC No. 12275325, 12275323, 12205346.

† yangxd@impcas.ac.cn.

ISBN: <ask the JACoW BoD> ISSN: <ask the JACoW BoD> doi: 10.18429/JACoW-HB2025-THPT32

# $H^-$ BEAM HALO COLLIMATION USING STRIPPING AND APPLICATIONS OF THE SECONDARY PROTON BEAM

Z. P. Li*[,1,2], X. J. Nie[1,2], Q. Li[1,2], K. Zhou[1,2], M. Y. Huang[1,2], J. Peng[1,2]
[1]Institute of High Energy Physics, Chinese Academy of Sciences, Beijing, China
[2]Spallation Neutron Source Science Center, Dongguan, China

*Abstract*

To mitigate beam loss during RCS injection and in the transport line from the linac to the ring, a novel transverse beam halo collimation system was developed for the CSNS LRBT beamline. The system employs three sets of stripping foils arranged with a 60° phase shift, using twelve carbon foils to convert peripheral $H^-$ ions with beam power below 2 kW into protons. Experimental results demonstrate that the collimators effectively reduce injection beam loss and contribute to RCS beam power enhancement. Moreover, the resulting proton beams enable medium-energy proton irradiation experiments and isotope production, thus achieving dual objectives of beam loss control and secondary beam utilization. This work demonstrates an effective approach for beam halo management in high-power proton accelerators.

## INTRODUCTION

The China Spallation Neutron Source (CSNS) [1] is a high-power pulsed spallation neutron source facility, comprising a proton accelerator, a target station, and multiple spectrometer systems. The accelerator chain primarily consists of a negative hydrogen ion ($H^-$) linear accelerator (linac) and a rapid cycling synchrotron (RCS). The $H^-$ beam at 80 MeV from the linac is injected into the RCS via a multi-turn charge-exchange injection scheme and is accelerated to a final energy of 1.6 GeV. Currently, CSNS operates at an average beam power of 170 kW, which is planned to be further increased to over 500 kW following the ongoing Phase II upgrade project [2].

The CSNS linear accelerator operates at a peak beam current of 15 mA. Owing to space charge effects and other sources of error, a fraction of the beam particles forms a halo at the periphery of the beam bunches [3]. Although these halo particles represent only a small fraction of the beam, their relatively high emittance makes them susceptible to beam loss during transport and injection into the subsequent accelerator. This beam loss consequentlyleads to an increase in radiation dose.

In the CSNS-II upgrade, the design peak beam current of the linear accelerator will be increased to 50 mA. This is anticipated to generate a greater number of halo particles with even larger emittance, posing a significant challenge for linac design. Although a beam transport channel with larger acceptance has been designed, halo particles with high emittance may still be lost in the injection region, where the aperture is relatively restricted. Furthermore, high-emittance particles can also constrain the painting range of the injected beam in the RCS, thereby limiting the potential for further enhancement of the beam power [4].

To effectively suppress beam halo effects generated in the linear accelerator, a halo collimation system based on $H^-$ stripping was designed and installed in the LRBT beam transport line between the linac and the RCS during the CSNS Phase I project, and its feasibility has been experimentally validated. Experimental results demonstrate that the carbon foil-based stripping collimation scheme effectively reduces the transverse beam emittance and mitigates beam loss during downstream transport and injection. Furthermore, the stripped proton beams can be utilized for medium-energy proton beam experiments, operating concurrently with the main $H^-$ beam, thereby expanding the application capabilities of the CSNS accelerator.

## HALO COLLIMATION BY STRIPPING FOILS

Three sets of foil collimators have been installed in the straight section of the LRBT beam transport line to effectively suppress beam halo effects. Each collimator unit is equipped with four carbon foils (top, bottom, left, and right), designed to progressively remove halo particles in three steps while minimizing significant beam loss [5].

The straight section of the LRBT beam transport line employs a triplet periodic lattice structure, where the beam envelope forms waists between each unit, with complete overlap of the horizontal and vertical waist positions. A foil collimator is installed at each of the three waist positions corresponding to the final three triplet units. Each collimator is equipped with stripping foils in both transverse directions, forming a square beam aperture in real space. When the beam passes through, $H^-$ particles at the periphery of the channel interact with the stripping foils and are converted into protons along with a small fraction of hydrogen atoms.

The lattice is specifically designed with a phase advance of 60° per cell in both planes. This specific value is chosen to ensure that the transverse phase space is properly rotated between successive collimators, thereby optimizing their effectiveness in progressively removing the beam halo. The three sets of stripping foils, capable of simultaneous X and Y halo collimation, are positioned at the three double-waist locations, collectively enabling effective control of beam emittance. After passing through the three-stage collimation system, the beam particles exhibit a hexagonal distribution in normalized phase space, as shown in Fig. 1.

* lizp@ihep.ac.cn

ISBN: <ask the JACoW BoD> ISSN: <ask the JACoW BoD> doi: 10.18429/JACoW-HB2025-THPT33

# HIGH-INTENSITY BEAM TESTS IN THE CERN PROTON SYNCHROTRON

H. Damerau*, S. Albright, F. Asvesta, M. Bozatzis, A. Huschauer, A. Lasheen, T. Prebibaj
CERN, Geneva, Switzerland

*Abstract*

A study campaign to identify potential limitations at highest intensities has been performed in the Proton Synchrotron (PS) in view of future requirements for fixed-target beams at CERN. Previous explorations of the maximum intensity date back more than two decades, and they required two injections from the PS Booster (PSB) with a long flat-bottom in the PS. This scheme resulted in unacceptably high beam loss. The limitations in the PSB have been removed with the upgrades in the framework of the LHC Injectors Upgrade (LIU) project. In combination with improvements to the PS RF systems, these upgrades enabled the acceleration of more than $4 \times 10^{13}$ protons for the first time. Coupled-bunch instabilities during the first part of acceleration are mitigated by a dipole mode feedback system. Additionally, careful adjustment of the working point at transition crossing was vital for reducing beam loss. A barrier-bucket RF system with a wideband cavity introduces a gap in the longitudinal distribution for the extraction kicker. The focus recently moved to evaluating the impact of beam induced voltage in this cavity, as well as the residual population of the gap.

## INTRODUCTION

The beam intensity in the CERN Proton Synchrotron (PS) continuously increased until the late 1990s [1], when the focus moved from fixed-target to high-brightness beams for the Large Hadron Collider (LHC) [2]. The improvements in the framework of the LHC Injectors Upgrade (LIU) project [3] culminated in the demonstration of the beam parameters for the High-Luminosity (HL) LHC.

The last campaign of exploratory high-intensity beam tests in the PS was performed in the early 2000s [4]. With two injections from the PS Booster (PSB) at maximum close to $3.9 \times 10^{13}$ protons were accelerated to a momentum of 14 GeV/c [5]. However, the large losses with twice $2.4 \times 10^{13}$ protons injected from the PSB, together with the Continuous Transfer (CT) extraction scheme [6, 7], would not have allowed operation under these conditions, and the scheme had to be abandoned.

The implementation of the Multi-Turn Extraction (MTE) [8] technique, combined with the barrier-bucket to deplete a gap for the kicker rise time [9], removed the losses at extraction from the PS almost completely. Along with the LIU upgrades of the entire PS complex, this paved the way to beam intensities well above the present operational level of about $2 \times 10^{13}$ protons per pulse (p/p).

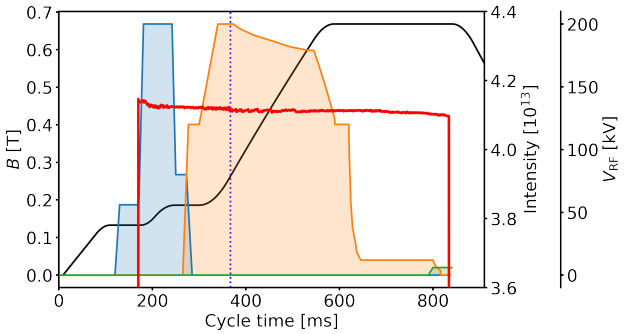


Figure 1: Bending field, $B$ (black) together with the RF voltage, $V_{\mathrm{RF}}$ programs at $h_{\mathrm{PS}} = 8$ (blue) and $h_{\mathrm{PS}} = 16$ (orange) during the fixed-target cycle. The voltage in the wideband cavity (green) generating the barrier bucket is only activated close to extraction. The beam intensity (red) is measured with a current transformer (BCT). Cycle time (Ctime) refers to the time with respect to the start of the cycle, injection being at 170 ms, i.e., C170. The blue vertical line marks the instant of transition crossing.

To explore the capability of providing fixed-target beam at much higher intensity from the PS, an extensive set of beam studies has been pursued since 2023. Thanks to Linac4, as well as the PSB energy and RF upgrades, each of the four rings can now deliver much more than $1 \times 10^{13}$ protons [10–12], well above the intensity the PS can presently handle.

The acceleration cycle of fixed-target beam for the Super Proton Synchrotron (SPS) is most suited for high-intensity beam tests in the PS. Firstly, one single transfer from the PSB allows to fill the entire ring, removing the need for a second injection and a long flat-bottom at low energy. Secondly, with all RF buckets populated equally, any difficulties related to transient beam loading are removed. Finally, hardware changes planned during the next long shutdown (LS3) also motivate to confirm the intensity reach of the barrier-bucket MTE.

## INTENSITY REACH AND TRANSMISSION

Eight bunches, two from each PSB ring, are injected into the PS at a kinetic energy of 2 GeV. With all buckets occupied, the beam is accelerated to an intermediate plateau at about 3.1 GeV at the RF harmonic, $h_{\mathrm{PS}} = 8$ (Fig. 1). A bunch pair splitting to $h_{\mathrm{PS}} = 16$ doubles the number of bunches [13], while halving the intensity per bunch. The longitudinal emittance is moreover increased by controlled blow-up with a phase modulated higher-harmonic RF system at 200 MHz [14] during the intermediate plateau. Transition energy (Lorentz factor at transition, $\gamma_{\mathrm{tr}} = 6.1$) is crossed

* heiko.damerau@cern.ch

ISBN: <ask the JACoW BoD> ISSN: <ask the JACoW BoD> doi: 10.18429/JACoW-HB2025-THPT35

# IMPACT OF LONGITUDINAL BEAM FEEDBACK ON SINGLE-BUNCH INSTABILITIES

L. Intelisano*, H. Damerau, I. Karpov, CERN, Geneva, Switzerland

*Abstract*

Beam feedback systems are crucial in high-energy circular accelerators to suppress undesired bunch oscillations and prevent beam quality degradation. In the longitudinal plane, the CERN Super Proton Synchrotron (SPS) is equipped with beam phase and synchronization loops. The phase loop locks the rf phase of the accelerating voltage to the one of the bunches detected by a pickup, while the synchronization loop maintains the average rf frequency at a programmed reference. During the acceleration ramp, a bunch length excitation leading to significant emittance growth has been observed for different beam types. These longitudinal oscillations vanish when the beam feedback is disabled. A refined simulation model of the SPS beam control loops has been developed for the BLonD simulation suite, allowing to study the impact of longitudinal feedback on single-bunch instabilities. The findings suggest that the instability is intrinsic to the beam due to the radial mode-coupling of the sextupole azimuthal mode, albeit modified by the action of the loops.

## INTRODUCTION

Beam feedback systems are essential parts of high-energy synchrotrons, where they mitigate collective instabilities by suppressing uncontrolled bunch oscillations and thereby preserving beam quality. At the CERN Super Proton Synchrotron (SPS), for proton beams not crossing transition energy, two key feedback loops are employed in the longitudinal plane. The beam phase loop (PL) locks the rf phase of the accelerating voltage $\phi^{\mathrm{rf}}$, to one of the bunches detected by a pickup. The synchronization loop (SL) regulates the rf phase on an external reference $\phi^{\mathrm{syn}}$ [1].

It has been observed for various types of beams in the SPS that an uncontrolled bunch oscillation occurs with these beam control loops enabled. For the AWAKE-type beam, the most demanding single-bunch SPS operating mode due to its stringent beam specifications in intensity and bunch length [2], Figure 1 shows an unexpected instability (blue) due to the presence of the PL. This uncontrolled bunch length oscillation vanishes when the PL is disabled (orange).

A similar destabilizing effect of the feedback on beam stability has been observed across different accelerators in both transverse and longitudinal planes [3–5].

This work investigates the impact of longitudinal feedback in the single-bunch regime. A refined SPS beam feedback model has been developed and integrated into the macroparticle tracking code BLonD [6]. The findings reproduce the detrimental effect of the PL on the AWAKE beam, in very good agreement with observations.

* leandro.intelisano@cern.ch

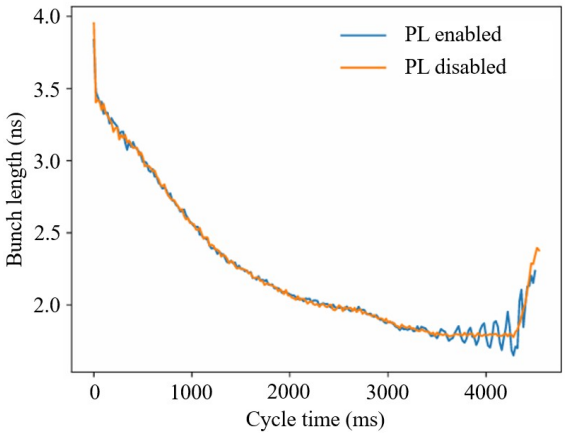


Figure 1: Measured bunch length evolution during the AWAKE-cycle beam with PL enabled (blue) and disabled (orange).

## BEAM FEEDBACK IN THE SPS

In the framework of the CERN LHC Injectors Upgrade (LIU), the SPS underwent an extensive upgrade to double the extracted proton intensity for the Large Hadron Collider (LHC) [7]. The beam control system was exchanged, transitioning from a mostly analog to a digital system [1], making its transfer functions readily accessible for high-fidelity simulations.

Figure 2 shows a simplified block diagram of the beam feedback system in the SPS, with PL and SL branches highlighted by red and green dashed lines, respectively. Specifically, the PL block computes the bunch-phase displacement at turns $n$ and $n-1$ and applies a frequency correction through appropriate gains $K_{\tilde{\phi}_n}$ and $K_{\tilde{\phi}_{n-1}}$.

The SL takes as an input the rf phase provided by the Numerically Controlled Oscillator (NCO) [8] and computes the SL phase error, $\epsilon$, defined as

$$\epsilon_n = \phi_n^{\mathrm{rf}} - \phi_n^{\mathrm{syn}} , \tag{1}$$

along with its discrete-time integral $Z_n$.

In this five-state control system, with state-vector $\mathbf{X}_n$, the correction $\Delta\omega_n^{\mathrm{rf}}$, is applied to the rf frequency $\omega_n^{\mathrm{rf}}$, of the fundamental cavity system through the feedback gain matrix $\mathbf{K}$. According to the state-feedback control law [9], we have

$$\Delta\omega_{n+1}^{\mathrm{rf}} = -\mathbf{K}\,\mathbf{X}_n , \tag{2}$$

ISBN: <ask the JACoW BoD> ISSN: <ask the JACoW BoD> doi: 10.18429/JACoW-HB2025-THPT36

# IMPEDANCE IN MATTER*

E. Métral†, CERN, Geneva, Switzerland

*Abstract*

The delivery of a high-brightness muon beam through ionisation cooling is essential to produce sufficient luminosity in a muon collider. The ionisation cooling technique has been demonstrated in principle by the Muon Ionisation Cooling Experiment (MICE) but the potential detrimental impacts of collective effects still need to be carefully investigated. Using the same formalism as the one developed two decades ago for the CERN LHC collimators (which revealed a new and beneficial physical regime), the longitudinal and transverse beam coupling impedances in matter have been computed analytically for the case of a cylindrically symmetric material characterised by any electrical conductivity, permittivity and permeability, surrounded by a perfect conductor and with a longitudinal size much larger than the transverse one.

## INTRODUCTION

Approximately twenty years ago, the long-standing subject of the longitudinal and transverse resistive-wall impedances experienced a revival of interest due to the important role of resistive-wall effects for collective beam stability in large circular accelerators or colliders (corresponding to low machine revolution frequency $f_0$). In particular, a new physical regime was revealed at low frequencies by the CERN LHC collimators, where a small beam aperture paired with a large wall thickness asked for a different physical picture of resistive-wall effect than the classical one. Starting from Maxwell equations and using field matching, a consistent derivation of the longitudinal and transverse (resistive-)wall impedances of an infinitely long cylindrical beam pipe was performed for one and two layers (surrounding the vacuum region where the beam circulates) [1] (and references therein), whose results should be valid for any beam velocity, frequency, conductivity, permittivity and permeability. These results were later extended to any number of layers for both a cylindrical beam pipe and two parallel plates [2] and the ImpedanceWake2D (IW2D) code was developed and made available to the community [3].

In the framework of the studies to design a muon collider, an additional extension of this formalism is required to evaluate the impedance in matter, i.e., when the beam propagates through material media instead of vacuum. This is required because the essential process of ionisation cooling reduces the beam emittances by transmitting the beam through a series of absorbers.

This paper begins by outlining the general rule for relating impedances in vacuum to those in matter. It then examines the consequences for both longitudinal and transverse impedances in a simplified scenario: a single layer of perfect conductor surrounding matter characterised by conductivity, permittivity, and permeability, which may be arbitrary and frequency-dependent.

## GENERAL RULE

Following the formalism of field matching discussed in Ref. [1], the only difference between the case of a beam circulating in vacuum (defined by zero conductivity $\sigma = 0$ and the free-space permittivity $\epsilon_0$ and permeability $\mu_0$) and a beam circulating through matter (defined by any conductivity $\sigma$, permittivity $\epsilon = \epsilon_0\epsilon_1$ and permeability $\mu = \mu_0\mu_1$) can be deduced from the right-hand-side of the scalar Helmholtz equation for the longitudinal electric field component in the circular cylindrical coordinates $(r, \theta, z)$ (see Eq. (2) of Ref. [1]). In the frequency domain, the (source) charge density $\rho$ is proportional to $e^{-jkz}$, with $j$ the imaginary unit and $k = \omega/v$ the wave number (with $\omega = 2\pi f$ the angular frequency and $v = \beta c$ the beam velocity), which leads to

$$\frac{1}{\epsilon}\frac{\partial \rho}{\partial z} + j\omega\mu\rho v = -\frac{j\rho k}{\epsilon_0}F, \tag{1}$$

where the general factor $F$ is given by

$$F = \frac{1}{\epsilon_1} - \mu_1\beta^2. \tag{2}$$

Writing

$$\epsilon_1 = \epsilon_r + \frac{\sigma}{j\epsilon_0\omega}, \tag{3}$$

yields

$$F = \frac{j\epsilon_0\omega}{\sigma + j\epsilon_0\epsilon_r\omega} - \mu_1\beta^2. \tag{4}$$

In vacuum, this factor $F$ becomes $1 - \beta^2 = 1/\gamma^2$ and therefore the general rule to deduce the longitudinal and transverse impedances in matter is to use the formulae of longitudinal and transverse impedances in vacuum (see Eqs. (17) and (24) of Ref. [1]) and replace the term $1/\gamma^2$ by the factor $F$ given by Eq. (4). Furthermore, the radial propagation constant in vacuum $\nu_{\rm vac} = k/\gamma$ should be replaced by the general radial propagation constant in matter $\nu_{\rm mat} = k\sqrt{1 - \epsilon_1\mu_1\beta^2}$. Therefore, in the Eqs. (17) and (24) of Ref. [1], one should also replace $s = ka/\gamma$ by $x_0 = \nu_{\rm mat}a$, where $a$ is the beam radius, and $x_1 = kb/\gamma$ by $x_1 = \nu_{\rm mat}b$, where $b$ is the inner beam pipe radius.

## LONGITUDINAL IMPEDANCE

Applying the general rule discussed in the previous section, the total (i.e., direct plus indirect) longitudinal impedance in matter (surrounded by a perfect conductor) in

* This work was supported by the European Union grant agreement 101094300 and it was endorsed by the IMCC

† Elias.Metral@cern.ch

ISBN: <ask the JACoW BoD> ISSN: <ask the JACoW BoD> doi: 10.18429/JACoW-HB2025-THPT37

# MODIFIED ENVELOPE EQUATIONS WITH CONSIDERATION OF ACCELERATION AND ITS APPLICATIONS IN BEAM DYNAMICS STUDY*

Xin-Miao Wan, Zhi-Qiang Ren, Xuan-Kai Chang, Long Ma, Yi-Xin Wu, Shi-Qi Li, Ning-Xuan Li, Bin Tang, Zhi-Hui Li†
The Key Laboratory of Radiation Physics and Technology of Ministry of Education, Institute of Nuclear Science and Technology, Sichuan University, Chengdu, China

*Abstract*

This research presents a new numerical method of the beam envelope equations in the presence of acceleration. By using a scanning technique, a matched solution set with acceleration has been obtained. With focusing cases as constant wave number per unit length, it is found that the conventional adiabatic approximation theory fails when dealing with high acceleration gradients. Moreover, for matched cases, a scaling law of matched beam envelope as a function of beam energy is derived, which can be applied for the design and optimization for linacs. For mismatch cases, we found that the well-known wave number formula for mismatched envelope oscillations in the low-energy region requires revision when considering acceleration, since the oscillation wave numbers of low energy beams are largely affected by the accelerating effects. By using the Particle-Core Model (PCM) simulations, with acceleration, the amplitudes of particle transverse oscillations near the 2:1 resonance island are dramatically suppressed. This work could have potential applications on analysing and depressing beam dynamical instability with strong accelerating fields in future linacs.

## INTRODUCTION

As a core device in basic science and engineering applications, the High-Power Proton Linear Accelerator serves an irreplaceable role [1]. Following decades of intensive research, the academic community has deepened its understanding of beam dynamics under high-current conditions [2]. However, current studies remain limited: most only interpret phenomena from multi-particle simulations, failing to integrate acceleration effects into theoretical analyses or uncover the underlying mechanisms [3]. Thus, the theoretical system of beam dynamics under acceleration still needs further development.

To address this gap, this study develops a numerical method for solving the matching envelope equation that accounts for acceleration effects. Using this method, two key findings are obtained: first, it identifies limitations in the mismatched envelope oscillation wavelength formula of the traditional adiabatic approximation; second, combined with the Particle-Core Model (PCM), it reveals that acceleration enables particles in the 2:1 resonance island to break free from resonance and gradually approach the beam core.

## ENVELOPE EQUATIONS

Taking the motion of a particle in the x-direction as an example, its equation of motion can be expressed as:

$$\frac{dp_x}{dt} = F_x = -kx + F_s\,, \tag{1}$$

$$p_x = \gamma m_0 \frac{dx}{dt} = \gamma m_0 v x'\,, \tag{2}$$

where $k$ denotes the linear force constant of the linear external force; $F_s$ represents the space charge force; $\gamma$ is the Lorentz factor, defined as $\gamma = 1/\sqrt{1-\beta^2}$(with $\beta = v/c$, where $v$ is the particle velocity and $c$ is the speed of light in vacuum); $m_0$ is the rest mass of the particle; The angle of the particle's motion direction is defined as $x' = dx/ds$, where $s$ is the path length of the particle's motion.

By substituting Eq. (2) into Eq. (1) and taking $s$ as the independent variable, the following equation is obtained after rearrangement:

$$x'' + \frac{(\gamma v)'}{\gamma v}x' + \frac{k}{\gamma m_0 v^2}x - \frac{F_s}{\gamma m_0 v^2} = 0. \tag{3}$$

Based on Eq. (3), we further derive the RMS envelope equation under acceleration conditions. Let $a$ be the RMS envelope radius in the $x$-direction, $\epsilon_r$ is the non-normalized RMS emittance, and $k_{0x}$ is the linear focusing coefficient on the $x$-direction. After substituting the relevant physical quantities and simplifying, the RMS envelope equation under acceleration is obtained:

$$a'' + (ln\beta\gamma)'a' + k_{0x}^2 a - \frac{\epsilon_r^2}{a^3} - \frac{\overline{F_s x}}{a} = 0. \tag{4}$$

To simplify the form of the equation under acceleration, an auxiliary function $f = 1/\sqrt{\beta\gamma}$ is introduced, and a normalized envelope parameter $A$ is defined, which satisfies the relation $a = f * A$. After rearrangement, the "quasi-envelope equation" under acceleration is derived:

$$A'' + \left[\frac{f''}{f} + \frac{(ln\beta\gamma)'f'}{f} + k_{0x}^2\right]A - \frac{\overline{F_s x}}{f^2 A}\frac{1}{\gamma m_0 c^2 \beta^2} - \frac{\epsilon_{n,r}^2}{A^3} = 0. \tag{5}$$

Here, $\epsilon_{n,r}$ is the normalized RMS emittance, which characterizes the quality stability of the particle beam during acceleration.

In summary, through the normalization relation $a = f * A$, the complete envelope equation for particle motion under acceleration can be inferred from the "quasi-

* Work supported by the National Natural Science Foundation of China (Grant Nos. 11375122 and 11875197)
† lizhihui@scu.edu.cn

ISBN: <ask the JACoW BoD> ISSN: <ask the JACoW BoD> doi: 10.18429/JACoW-HB2025-THPT39

# LONGITUDINAL LOCALIZED EXCITATION SLOW EXTRACTION METHOD*

Y. Xiong[1,2], H. J. Yao[1,2], Z. J. Wang[1,2], C. H. Li[1,2], S. X. Zheng†,[1,2], Key Laboratory of Particle & Radiation Imaging, Tsinghua University, Ministry of Education, Beijing, China
[1]also at Laboratory for Advanced Radiation Sources and Application, Tsinghua University, Beijing, China
[2]also at Department of Engineering Physics, Tsinghua University, Beijing, China

*Abstract*

Resonant slow extraction is widely utilized in hadron synchrotron accelerators. This paper proposes a longitudinal localized excitation method for slow extraction, in which transverse excitation is applied only within a limited phase interval located at the edge of the longitudinal phase space. As a result, only particles situated in this region are excited and subsequently extracted. This approach offers several advantages, including mitigating adverse space charge effects, reducing spill fluctuations, and enabling adjustment of the extracted beam's momentum spread. These capabilities make the method suitable for various applications with specific beam requirements. Several application examples of the longitudinal localized excitation slow extraction method are presented in this paper.

## INTRODUCTION

Synchrotrons are the predominant type of high-energy particle accelerators today and are also highly competitive in the medium- and low-energy accelerators. Resonant slow extraction [1] is a common method used in synchrotrons.Taking third-order resonant slow extraction as an example, its basic principle involves moving the ring's working point close to the resonance line prior to extraction and applying a sextupole field at a suitable location. This will create stable and unstable regions in the transverse phase space. Particles in the unstable region gradually deviate from the reference orbit and enter the extraction channel to be extracted. To ensure continuous beam extraction, particles must continuously move from the stable region into the unstable region. The RF-KO (Radio Frequency Knock-Out) method [2] is a commonly used technique to realize this. The RF-KO signal applies continuous and regular transverse excitations to the beam, causing the transverse emittance to grow continuously. Particles with increased emittance are extracted once they move beyond the boundary of the stable region.

Beam quality is of great importance in slow extraction, including beam intensity, momentum spread and beam uniformity. Different application requires different beam characteristics. To obtain high intensity beam, we need to improve the extraction efficiency. But high momentum spread can lead to an increased beam envelope, raising the risk of beam loss inside the ring during extraction, thus reducing extraction efficiency. Besides, the beam with high intensity suffers from strong space charge effects. In RF-KO excitation process, space charge effects will result in beam center oscillations and the growth rate of transverse emittance will be slowed down [3]. These effects will make the extracted beam have a huge nonuniformity.

To improve the beam quality of third-order resonant slow extraction based on RF-KO, especially addressing the detrimental effects of high momentum spread, high spill fluctuation and strong space charge, a longitudinal localized excitation method for transverse slow extraction is proposed.

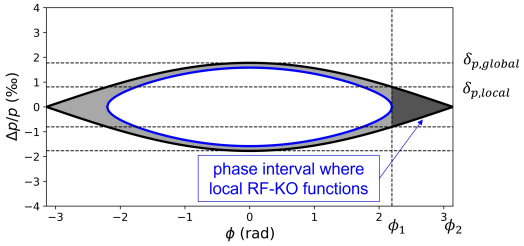


Figure 1: Longitudinal phase space of kicked particles and extracted particles. The boundary of the stable region (bucket) is depicted by the black line.

## LONGITUDINAL LOCALIZED EXCITATION SLOW EXTRACTION

In traditional slow extraction, to minimize the adverse effects of high momentum spread, the RF voltage must be ramped down prior to beam extraction. This process is intentionally conducted in a slow, quasi-adiabatic manner to preserve the longitudinal emittance. The conservation of longitudinal emittance implies a minimum value for the momentum spread of the extracted beam, given by the area occupied by the beam in longitudinal phase space divided by $2\pi$. This minimum value is achieved when the RF cavity voltage is reduced to zero. However, since the cavity voltage is typically not zero during the extraction process, the actual momentum spread of the extracted beam is often larger than this lower limit.

The longitudinal phase space with nonzero RF cavity voltage and zero synchronous phase is shown in Fig. 1.

For some applications, the theoretical lower limit is insufficient to meet the demanded beam momentum spread. To achieve a smaller momentum spread in the extracted

* Work supported by the National Natural Science Foundation of China (No. 12075131).
† zhengsx@tsinghua.edu.cn

ISBN: <ask the JACoW BoD> ISSN: <ask the JACoW BoD> doi: 10.18429/JACoW-HB2025-THPT47

# POSITION-PHASE ERROR CANCELLATION EFFECTS IN BEAM-BASED LINAC ALIGNMENT AND SYNCHRONIZATION

Haoyu Zhou[1,2,*], Jonathan Wong[1,2,3], Chi Feng[1,3], Yu Du[1,2], Tielong Wang[1,2], Binghui Ma[1,2]
[1] Institute of Modern Physics, Chinese Academy of Sciences, Lanzhou, China
[2] University of Chinese Academy of Sciences, Beijing, China
[3] Advanced Energy Science and Technology Guangdong Laboratory, Huizhou, China

*Abstract*

As prerequisites for automatic phase setting and fault compensation, precise longitudinal alignment and RF phase calibration are critical for high-intensity superconducting hadron linacs. While multiple facilities have successfully aligned or synchronized their linacs with time-of-flight (TOF) beam-based methods, existing error analyses typically assume uncorrelated position and phase uncertainties. This work rigorously derives intrinsic correlations between position and phase errors in beam-calibrated linacs. We demonstrate how these correlations can induce error cancellation effects that improve the accuracy of energy measurements and phase setting. Having validated these effects through simulations, we analyzed their implications for beam-based calibration experiments with applications to HIAF and CiADS commissioning.

## INTODUCTION

During the tuning of a linear accelerator, each cavity must be correctly phased to achieve the designed energy distribution and maintain stable longitudinal beam dynamics. Consequently, accurate phase setting has long been a technical challenge for linac operations. Traditionally, phase setting is performed through phase-scan methods, which require sequential scanning of each cavity and are therefore time-consuming. To meet the demand for rapid tuning, automated phase-setting techniques have been developed, enabling phase calibration to be completed within minutes [1, 2].

Among them, the Institute of Modern Physics (IMP) proposed a beam-based calibration method that employs time-of-flight (TOF) measurements to simultaneously determine both the cavity phase offset and the position/phase of beam position monitors (BPMs) [3]. As illustrated in Fig. 1, a pair of pre-calibrated BPMs is installed downstream of the beamline to calibrate the relative position and phase offset between a reference BPM and the BPM under test. However, experimental results showed that the beam velocity error measured using the calibrated parameters was much smaller than expected. This observation suggests the presence of an intrinsic cancellation between position and phase calibration errors, leading to a remarkably high accuracy in the measured beam velocity.

The structure of this paper is as follows. The first section analyzes in detail how position and phase errors cancel each other when systematic calibration errors exist between BPMs. The second section investigates whether similar error cancellation effects occur in the calibration between the cavity and BPM under both systematic and random errors, and derives how the effectiveness of error cancellation varies with the velocities of the calibration and test beams. The final section summarizes the findings and outlines directions for future work.

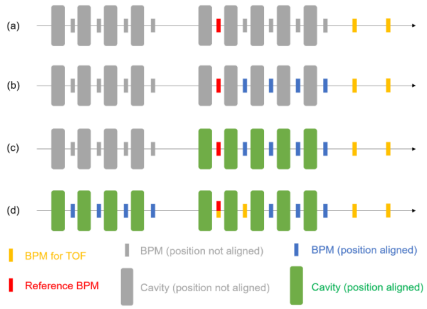


Figure 1: Schematic diagram of position alignment of the entire linac that proceeds as follows: (a) the original setup; (b) the alignment of BPMs; (c) the alignment of cavities; and (d) if applicable, the use of aligned BPMs for TOF measurements to align elements further upstream.

## VERIFICATION OF BPM INTER-ERROR CANCELLATION RELATIONSHIP

We select a relatively simple pair of BPM models in automatic phase setting to verify the error cancellation relationship. Using a beam with velocity $V_0$ to calibrate the distance and phase deviation $\Delta\varphi$ between two BPMs, as shown in Fig. 2. The readings of the two BPMs are $t_1$ and $t_2$ , and their difference is represented by $t_d$ . We convert the phase deviation into a time deviation, defining $\tau$ as the time difference corresponding to $(\varphi_{b,offset} - \varphi_{a,offset})$, i.e., $\delta_{t_2} - \delta_{t_1}$ . If there is an $\Delta L$ error in the actual distance between the two BPMs compared to the calibration distance, we want to observe how this error affects the final measurement accuracy of the beam velocity [4].

This distance error $\Delta L$ will lead to a shift in the calibration of the time deviation $\tau$ :

* zhouhaoyu@impcas.ac.cn

ISBN: <ask the JACoW BoD> ISSN: <ask the JACoW BoD> doi: 10.18429/JACoW-HB2025-THPT49

# PROGRESS OF CNT MULTI-WIRE SCANNERS FOR CSNS-II*

Zhijun Lu[1,2], Renhong Liu[1,2], Renjun Yang†[,1,2], Biao Zhang[1,2], Zhihong Xu[1,2], Ruiyang Qiu[1,2], Fang Li[1,2], Weiling Huang[1,2], Lei Zeng[1,2], Rehman M, Rui Yang[1,2], Pengcheng Wang[1,2], Jiaming Liu[1,2], Yigang Wang[1,2], Xiaoyang Sun[1,2]
[1]Institute of High Energy Physics, Chinese Academy of Sciences, Beijing, China
[2]Dongguan Research Department, Dongguan, China

*Abstract*

In the China Spallation Neutron Source II (CSNS-II), the $H^-$ beam will be accelerated in the Linac to 300 MeV. Subsequently, the electrons are stripped from the $H^-$ ions through a stripping foil during injection into the Accumulator Ring, converting them into a proton beam. Wire scanners are employed to measure the transverse beam size and position in the injection area. This paper presents thermal analysis of the wire scanners. To meet measurement requirements, the beam pulse length will be 575 μs, and the current will be approximately 30 mA. Given these parameters, carbon nanotube (CNT) or tungsten wires are considered as potential materials for measuring beam profiles throughout the facility. However, when the beam pulse length exceeds 200 μs, the temperature of a 33 μm tungsten wire surpasses its sublimation threshold (3000 K), approaching its melting temperature. By comparing the temperature of different wire materials, the results indicate that under the specified beam parameters, CNT wires exhibit a significantly lower temperature increase, making it the optimal choice.

## INTRODUCTION

In the beginning of RCS commissioning, it's crucial to quickly establish a loss-free injection line orbit. Therefore, multi-wire scanners (MWS) have been selected as the injection beam monitor. This choice is due to their nature as interceptive devices, which provide reliable beam size and position information. Furthermore, their spatial resolution, which depends on the motor scanning precision, is critical for accurate beam characterization, thus facilitating the rapid establishment of a loss-free orbit.

In the Phase II upgrade of the China Spallation Neutron Source (CSNS) [1], the beam parameters in the injection region have been significantly enhanced (Table 1). The original CSNS multi-wire target design utilized 33μm tungsten wires. However, with the upgraded beam parameters, these wires are now susceptible to melting and destruction. This is primarily because the deposited energy and the resulting temperature rise of the wire are determined by the beam parameters and the wire's material. Consequently, even during 1 Hz Rapid Cycling Synchrotron (RCS) commissioning, when the beam pulse length reaches 200 μs, the tungsten wire already attains its melting point, leading to its structural failure.

Table 1: Beam Properties

| Parameters | No. |
|---|---|
| Beam energy (MeV) | 300 |
| Peak current (mA) | 30 |
| Pulse width (μsec) | 575 |
| Reputation rate (Hz) | 25 |

To meet the new beam parameter requirements, this study employed carbon nanotube (CNT) wire. Given that this marks the first international application of this material in the MWS, a systematic investigation was consequently undertaken in this paper.

## WIRE ANALYSE

### *Wire Material Choice*

Research indicates that tungsten (W), SiC, and carbon fibre (CF) [2,3] have been considered for use in MWS, with their respective material parameters detailed in Table 2. However, W and carbon wire face significant limitations at elevated temperatures. When operating temperatures exceed 2000 °C [4], both the thermionic emission effect and a high sublimation rate substantially impair wire lifespan and signal stability, leading to rapid thinning and eventual breakage. And SiC materials are recommended for use at temperatures not exceeding 1250 °C.

Table 2: Material Properties

| Material | CNT | CF | W | SiC |
|---|---|---|---|---|
| Diameter (um) | 100 | 33 | 33 | 75 |
| Density (g/cm$^3$) | 1.08 | 1.8 | 19.35 | 2.89 |
| Thermal conductivity (W/m·K) | 350 | 24 | 173 | 340 |
| Tensile Strength (GPa) | 1.79 | 3 | 1 | 5.9 |
| Work Temperature (°C) | <2000 | <2000 | <2000 | <1250 |

According to simulation results, when the beam pulse length is 200 μs, the tungsten wire's temperature reaches its melting point 3200 °C (Fig. 1), rendering it unsuitable for the long-term stable operation of the device. Similarly, SiC simulation temperature also surpasses its material tolerance limits, thus failing to meet operational requirements.

* Work supported by National Natural Science Foundation of China (No. 12305166) and the Natural Science Foundation of Guangdong Province, China (No. 2024A1515010016)
† yangrenjun@ihep.ac.cn.

ISBN: <ask the JACoW BoD> ISSN: <ask the JACoW BoD> doi: 10.18429/JACoW-HB2025-THPT51

# REDUCING ENERGY SPREAD OF LOW-ENERGY SLOW EXTRACTED BEAM USING LONGITUDINAL LOCALIZED EXCITATION METHOD *

C. H. Li[1, 2], H. J. Yao[1, 2], Y. Xiong[1, 2], S. X. Zheng†, [1, 2], Key Laboratory of Particle & Radiation Imaging (Tsinghua University), Ministry of Education,Beijing, China
[1]also at Laboratory for Advanced Radiation Sources and Application, Tsinghua University, Beijing, China
[2]also at Department of Engineering Physics, Tsinghua University, Beijing, China

*Abstract*

High-current or low-energy slow extraction from proton synchrotron suffers from strong space charge effect. Longitudinal localized excitation slow extraction method is proposed in this paper to reduce the spill energy spread arising from a large longitudinal emittance, while mitigating space charge effects. This method applies transverse excitation within limited phase intervals which locate at the edge of the longitudinal phase space. By using SynTrack particles tracking code, we simulated low-energy slow extraction under strong space charge conditions for two cases: global excitation and localized excitation. The simulation results indicate that the momentum spread of the extracted beam in localized excitation mode can be significantly lower than that in the global excitation mode. Due to the influence of longitudinal motion, excited particles may also move out of the excitation phase interval before being extracted, so it cannot be fully guaranteed that the extracted particles remain within the excitation phase interval. The mechanism of this leakage phenomenon and corresponding suppression methods are investigated. Furthermore, the hardware design implementing the localized excitation function were presented.

## INTRODUCTION

Currently, the vast majority of proton therapy facilities and space radiation simulation facilities utilizing synchrotron as the main accelerator have adopted the resonance slow extraction scheme, among which the third-order resonance is a typical scheme. The extraction efficiency and beam uniformity in resonant slow extraction of the low-energy beam are affected by various adverse factors, including stronger space charge effect, lager longitudinal emittance, higher magnetic field ripple and greater magnetic field error. And the space charge effect is the most significant and its mechanism of action is the most complex. It induces a central oscillation in the proton beam under RF excitation, which significantly slows transverse emittance growth and complicates high-uniformity extraction [1]. Through theoretical and experimental research [2], Dr. Yang Ye from Tsinghua University proposed that the application of high-order harmonic RF excitation can effectively solve this issue. By designing an extraction scheme with the working point slightly below the third-order resonance line, his team achieved slow extraction of a 10 MeV proton beam under conditions where the maximum incoherent tune shift due to space charge was -0.06 for the first time.

The energy spread of the extracted beam is a key indicator of beam quality. To realize a narrower energy spread, we propose a new RF-KO (RF-Knockout) excitation mode in third-order resonance slow extraction: longitudinal localized excitation slow extraction method. In contrast to the conventional RF-KO approach,in which particles are excited continuously at any longitudinal phase and are all eventually extracted - hence the term "global excitation", this method only applies transverse excitation within a limited phase interval at the edge of the longitudinal phase space. Due to the reduced particle density within the excitation range, the strong space charge effect is also significantly mitigated. Furthermore, when extracting below the resonance line, the stable triangle of particles with large momentum dispersion more easily moves to the outside of electrostatic deflector(ESe), resulting in the particles being unable to enter the ESe at a suitable angle, and the extraction efficiency is reduced. Thus the localized excitation method improves extraction efficiency by mitigating losses from particles with large momentum spread.

Preliminary simulations of the longitudinal localized excitation slow extraction method are presented, utilizing the Xi'an Proton Application Facility (XiPAF) [3].

## LONGITUDINAL LOCALIZED EXCITATION SLOW EXTRACTION METHOD

The longitudinal dynamics of particles in a synchrotron can be described by the Hamiltonian [4]:

$$H(\phi, \delta_p) = \frac{1}{2} h \omega_s \eta_s \delta_p^2 + \frac{\omega_s e V_0}{2\pi \beta_s^2 E_0} [\cos\phi - \cos\phi_s + (\phi - \phi_s)\sin\phi_s], \quad (1)$$

where the subscript $s$ represents synchronous particles, and $\omega_s = \beta_s c / R_s$ is the angular cyclotron frequency of the synchronous particle, $\eta_s$ is the slip factor, $\delta_p$ is the relative momentum deviation, $V_0$ is the high frequency accelerating voltage, $\beta_s$ is the relative velocity, $E_0$ is the total energy of the particle, $h$ is the harmonic number, and $\phi_s$ is the synchronous phase.

* Work supported by the National Natural Science Foundation of China (No. 12075131)

† zhengsx@tsinghua.edu.cn

ISBN: <ask the JACoW BoD> ISSN: <ask the JACoW BoD> doi: 10.18429/JACoW-HB2025-THPT57

# SIMULATION STUDY ON MAGNET AND RF FAILURES IN THE LINEAR ACCELERATOR OF CSNS-II

Y. Yuan[1,2], J. Peng[1,2], Z. P. Li[1,2]
[1]Institute of High Energy Physics Chines Academy Sciences, Beijing, China
[2]Spallation Neutron Source Science Center, Dongguan, China



*Abstract*

China Spallation Neutron Source (CSNS) is a large multidisciplinary experimental facility that generates neutrons by targeting a strong current proton accelerator. Its linear accelerator consists of a front-end accelerator, a 3 MeV Radio Frequency Quadrupole (RFQ) accelerator, and an 80 MeV Drift Tube Linac (DTL). The second phase of the project will upgrade the linear accelerator by installing superconducting cavities after the DTL exit, increasing the beam energy to 300 MeV and the beam power extracted from the ring to 500 kW. This paper will present a simulation study that examines the effects of different magnets and cavity failures in the linear accelerator mainly on beam loss.

## INTRODUCTION

The layout of the CSNS [1] Phase II linac is shown in Fig. 1. Medium energy beam transport (MEBT) section comprises 10 quadrupoles and 2 buncher cavities. DTL consists of four physical tanks, which contain 64, 37, 30, and 26 accelerating cells, respectively. Transverse focusing in Phase I is provided by an FFDD focusing lattice. In Phase II this may be replaced by an FDFD lattice, which can realize a smaller transverse beam envelope but imposes higher magnet-gradient requirements. The superconducting section is formed by 20 double-spoke cavities and 24 elliptical cavities, with an intermediate transport matching section.


Figure 1: Layout of the CSNS Phase II linac.

The simulation study focuses on the impact of RF-cavity failures and magnet power-supply failures on beam loss in the linac straight sections. Beam losses arising from mismatch after the triplet bend and during ring injection due to energy shifts or changes in the transverse Twiss parameters are not considered at this stage. Two failure scenarios are examined (RF cavity failure and magnet failure) to preliminarily identify loss locations, loss fractions, and deposited power, with particular attention to whether significant losses occur in the superconducting section.

### *Impact of RF-Cavity Failure on Beam Loss*

For the simulations, one cavity is selected from each of the following groups: Buncher01, Buncher02, DTL1–4, double-spoke cavities, and elliptical cavities. Beam dynamics is simulated using TraceWin code. The beam is tracked from the RFQ exit to the exit of the LRBT (linac-to-ring beam-transport) straight section. The beam current is 50 mA, 100,000 macroparticles are used, and error effects are not included. Beam-loss results for RF-cavity failure are reported, including the total loss fraction and the locations of both concentrated losses and minor losses. Table 1 summarizes the beam-loss conditions resulting from RF-cavity failure. “Major” denotes locations of concentrated beam loss, while “Minor” denotes locations of minor (distributed) beam loss.

Table 1: Beam-Loss Resulting from RF-Cavity Failure

| Cavities | Beam loss (%) | Major | Minor |
|---|---|---|---|
| Buncher01 | 16.19 | DTL | Spoke |
| Buncher02 | 24.99 | DTL | Spoke |
| DTL1 | 82.50 | DTL+Spoke | LRBT |
| DTL2 | 50.49 | DTL+Spoke | LRBT |
| DTL3 | 25.34 | Elliptical+LRBT | DTL+Spoke |
| DTL4 | 4.30 | Elliptical+LRBT | None |
| Spoke | 0 | None | None |
| Elliptical | 0 | None | None |

### *Impact of Magnet Failure on Beam Loss*

The magnet-failure study specifically refers to magnet power-supply failures. A one-to-one power-supply failure is equivalent to the failure of a single magnet, whereas a one-to-many failure corresponds to simultaneous failures of multiple magnets supplied by the same power supply. For the simulations, magnets at the upstream end, downstream end, and midpoint of each subsystem (MEBT; DTL1–4; the double-spoke section; and the elliptical-cavity section) were selected as failure cases. Special consideration is given to the DTL because its magnet circuits include one-to-many supplies; all other magnet power supplies are one-to-one. Table 2 presents the beam-loss results for different magnet power-supply failure scenarios in the MEBT. Figure 2 shows the layout of magnets and RF cavities in the MEBT, comprising 10 quadrupole magnets and 2 buncher cavities.

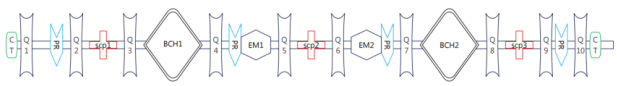


Figure 2: Layout of MEBT.

ISBN: <ask the JACoW BoD> ISSN: <ask the JACoW BoD> doi: 10.18429/JACoW-HB2025-THPT59

# TRANSVERSE BEAM EMITTANCE MEASUREMENT AT CSNS RCS

Y. Li[1,2*], Z. P. Li[1,2], M. Y. Huang[1,2], Z. H. Xu[1,2], Y. S. Yuan[1,2]
[1]Institute of High Energy Physics, Chinese Academy of Sciences, Beijing, China
[2]Spallation Neutron Source Science Center, Dongguan, China



*Abstract*

The transverse beam emittance at the Rapid Cycling Synchrotron (RCS) of the China Spallation Neutron Source (CSNS) is recognized as a crucial parameter, with its precise measurement being essential for investigating space charge effects and enhancing beam quality under high-power operation. However, no reliable diagnostic tools are currently available for direct or indirect measurement of the transverse beam emittance at the CSNS RCS . To address this limitation, this paper proposes an alternative method of early beam extraction at 5 ms combined with wire scanner measurements to indirectly obtain the beam emittance. Using this approach, transverse emittance was successfully measured across a beam power range of 50 kW to 170 kW. Furthermore, issues encountered during the measurements are discussed, and future optimization directions are proposed.

## INTRODUCTION

The China Spallation Neutron Source [1] is a high-power pulsed spallation neutron source facility driven by a proton accelerator. During operation, the $H^-$ beams are injected into the RCS via a multi-turn charge-exchange, accelerated to 1.6 GeV within 20000 turns in the RCS, and extracted to shoot the tungsten target with a repetition frequency of 25 Hz for neutron production. The design beam power for CSNS was 100 kW, and the upgrade project (CSNS-II) aims to achieve 500 kW. The beam commissioning of the CSNS RCS started in May 2017, followed by a series of experimental study on beam loss suppression. In February 2020, the design goal of 100 kW beam power has been successfully achieved with a tolerable beam loss level [2].The facility is currently operated stably at a beam power of 170 kW.

With the continuous increase in beam power, in-depth investigation of beam dynamics behavior has become particularly important. Among key beam parameters, the transverse beam emittance, which characterizes the beam distribution in phase space, directly reflects beam quality and stability. Under high-power operation, the space charge effects are found to significantly influence beam emittance, subsequently leading to increased beam loss. Therefore, accurate emittance measurement is not only of great scientific significance for understanding the evolution of high-intensity beams, but also provides a crucial basis for accelerator tuning and performance optimization.

Transverse emittance can be measured directly using double scanning slit system or indirectly obtained through wire scanner measurements of the beam profile. For circular accelerators such as the RCS, IPM is regarded as an ideal diagnostic tool for beam profile measurements due to its capability for turn-by-turn measurements and non-intercepting characteristics [3, 4]. Consequently, an IPM system was installed in the CSNS RCS during the summer maintenance period in 2019. Unfortunately, strong electromagnetic interference in the tunnel has resulted in a consistently unsatisfactory signal-to-noise ratio, preventing it from providing reliable beam profile for emittance analysis. To address the issue of IPM system failure, an alternative measurement scheme based on early beam extraction and wire scanner measurement is innovatively proposed in this paper.

The structure of this paper is organized as follows: the measurement scheme for emittance is elaborated in the first part, including the design of the extraction scheme, the layout of the beamline, and the associated beam transport theory. In the second part, the measurement results obtained under different beam power conditions are presented, along with an overall analysis. Finally, there is a summary and discussion. The results of this study not only provide important experimental data for beam optimization of the CSNS RCS, but also offer valuable references for emittance measurement in other high-power proton accelerators.

## MEASUREMENT METHOD

An indirect measurement scheme based on "5 ms early extraction and wire scanner scanning" is adopted in this study. The technical approach mainly consists of the following steps: 1) Achieving beam extraction through kicker magnet timing control; 2) Completing beam transport and optical matching in the diagnostic beamline; 3) Using a multi-wire scanner system to obtain beam envelope; 4) Calculating the beam emittance combined with beam optics parameters. This scheme, which is based on mature wire scanner technology, effectively ensures the reliability of the measurement data.

### *Extraction Timing Control*

It is recognized that earlier beam extraction is more advantageous for studying beam loss under high-power conditions. However, earlier extraction leads to longer bunch length, and due to the limited flat-top time of the kicker, 100 % extraction efficiency cannot be achieved. Considering that the space charge effect is strongest during the first 5 ms within the 20 ms acceleration cycle, an extraction strategy at 5 ms was ultimately selected after balancing extraction efficiency and research objectives.

To successfully extract the circulating beam from the RCS at 5 ms, a dedicated 5 ms extraction mode first needs to be established. This mode includes the setting of magnet currents in the extraction beamline and the adjustment of timing for the extraction kicker and corresponding beam diagnostic

* liyong@ihep.ac.cn

ISBN: <ask the JACoW BoD> ISSN: <ask the JACoW BoD> doi: 10.18429/JACoW-HB2025-THPT61

# THE EXPERIMENTAL EVALUATION OF THIRD-ORDER RESONANCE CORRECTION USING 8 TRIM-S IN J-PARC MR

Y. Tan*, Y. Morita, T. Yasui, S. Igarashi, T. Asami, H. Hotchi, M. Yoshii, Y. Sato, K. Miura,
KEK, Tokai, Japan
R. Sagawa, Universal Engineering, Mito, Japan
M. Yoshinari, NAT Corporation, Hitachinaka, Japan

*Abstract*

In the Japan Proton Accelerator Research Complex (J-PARC) main ring (MR), an upgrade project involving a total of 24 Trim-S units is underway to further suppress beam loss. This effort targets key resonances for on- and off-momentum particles, including third-order resonances $3\nu_x = 64$ and $\nu_x + 2\nu_y = 64$, and a fourth-order resonance $4\nu_x = 85$, which arises from the combination of $\nu_x = 21$ and $3\nu_x = 64$. With the installation of an additional 4 sets of Trim-S power supplies, beam studies using 8 sets of Trim-S units have been conducted for resonance scanning and correction. The results show that the beam survivals are consistent when using 4 or 8 sets of Trim-S units, and the resonance driving terms of $3\nu_x = 64$ and $\nu_x + 2\nu_y = 64$ are almost identical under both conditions. This indicates that third-order resonances $3\nu_x = 64$ and $\nu_x + 2\nu_y = 64$ for on-momentum particles have been corrected effectively. However, no new resonance sources have been discovered in the study using 8 sets of Trim-S units. Further investigations are required to search for the uncorrected third-order resonances for off-momentum particles.

## INTRODUCTION

Measurement and correction of nonlinear resonances are crucial for particle accelerators in mitigating beam loss. In Large Hadron Collider (LHC), beam studies measuring tune and coupling upon application of closed orbit bumps are used to validate and refine the magnetic model of the collider for nonlinear optics corrections [1]. In Diamond Light Source, based on spectral line derived from the turn-by-turn data from Beam Position Monitors (BPMs) upon the pinger magnets, the sextupole components can be reconstructed by minimizing the discrepancy between the real accelerator and the model [2].

In the Japan Proton Accelerator Research Complex (J-PARC) main ring (MR), third-order resonances of $3\nu_x = 64$ and $\nu_x + 2\nu_y = 64$ have been significantly corrected using 4 sets of Trim-S [3, 4] during 800 kW beam operation. With the beam power to be increased to 1.3 MW for the startup of Hyper-Kamiokande [5], given that hands-on maintainability requires beam loss to be kept below 3.5 kW [6], third-order resonances need to be further corrected to suppress beam loss. The numerical simulation with error field on dipole magnets which contain intrinsic sextupole components shows that 24 sets of Trim-S can correct the resonance for both on- and off-momentum resonance particles of $3\nu_x = 64$ and $\nu_x + 2\nu_y = 64$ and fourth-resonance of $4\nu_x = 85$ which is driven by the combination of $\nu_x = 21$ and $3\nu_x = 64$ [7]. So, search of the sextupole error field is conducted in order to evaluate the resonance driving term for further planning [8,9]. However, the sextupole error field on the zero dispersion area cannot be evaluated because of the limitation of this scheme.

In contrast to the previous method, beam-based optimization of the lifetime via scans of the relevant correctors provides another possibility to search and correct uncorrected or unclear resonance [10]. In this method, the correctors act as knobs, and they are used to perform the scans. The number of correctors must be greater than or equal to the number of knobs necessary to compensate the driving terms. For example, in the case of correcting one third-order driving term for on-momentum particles, we need at least 2 knobs since it is a complex number consisting of a real and a imaginary part. The step-by-step project of 24 sets of Trim-S units in J-PARC MR enables such scan experiments. An additional 4 newly selected sets of Trim-S magnets have been available in J-PARC MR for further research [11, 12], providing 4 additional knobs for resonance scans and corrections. This paper reports and analyses the beam study results using 8 sets of Trim-S units.

Section 2 introduces the background of the experiment and gives the result of initial current calculation. Section 3 describes the experimental procedure which includes the scans of individual 4 sets of Trim-S and all 8 sets of Trim-S by using the quadratic fitting method. Section 4 presents the experimental results by comparing the beam loss and the estimated driving terms between 4 sets and 8 sets of Trim-S. Then, the scan range is presented and compared between different configurations. Finally, Section 5 summarizes the findings regarding the consistency of all conditions and outlines future plans for further research.

## BACKGROUND

The distribution of 24 Trim-S units planned in the J-PARC MR is shown in Fig. 1 in [12]. The Trim-S units are trim coils of the sextupole magnets, with an identical winding configuration to the main coils. The areas enclosed by the red dashed line indicate Trim-S units that have been powered by supplies (PSs) at the D2 and D3 buildings. The Trim-S 048, 055, 062, 069 located at D2, as well as 134, 141, 171, and 178 located at D3 are selected based on two principles of wide distribution of phase of the driving terms and minimization

* yulian.tan@kek.jp

ISBN: <ask the JACoW BoD> ISSN: <ask the JACoW BoD> doi: 10.18429/JACoW-HB2025-THPT62

# THE FIELD MEASUREMENT OF THE INJECTION PAINTING BUMP MAGNETS FOR THE CSNS-II/RCS

Z. X. Pang[1, 2, 3], M. Y. Huang*, [1, 2, 3], H. W. Ha[1, 2], C. D. Deng[1, 2], W. Q. Zhang[1, 2], G. D. Zhao[1, 2], X. Qi[1, 2]
[1]Institute of High Energy Physics, Chinese Academy of Sciences, Beijing, China
[2]Spallation Neutron Source Science Center, Dongguan, China
[3]University of Chinese Academy of Sciences, Beijing, China

*Abstract*

For accumulating high-intensity beam, the $H^-$ stripping injection is adopted in the rapid cycling synchrotron(RCS) of the China Spallation Neutron Source (CSNS). For the CSNS-II, the painting injection is a key solution, which is performed in a straight section of RCS by the bump magnets, including four BCH magnetsfor horizontal painting, four BV magnets for the vertical painting and one LRBD magnet for the horizontalsweeping compensation. The fabrication and the field measurement of the magnets have been completed. Themeasurement items include magnetic field response error, magnetic field uniformity, leakage field, and so on. The measurement system and the results of the magnetic field measurement are presented in this paper.

## INTRODUCTION

To reduce the space charge effect, the CSNS-II RCS increases the injection beam energy from 80 MeV to 300 MeV and adds a second-harmonic radio frequency system to enhance the beam bunching factor. To meet the requirements for injecting 300 MeV energy beams and achieve better injection painting, the injection scheme has been redesigned. It adopts an $H^-$ stripper injection scheme to meet the demand for high injection efficiency [1].

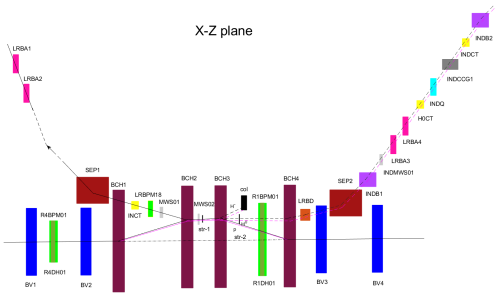


Figure 1: Layout of the CSNS-II RCS injection area hardware.

The hardware layout of the injection area is shown in Figure 1. The main magnets include: 4 horizontal painting magnets, 4 vertical painting magnets, 2 septum dipole magnets, 1 pulsed septum magnet, 2 DC dipole magnets, 4 vertical DC bump magnets (one of which is equipped with auxiliary windings), and 1 DC quadrupole magnet. All 8 painting bump magnets are distributed in the RCS section of the injection system. Among them, 4 horizontal bump magnets (BCH) are used for horizontal painting, and 4 vertical bump magnets (BV) are used for vertical painting. The 4 DC bump magnets (LRBA) are distributed in the LRBT section of the injection system, and they provide a fixed vertical bump amplitude during the injection phase to enable the correlated painting mode using the falling edge of the pulsed power supply.

This work mainly focuses on measuring the integrated magnetic field uniformity, leakage field, magnetic field response characteristics of 9 pulsed magnets, including 4 horizontal painting magnets, 4 vertical painting magnets, and 1 pulsed cutting magnet, and the edge field of BCH2/3.

Table 1: Physcial Design Requirement of the Pulsed Magnets

| Magnet | Uniformity | Response error | Leakage ratio |
|---|---|---|---|
| BCH1 | $\leq \pm 1.5\%$ | $\leq \pm 0.15\%$ | $\leq \pm 0.25\%$ |
| BCH2 | $\leq \pm 1.5\%$ | $\leq \pm 0.15\%$ | |
| BCH3 | $\leq \pm 1.5\%$ | $\leq \pm 0.15\%$ | |
| BCH4 | $\leq \pm 1.5\%$ | $\leq \pm 0.15\%$ | |
| BV1 | $\leq \pm 1.5\%$ | $\leq \pm 0.15\%$ | |
| BV2 | $\leq \pm 1.5\%$ | $\leq \pm 0.15\%$ | |
| BV3 | $\leq \pm 1.5\%$ | $\leq \pm 0.15\%$ | $\leq \pm 0.25\%$ |
| BV4 | $\leq \pm 1.5\%$ | $\leq \pm 0.15\%$ | |
| LRBD | $\leq \pm 1.5\%$ | $\leq \pm 0.15\%$ | $\leq \pm 0.25\%$ |

## PULSED MAGNET MEASUREMENT SYSTEM

A test system based on a PCB coil array [3] is used to measure various parameters of the pulsed magnets, as shown in Figure 2 [4]. The system mainly includes: a PCB array coil, an RC integrator, a data acquisition unit, and a current sensor. Among these components, the data acquisition unit has four channels with adjustable measurement ranges. Displacement stages are installed at both ends of the magnet under test, enabling the displacement of the induction coil within the good field region. When an external trigger signal arrives, the excitation power supply outputs a pulsed current, which generates a pulsed magnetic field in the magnet under test.

The induction coil then detects the change in magnetic flux at its center. Two RC integrators are used to integrate the

* huangmy@ihep.ac.cn

ISBN: <ask the JACoW BoD> ISSN: <ask the JACoW BoD> doi: 10.18429/JACoW-HB2025-THPT65

# THE STUDY OF THE ENERGY SPREAD MEASUREMENT AT LINAC OF CSNS *

Yanliang Han†,1, Jun Peng[1], Zhiping Li[1]
IHEP, CAS, Beijing, China
[1] also at Spallation Neutron Source Science Center, Dongguan, China

*Abstract*

In accelerator-based spallation neutron sources, which include a rapid cycling synchrotron (RCS), the energy spread at the end of the linac is a crucial parameter that significantly impacts the operational efficiency of the downstream RCS ring. However, in recent years, the energy spread at the linac of the Chinese Spallation Neutron Source has been inadequately measured due to limited methods for longitudinal phase space measurement. This paper presents a study on measuring the energy spread using wall current monitors at the linac. The results indicate that the energy spread is at the $10^{-3}$ level, consistent with simulations. Nevertheless, the uncertainty remains relatively high, necessitating further efforts to improve measurement accuracy in the future.

## INTRODUCTION

The China Spallation Neutron Source (CSNS) is an accelerator-based pulsed neutron source located in Guangdong Province, southern China. Construction began in 2011 and was completed in 2018 [1, 2]. The design beam power is 100 kW with plans to upgrade it to 500 kW in the next few years.

The CSNS comprises an 80 MeV linac, a rapid cycling synchroton ring which boost the beam energy to 1.6 GeV, a spallation target and two transfer line LRBT and RTBT, as illustrated in Fig. 1. This paper focuses on the linac, which acts as the injector for the RCS. The linac includes a negative hydrogen ion source, a low energy beam transfer line (LEBT), an RFQ, a medium energy beam transfer line (MEBT), and four drift tube linacs (DTL).

Several types of instrumentation equipment are installed along the linac, such as BPM position monitors for transverse positions, current transformers (CT) for beam current, fast current transformers for beam phase, and wire scanners for transverse beam size. These instruments enable the measurement of beam orbit, current, phase, and transverse emittance. Over the years, the linac has provided high-quality negative hydrogen beams for the RCS. However, some longitudinal beam properties, such as bunch length and energy spread, have not been measured. While bunch length is less critical for RCS injection due to the larger phase acceptance in the RCS compared to the linac, energy spread is a crucial parameter. Improper energy spread can lead to beam loss during RCS operation, particularly in the future CSNS-II. An energy spread study based on the wall current transformer (WCM) in the RCS [3] for the accumulated initial beam in the RCS indicates an energy spread of 0.17 %. In contrast, simulations in the linac suggest a momentum spread of around 0.1 %. This discrepancy underscores the importance of directly measuring the energy spread at the end of the linac.

In this paper, we present a study of the energy spread in the linac of the CSNS, utilizing the three WCMs installed in the linac.

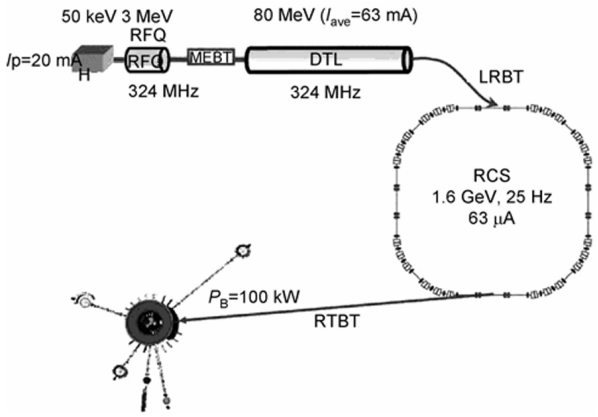


Figure 1: The layout of the CSNS facility.

## THE PRINCIPLE OF MEASUREMENT

At the end DTL, the transfer line LRBT will delivery the $H^-$ beam to RCS. In the LRBT, there are three WCMs installed which can give the bunch length information in the linac, as shown in Fig. 2. When the $H^-$ bunches pass through these WCMs, their length will increase due to the no-zero energy spread.

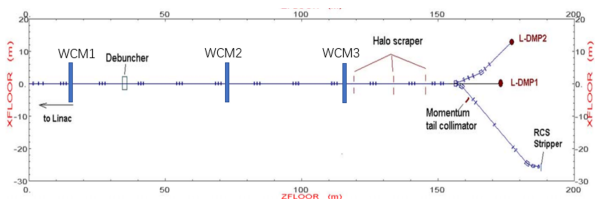


Figure 2: The layout of WCM in the LRBT.

The longitudinal transfer matrix in the drift space can be expressed as:

* Work supported by Open Research Foundation of Songshan Lake, DG24313511 and IHEP Talent Recruitment Program Foundation No. E15156U110.

† Email: ylhan@ihep.ac.cn

ISBN: <ask the JACoW BoD> ISSN: <ask the JACoW BoD> doi: 10.18429/JACoW-HB2025-THPT69

# TUNE OPTIMIZATION FOR CSNS-II RCS: SIMULATIONS AND MACHINE STUDIES*

J. L. Chen[1], Y. W. An[1], Y. Li[1], H. Y. Liu[1], J. J. Tan[1], M. Y. Huang †,[1],
Institute of High Energy Physics, Chinese Academy of Sciences, Beijing, China
[1]also at Spallation Neutron Source Science Center, Dongguan, China



*Abstract*

Based on the beam commissioning of CSNS-I RCS, the current tune above the half-integer resonance exhibits extremely narrow parameter margins and severe instabilities. Therefore, to further increase the beam power in Phase II, significant optimization of the tune is required.

First, we conducted a series of simulations. A total of 97 tunes were selected on the resonance diagram, and the beam transmission efficiency was simulated, taking into account space charge effects and instabilities. The results demonstrate that the tunes below the half-integer resonance (near 4.3/5.3) are instability-free and can achieve transmission efficiencies exceeding 99 % (up to 140 kW in Phase I and 700 kW in Phase II).

Subsequently, to verify stable operation at the tunes near 4.3/5.3 in the actual machine, we performed a series of mechine studies. The results confirm that these tunes remain instability-free and can achieve stable beam supply at 140 kW (corresponding to 700 kW in Phase II under equivalent space charge tune shift conditions). This provides strong evidence that the selected tunes can support stable 700 kW beam operation during Phase II commissioning.

## INTRODUCTION

The Rapid Cycling Synchrotron (RCS) is a key component of China Spallation Neutron Source (CSNS), which is designed to accelerate proton beam pulses to 1.6 GeV for striking a solid metal target to produce neutrons [1, 2]. The design of Phase I of RCS is to accumulate and accelerate proton particles from 80 MeV to 1.6 GeV at a repetition rate of 25 Hz, with a designed beam power of 100 kW. In the future, we will carry out the Phase II upgrade. The main change in parameters will be an injection energy of 300 MeV, which will enable RCS to have a smaller tune-shift caused by the space charge effect, and the beam power will be increased to 500 kW. Additionally, trim quadrupoles will be adopted in Phase II. A comparison of the parameters between Phase I and Phase II is shown in Table 1.

For RCS, tunes are critical. Based on Phase-I beam commissioning experience, the current tune offers minimal parameter margins and exhibits severe instabilities [3]. Threrfore, for Phase-II, it requires significant tune optimization to support higher beam power. We have conducted extensive simulation work. Based on the simulation results, the tunes below the half-integer exhibit no instabilities and achieve a high tansmission rate under higher beam power. To verify the simulation results, we carried out machine studies under the beam conditions of Phase I. The current research results show that the tunes below half-integer remain instability-free and can achieve stable beam supply at 140 kW (corresponding to 700 kW in Phase II under equivalent space charge tune shift conditions). This provides strong evidence that the selected tunes can support stable 700 kW beam operation during Phase II commissioning.

Table 1: CSNS RCS design parameters

| Parameter (Unit) | Phase I | Phase II |
|---|---|---|
| Extraction Beam Power (kW) | 100 | 500 |
| Injection Beam Power (MeV) | 80 | 300 |
| Extraction Beam Energy (MeV) | 1600 | 1600 |
| Repetition Rate (Hz) | 25 | 25 |
| Space Charge Tune Shift | 0.28 | 0.19 |
| Beam Average Current (μA) | 62.5 | 312.5 |
| Number of Dipoles | 24 | 24 |
| Number of Main Quadrupoles | 48 | 48 |
| Number of Trim Quadrupoles | / | 16 |

## SIMULATION

Our simulation focused on identifying the tunes that can achieve a transmission rate of over 99 % at 800 kW, with considerations for injection painting, space charge effects, and beam instabilities. A total of 97 sets of tunes were selected for the simulation, as shown in Fig. 1. Ultimately, we have determined the range for selecting tunes: 4.35-4.45 in $x$ plane and 5.25-5.45 in y plane (below half-integer resonances), as shown in Fig. 2. And the simulation results show that the transmission rate reached above 99 % and there is no beam instabilities, as shown in Fig. 3.

## MACHINE STUDIES

The space charge effect of 100 kW-160 kW (Phase I) is equivalent to that of 500 kW-800 kW at an injection energy of 300 MeV (Phase II).

### *Beam Commissioning at* 100 kW

At the beginning of beam commissioning, the beam loss in the injection region has decreased significantly and the transmission rate of the RCS was very low (< 97 %).

We adopted the following optimization methods:

1. Optimize the global orbit
2. Replace the RF curve

* Work supported by the Young Scientists Fund of the National Natural Science Foundation of China (Category C, Grant No. 12405175)

† huangmy@ihep.ac.cn

ISBN: <ask the JACoW BoD> ISSN: <ask the JACoW BoD> doi: 10.18429/JACoW-HB2025-THPT71

# Xsuite FOR SIMULATING HIGH-BRIGHTNESS, HIGH-INTENSITY HADRON BEAMS

X. Buffat, R. De Maria*, G. Iadarola, S. Łopaciuk, F. F. Van der Veken, CERN, Geneva, Switzerland

*Abstract*

Accurate simulation of high-brightness, high-intensity hadron beams is essential for the design, commissioning, and optimization of modern accelerators such as the LHC injector complex, the LHC, and future high-energy machines. Xsuite is a modern, modular framework developed at CERN, implemented primarily in Python, and designed to address the challenges posed by simulating these processes. It supports six-dimensional symplectic tracking with detailed modeling of nonlinearities, field errors, and collective effects; advanced models for space charge, impedance, beam-beam forces, and intrabeam scattering; and particle-matter interactions through its internal scattering engine together with interfaces to FLUKA and Geant4. Designed for high-performance computing, Xsuite leverages GPU acceleration and massive parallelization to enable large-scale simulations. This contribution outlines Xsuite's capabilities and illustrates its application in current and future accelerator projects.

## INTRODUCTION

The Xsuite [1, 2] system comprises Python packages that provide physics functionality (Xtrack [3], Xpart [4], Xfields [5], Xcoll [6], Xwakes [7]). These packages interoperate via a common low-level performance library (Xobjects [8, 9]) and a high-level control library (Xdeps [9, 10]). Additional packages such as Xplt [11] and Xnlbd [12, 13] expand post-processing capabilities. The main Xsuite package [14] serves as the entry point to install the suite and its dependencies. The physics models and methods implemented in the code are documented in the Xsuite Physics Manual [15].

This paper presents the main features of the modules and illustrates a subset of use cases.

## MODULES

### *Tracking*

Tracking forms the backbone of the Xsuite physics suite packaged in the Xtrack module. The module allows users to create an environment that gathers machine parameters, elements, particles, lines, tracking loops, and Twiss and matching methods. The Xtrack package contains typical beam-line elements, such as magnets, that are sufficient to define a lattice. Additional modules and users can implement an element class that defines user-defined tracking maps in Python or C. Forward and backward tracking is supported. Xsuite supports fringe fields maps from PTC [16], and work is in progress to support general fringe fields based on field derivative expansion [17].

### *Optics*

Direct element-by-element tracking is used to extract optics functions. Transfer functions of first and second order can be extracted using finite differences. The eigenvector problem is solved to obtain coupled Twiss parameters using Ripken formalism and derivative quantities [18].

### *Space Charge*

Xsuite provides three models of space-charge forces:

**Frozen** A static charge distribution is used to compute the space-charge forces. The tracked particles do not affect each other.

**Quasi-frozen** As in the frozen model, but the properties of the charge distribution (transverse r.m.s. sizes and transverse positions) are updated at each interaction based on the particle distribution.

**PIC** The forces are computed using the actual tracked distributions, without assumptions about the bunch shape. The particle-in-cell method (2D and 3D) is used, using a fast and accurate FFT Poisson solver and integrated Green functions, [19].

*Frozen* and *Quasi-frozen* use a 2D Gaussian distribution for the transverse part $\rho_\perp(x,y)$ and uniform or q-Gaussian for the longitudinal part $\lambda_0(\zeta)$:

$$\rho_0(x,y,\zeta) = q_0\lambda_0(\zeta)\rho_\perp(x,y), \tag{1}$$

with the following normalization:

$$\int \rho_\perp(x,y)\,dx\,dy = 1 \quad \text{with} \quad \int \lambda_0(\zeta)\,d\zeta = N, \tag{2}$$

where $N$ is the bunch population. The field generated by the distribution assumes free-space boundary conditions. The space-charge force (expressed by the gradient of the potential $\phi_\perp(x,y)\lambda(\zeta)$) is integrated over a given length $L$, and the effect is approximated by the following kick:

$$\Delta p_x = \frac{m_0}{m}\frac{\Delta P_x}{P_0} = -\frac{qq_0L(1-\beta_0^2)}{m\gamma_0\beta_0^2c^2}\,\lambda_0(\zeta)\,\frac{\partial\phi_\perp}{\partial x}(x,y) \tag{3}$$

$$\Delta p_y = \frac{m_0}{m}\frac{\Delta P_y}{P_0} = -\frac{qq_0L(1-\beta_0^2)}{m\gamma_0\beta_0^2c^2}\,\lambda_0(\zeta)\,\frac{\partial\phi_\perp}{\partial y}(x,y) \tag{4}$$

$$\begin{aligned}\Delta\delta \simeq \Delta p_z &= \frac{m_0}{m}\frac{\Delta P_z}{P_0} \\ &= -\frac{qq_0L(1-\beta_0^2)}{m\gamma_0\beta_0^2c^2}\,\frac{d\lambda_0}{d\zeta}(\zeta)\,\phi_\perp(x,y)\,,\end{aligned} \tag{5}$$

where $q_0$, $m_0$ are the charge and mass of the reference particle and $q$, $m$ the charge and mass of the tracked particle.

* riccardo.de.maria@cern.ch

ISBN: <ask the JACoW BoD> ISSN: <ask the JACoW BoD> doi: 10.18429/JACoW-HB2025-FRIAA02

# AUTOMATION FOR CERN'S ACCELERATOR FLEET – STATUS AND NEXT STEPS

M. Schenk*, R. Alemany Fernandez, M. M. Algelly, A. Beeckman, A. S. Bram, A. Calia, M. Fleischhacker, L. Foldesi, J. C. Garnier, R. Gorbonosov, M. Hostettler, A. Huschauer, F. Irannejad, V. Kain, A. Lu, A. Menor de Oñate, K. Papastergiou, C. Petrone, B. Rodriguez Mateos, M. Sobieszek, G. Trad, F. M. Velotti, J. A. Wulff
CERN, Geneva, Switzerland

*Abstract*

Growing demands on accelerator performance, together with recent advances in computational sciences, provide a remarkable opportunity to rethink how CERN's accelerator complex is operated. Moving beyond traditional approaches, greater automation and improved optimisation methods promise measurable benefits, including reduced costs and energy use, shorter setup times, consistent beam quality, and higher overall reliability. Delivering these gains requires, among others, new algorithms, ranging from classical optimisation to machine learning, and infrastructure that evolves to meet new requirements. Applications extend beyond beam quality optimisation to include equipment-related tasks such as automated setup and recovery, fault prediction and diagnostics, and predictive maintenance. First use cases already support optimisation tasks in daily operation, while further developments are underway. This contribution will review the current status and outline the path toward wider operational use, with emphasis on the Efficient Particle Accelerators (EPA) project as the framework that links these activities into a coherent roadmap from studies to deployment and toward future facilities.

## INTRODUCTION

Systematic accelerator automation at CERN took shape with the Intersecting Storage Rings (ISR) in the 1970s, where the complexity of beam stacking motivated efforts to make operation more manageable and reproducible [1]. The ISR control system was designed in a modular, hierarchical way, operating in high-level machine parameters rather than direct hardware values. Automated optimisation and sequencing were progressively introduced – concepts later formalised in the LHC Software Architecture (LSA, CERN's settings management system) [2], Sequencer [3], and feedbacks for orbit, tune, and other key parameters [4] – which together form an essential part of today's operations model.

Bottlenecks remain, however, such as switching between beam-production modes (fixed-target physics, LHC fills, machine development), costly on-site interventions, resource-intensive commissioning, maintaining beam quality, and optimising energy use [5]. The diversity of user requirements further increases flexibility demands while stretching available resources. For potential future facilities such as the FCC, the scale and cost would, for example, make frequent on-site interventions unsustainable, requiring equipment with built-in auto-diagnostics and recovery capabilities [6].

Since the late 2010s, CERN has entered a new phase of accelerator automation. This evolution was primarily enabled by the adoption of the Python ecosystem, advances in computing and machine learning (ML), improved interoperability through common APIs, and dedicated frameworks for optimisation and online data processing, all building on CERN's mature control infrastructure. In 2023, the Efficient Particle Accelerators (EPA) project was launched as a five-year initiative following the Efficiency Think Tank recommendations [7], providing a framework for the coordinated development and implementation of this new automation wave. It aims to modernise accelerator operation by improving efficiency and reliability, and by preparing equipment and controls for higher degrees of autonomy. Prototyping is underway during Run 3, with broader deployment planned for Long Shutdown 3 (LS3) starting in 2026. Beyond improving current operations, EPA also explores concepts for future machines, where beam and equipment automation will be core design principles.

This paper first covers part of the enabling infrastructure, then reviews the status and outlook of EPA activities.

## INFRASTRUCTURE

This section does not provide a comprehensive overview of CERN's control infrastructure but highlights recent developments that facilitate automation and the integration of ML. Established core components, such as settings management, continue to evolve with new requirements, adding important functionality for safe and efficient operation, including online consistency checks, improved cycle generation, Python "makerules", and continuous parameter optimisation.

Established in 2019, the Acc-Py ecosystem integrates the full Python environment into CERN's accelerator operations, providing package management, DevOps workflows with deployment tools and CI/CD pipelines, PyQt GUIs, and direct access to accelerator devices [8, 9]. As Python is the de facto standard for ML, Acc-Py makes scientific and ML libraries readily available within the protected Technical Network (TN) and provides a common platform to deploy such methods in accelerator operations easily.

The Unified Controls Acquisition and Processing framework (UCAP), also in production since 2019, provides the backbone for online data-processing pipelines [10]. It acquires and synchronises heterogeneous data streams, exe-

* michael.schenk@cern.ch

ISBN: <ask the JACoW BoD> ISSN: <ask the JACoW BoD> doi: 10.18429/JACoW-HB2025-FRCAA01

# AUTOMATION OF GSI KEY BEAM MANIPULATIONS WITH AI METHODS

S. Appel*, M. Bajzek, E. Kazantseva, P. Madysa, S. Pietri, S. Sorge, H. Weick
GSI Helmholtzzentrum für Schwerionenforschung, Darmstadt, Germany
H. Alsmeier, R. Findeisen, S. Hirt, E. Lenz, M. Pfefferkorn
TU Darmstadt, CCPS, Darmstadt, Germany
O. Boine-Frankenheim, D. Kallendorf, O. Kazinova, C. Reinwald
TU Darmstadt, TEMF, Darmstadt, Germany
B. Halilovic, S. Hirlaender
Paris Lodron Universität Salzburg, Salzburg, Austria

*Abstract*

We present the Geoff framework for automated accelerator tuning, demonstrated in real-world experiments at GSI. Using classical optimizers like BOBYQA, Geoff enables fast deployment, control room integration, and efficient beam optimization, reducing SIS18 injection losses from 45 % to 15 % and speeding up FRS setup. This work also reports the first application of multi-objective and multi-fidelity Bayesian optimization to SIS18 injection tuning. Complementary simulation studies employ model predictive control via model-based reinforcement learning for fast, constraint-aware tuning. These model-based methods outperform classical optimizers by guiding experiments with probabilistic surrogate and dynamic models.

Geoff's modular design supports easy switching between algorithms and integration with modern ML tools, bridging accelerator operations and data-driven optimization.

## GEOFF AT GSI/FAIR

The Facility for Antiproton and Ion Research (FAIR) is going to be an international center of heavy-ion accelerators, that will drive the forefront of heavy-ion and antimatter research [1]. The complexity of FAIR requires a high level of automation for future operation [2]. One part of this automation effort is to provide a framework that allows both machine experts and operators to solve concrete optimization problems, and to make these solutions reusable in an operational context. We call this project the "Generic Optimisation Frontend and Framework", or *Geoff* for short [3].

*Geoff* is based on the Python programming language, which is widely used in scientific research, has a vibrant ecosystem of machine learning (ML) algorithms, and is perceived as very beginner-friendly. Both language and framework have proven themselves flexible enough to be quickly adapted to new problems.

*Geoff* is used extensively at CERN—from linacs to SPS and ISOLDE—and is being deployed at GSI/FAIR [4]. It is usually embedded in a GUI application, but can also be used via command-line scripting to shorten the edit-check-run cycle between code changes and test runs. *Geoff* standardizes interfaces for optimization tasks [5] and provides adapters for various third-party packages, e.g., *SciPy*, *Stable Baselines 3*, and *Scikit-Optimize*. Optimization problems, implemented as plugin packages, can scale to arbitrary complexity and depend on any Python package. Custom figures can be generated and updated continuously to monitor the algorithm's progress. It can use any control system and communicate with external simulation tools, as long as Python bindings exist (see Fig. 1).

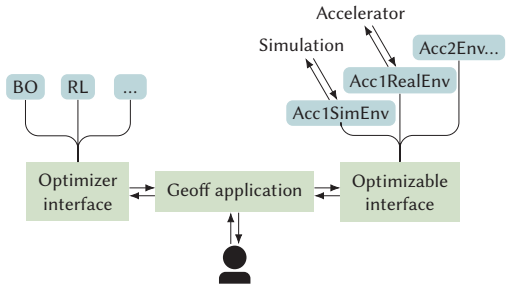


Figure 1: Model of *Geoff* and its components. The optimizer interface includes BOBYQA, Bayesian optimization (BO), and reinforcement learning (RL).

## MULTI-TURN INJECTION

The SIS18 serves as a booster for SIS100. Multi-turn injection (MTI) into it is a key bottleneck for achieving FAIR intensity goals. Beam loss–induced vacuum degradation limits intermediate-charge-state beam intensity, so injection losses—occurring at the septum or acceptance—must be minimized. Four time-varying bumper magnets create a closed-orbit bump, guiding each incoming beam into the available horizontal phase space near the previous injection [6, 7].

In November 2023 and May 2024, optimization runs at GSI evaluated the use of *Geoff*. The goal was to minimize SIS18 injection losses by adjusting five injection parameters—orbit bump amplitude and reduction, two septum steerers, and a timing offset—and four TK steerers. To avoid bias from favorable initial states, parameters were randomized before each run. Loss was estimated from the difference between ideal and measured SIS18 currents (Fig. 2). BOBYQA was chosen as the optimizer, with an initialization phase of $N = 19$ evaluations for nine parameters, as

* s.appel@gsi.de